NOISE CANCELLATION IN HEADPHONES FOR AUDIOMETRY

A dissertation submitted in
partial fulfillment of the requirements for the degree of

Master of Technology

by

Vinod Kumar Lohar
(09307053)

under the supervision of

Prof. P. C. Pandey

Department of Electrical Engineering
Indian Institute of Technology Bombay

June 2011

Indian Institute of Technology Bombay

M.Tech. Dissertation Approval

This dissertation entitled **"Noise cancellation in headphones for audiometry"**
by **Vinod Kumar Lohar** (Roll No. **09307053**)
is approved, after the successful completion of *viva voce* examination,
for the award of the degree of **Master of Technology in Electrical Engineering**
with specialization in **Electronic Systems.**

Supervisor	....	(Prof. P. C. Pandey)
Examiners	....	(Prof. Preeti Rao)
	....	(Prof. M. S. Shah)
Chairperson	....	(Prof. R. K. Joshi)

Date: 27th June 2011
Place: Mumbai

Declaration

I declare that this written submission represents my ideas and my own words and where other's ideas or words have been included, I have adequately cited and referenced the original sources. I also declare that I have adhered to all principles of academic honesty and integrity and have not mispresented or fabricated or falsified any idea/data/fact/source in my submission. I understand that any violation of the above will be cause for disciplinary action by the institute and can also evoke penal action from sources which have thus not been properly cited or from whom proper permission has not been taken when needed.

Vinodkumar

(Signature)

Vinod Kumar Lohar

(Name of the student)

09307053

(Roll No.)

Date: 27th June, 2011

Place: Mumbai

Vinod Kumar Lohar / Prof. P. C. Pandey (supervisor): "Noise cancellation in headphones for audiometry", *M. Tech. dissertation*, Electronic Systems Group, Department of Electrical Engineering, Indian Institute of Technology Bombay, June 2011.

ABSTRACT

Noise cancellation technique can be used to reduce the ambient noise level to improve the hearing of the desired sounds. The objective of this project is to study and develop a noise cancelling headphone (NCH), which can be used to reduce the effect of ambient noise in the testing environment for audiometry without using an acoustically isolated room. The noise level needs to be decreased to that corresponding to a typical audiometry room, without affecting the test signal. A real-time implementation of LMS-based adaptive filter for broad-band noise cancellation is not practical in this case because the delay in the processing path turns out to be larger than the propagation delay of the noise through the shell of the headphone. A method is proposed to find the frequency response of the filter needed for broad-band noise cancellation by using LMS-based adaptation for cancellation of an externally applied tone as the noise and sweeping the tone frequency. The adaptation is carried out in the absence of test stimulus. This frequency response is used for realizing a fixed adapted filter for noise cancellation. Simulations were carried out with various broad-band noises and an average noise reduction of 34.6 dB was observed. Initially real time implementation was carried out using dsPIC33FJ128GP802 which has 40 MHz clock speed and 16 KB on-chip memory. Real-time implementation was carried out with sampling frequency of 20 kHz and filter order of 250. Average noise reduction of 13.6 dB was observed for tones over frequency range of 260 Hz to 460 Hz. Next, TI TMS320C5515 with 120 MHz clock and 320 KB on-chip RAM was used for real-time implementation with sampling frequency of 24 kHz and filter length of 400. Average noise reduction of 20.2 dB was observed for tones over a range of 200-800 Hz. An average noise reduction for tonal noise swept over the frequency range of 200-800 Hz was 6.5 dB and filtered band-pass white Gaussian noise was 2.3 dB. Further investigations are needed for making the real-time implementation useful for cancellation of broad-band noise.

CONTENTS

LIST OF FIGURES

LIST OF TABLES

LIST OF ABBREVIATIONS

Abbreviation	**Term**
AAF	anti-aliasing filter
ABS	acrylonitrile butadiene styrene
A/D	analog-to-digital converter
ADC	analog-to-digital converter
AF	adaptive filter
ALU	arithmetic logic unit
AMP	amplifier
ANC	active noise cancellation
AUD	audiometer
CCS	code composer studio
CPU	central processing unit
D/A	digital-to-analog converter
DAC	digital-to-analog converter
DARAM	dual-access RAM
dB	decibel
DFT	discrete fourier transform
DMA	direct memory access
DSK	DSP starter kit
DSO	digital storage oscilloscope
DSP	digital signal processing
ECM	electret condenser microphone
EMIF	external memory interface
FIFO	first in, first out
FIR	finite impulse response
FRC	fast RC oscillator
FxLMS	filtered-x least mean square
HL	hearing level
IC	integrated chip
IDE	integrated development environment
IDFT	inverse discrete fourier transform

I2C	inter integrated circuit
I2S	inter-IC sound
I/O	input-output
LCD	liquid crystal display
LMS	least mean square
LPF	low-pass filter
MAC	multiply-accumulate
Mic	microphone
MSE	mean square error
NCH	noise cancelling headphone
NLMS	normalized least mean square
PC	personal computer
PGA	programmable gain amplifier
PLL	phase-locked loop
PNA	passive noise attenuation
RAM	random access memory
ROM	read only memory
RTC	real-time clock
RX	receiver
SAR	successive approximation register
SARAM	single-access RAM
SF	smoothing filter
SPI	serial peripheral interface
SPL	sound pressure level
SPR	speaker
TI	texas instruments
TX	transmitter
UART	universal asynchronous receiver/transmitter
USB	universal serial bus

Chapter 1
INTRODUCTION

1.1 Background

Various noise cancellation techniques have been developed to reduce ambient noise levels for improving the audibility of the desired sound. These noise cancellation techniques can be used to reduce the high noise level which may affect the auditory senses of human beings working under high noise condition. As cancelling the noise over a large space is very difficult, noise cancelling headphones have been found very useful, particularly for listening music and telecommunication [1].

Audiometric tests are conducted to determine the hearing threshold levels of an individual and the ability to discriminate speech accurately. Ambient noise affects on hearing threshold levels. Hence low ambient noise level is an important requirement for these tests [2]. Various methods used to reduce the ambient noise level include sound-proof testing room, passive attenuation using circum-aural headphone, and insert earphones [3]-[5]. Sound-proof testing rooms are expensive and difficult to maintain in many clinics [5]. In the circum-aural headphones, the ear is enclosed in a chamber made of passive attenuation material. This method gives non-uniform test results mainly due to improper fitting issues [4]. The insert earphones provide accurate test results in higher ambient noise field, but the results may vary due to improper fitting [3]. Active noise cancellation is an alternative method for noise reduction during audiometry. It reduces the ambient noise level by producing an anti-noise which has spectral components of the same amplitude as the noise but of opposite phase [1]. The anti-noise reduces the unwanted noise by destructive interference in the acoustical enclosure of the ear cup of the headphone.

1.2 Project objective

The objective of this project is to study and develop a noise cancelling headphone (NCH) which can reduce ambient noise during audiometric tests. Active noise cancellation (ANC) can be used to develop NCH to reduce the ambient noise levels and increase the accuracy of measured hearing threshold in noisy environment. NCH can be used along with an audiometer to conduct audiometric tests without the need of an acoustically isolated environment. Conventional ANC can affect the test signal itself due to adaptation. In audiometry, it is required to decrease the noise level over the audiometric frequency range of 125 Hz to 8 kHz without affecting the test signal. Assuming most patients undergoing hearing test have hearing threshold of 50 dB or higher and ambient noise present in a clinic does not exceed 80 dB, the active noise cancellation should provide an attenuation of 40 dB or higher.

Ambient noise is generally broadband and not concentrated at a single frequency. Earlier real-time implementation of the ANC using LMS algorithm showed that noise reduction was not significant for broadband noise [14]. The main objective of the project is to develop a technique which can cancel broadband noise effectively. To reduce the processing delay in realizing an adaptive filter, a fixed FIR filter for broadband noise cancellation needs to be designed.

1.3 Dissertation outline

Chapter 2 provides a review of some of the noise cancelation techniques. Brief information on audiometry and noise canceling headphones for audiometry using the ANC techniques are also presented. In Chapter 3, the proposed method to implement NCH for broadband noise cancellation is described. Results obtained from Matlab based simulation are presented. In the next two chapters, real-time implementation of active noise cancellation using two DSP chips is presented. The last chapter summarizes the work carried out along with some suggestions for future work.

Chapter 2
NOISE CANCELLING TECHNIQUES

Noise cancellation techniques are used to reduce the noise in the listening environment. These techniques are broadly classified into passive noise attenuation (PNA) and active noise cancellation (ANC). PNA can be achieved using passive sound absorbing materials such as foams used in the ear-cups. ANC works on the principle of destructive interference between noise and anti-noise. PNA is effective at high frequencies and ANC can be effectively used at low frequencies as shown in Fig. 2.1 [6]. Broadband noise reduction required by NCH can be achieved by using combination of PNA and ANC.

2.1 Passive noise attenuation

Enclosed headphones have sound absorbing materials which provide good passive attenuation for high frequency disturbances [6]. Construction of a supra-aural headphone, described by Sapiejewski [4] is shown in Fig. 2.2. It consists of a cup-shaped shell made of rigid plastic such as an acrylonitrile butadiene styrene (ABS) plastic and a cushion cover made of high acoustic impedance material such as foam. The shell and the cushion cover together enclose an interior volume. It also consists of a baffle assembly, including a baffle plate mounting and an acoustic driver having a diaphragm. The baffle divides the interior enclosed volume into two parts i.e. the front portion including the passageway and the acoustically open foam and the rear portion. Such an earphone is advantageous for supra-aural headphone, because the earphone can be made relatively small while having the large front enclosed volume for

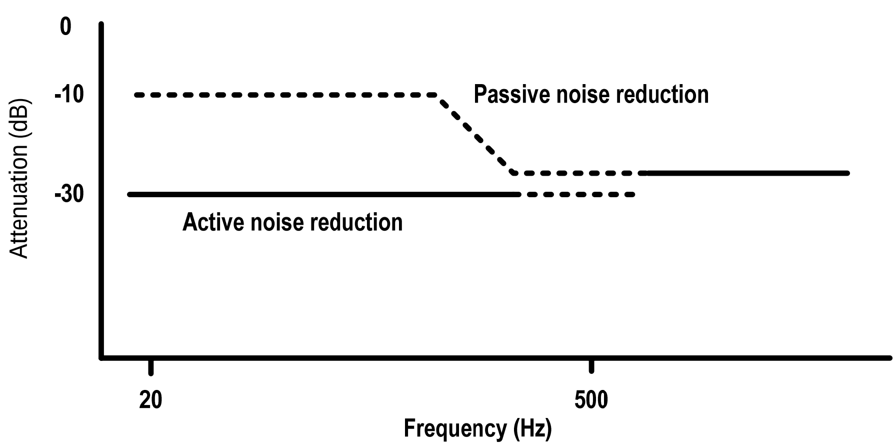

Figure 2.1 Operational range of active and passive noise reduction [6]

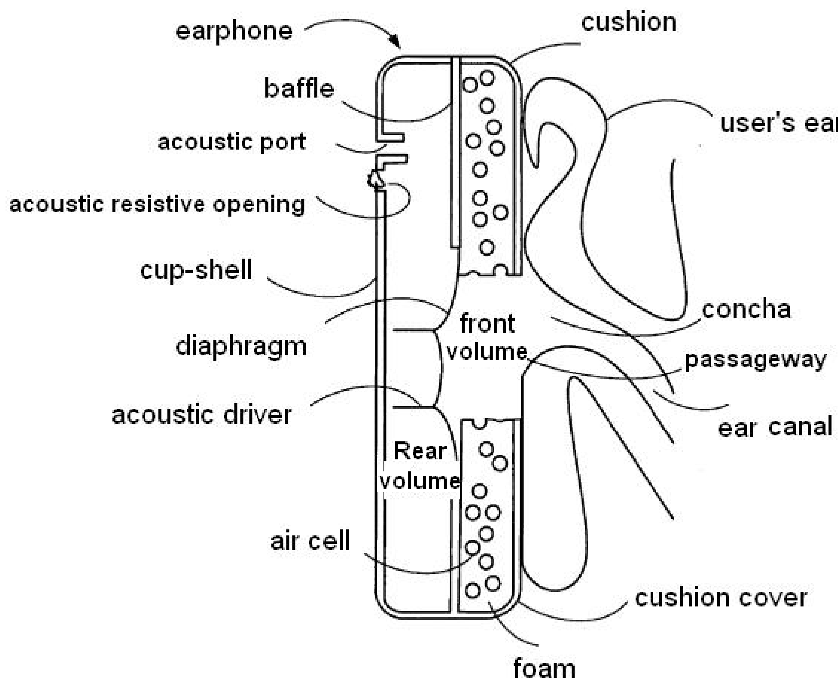

Figure 2.2 Cross section view of an earphone for passive noise attenuation [4]

passive noise attenuation and the large compliant sealing surface.

According to Rafaely and Furst [7], a well-designed closed-ear headphone can passively block high frequency noise down to about 500 Hz by nearly 30 dB, basically acting like a low pass filter. The size and mass of absorbing material required usually depends on the acoustic wavelength to be attenuated, making them bigger and more massive for attenuation of lower frequencies [6]. Thus PNA alone cannot be used for broadband noise cancellation.

2.2 Active noise cancellation

ANC can be carried out using feed-forward control or feedback control. In feed-forward control, a reference noise signal is picked up by reference microphone and processed by ANC system to generate an anti noise. In feedback control, the active noise controller attempts to cancel the noise without using a reference microphone.

2.2.1 Analog feedback ANC

In feedback system, an error sensor is used to measure the output and feedback of this sensed value is used to control the disturbance. Feedback ANC is used for applications in which it is not possible to sense the reference signal coherent with the disturbance. An NCH developed by Bose [8] using analog feedback control for ANC is shown in Fig. 2.3. It consists of an error microphone kept in the ear cup adjacent to the diaphragm to obtain feedback signal. The feedback signal is pre-amplified and combined with the audio signal to be reproduced. The

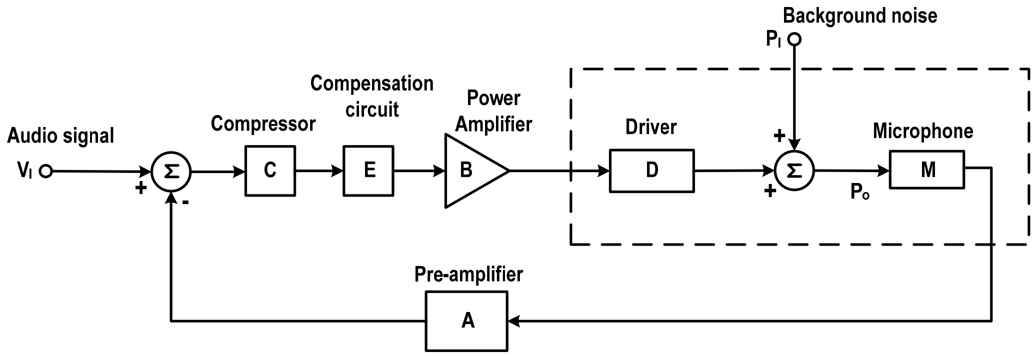

Figure 2.3 Block diagram of analog feedback control ANC system reported in [8]

compressor circuit is used to limit the high level of the combined signal. The compensation circuit ensures Nyquist stability criteria by controlling the open loop gain, so that the system will not oscillate in the closed loop. Power amplifier energizes the headphone driver to produce an acoustic signal in the ear cup cavity which gets acoustically combined with the background noise in the ear cup cavity. A noise reduction of 20 dB was achieved for low frequency noise up to 500 Hz and attenuation decreased with increasing frequency, becoming ineffective for frequencies above 1 kHz.

In analog feedback ANC, the gain is kept very low at higher frequencies to maintain the stability margins for an uncertain headset plant characteristic. Hence the noise reduction is not effective at high frequencies [9]. Thus there is a tradeoff between the performance and stability. Since this is not an adaptive approach, real-time modeling of the ear-cup transfer function cannot be carried out and hence the method cannot be used for high level of noise attenuation [10].

2.2.2 Adaptive feedback ANC

In a feedback system, unlike in a feed-forward system, a reference related to the noise is not available. The reference is regenerated from the error and the adaptive filter output. The adaptive filter is a digital filter in which the coefficients of the filter are updated using least mean square (LMS) algorithm to minimize the error. An adaptive feedback ANC system for headphone applications designed by Kuo *et al.* [11] is shown in Fig 2.4, where $d(n)$ is the primary noise at the error sensor location and $e(n)$ is the residual noise measured by the error sensor. $W(z)$ is adaptive weight vector of the controller and output is denoted as $y(n)$. $S(z)$ is the transfer function of the secondary path from the output of $W(z)$ to the error sensor, and it includes the digital-to-analog converter (DAC), reconstruction filter, power amplifier, loudspeaker, acoustic path from loudspeaker to the error microphone, error

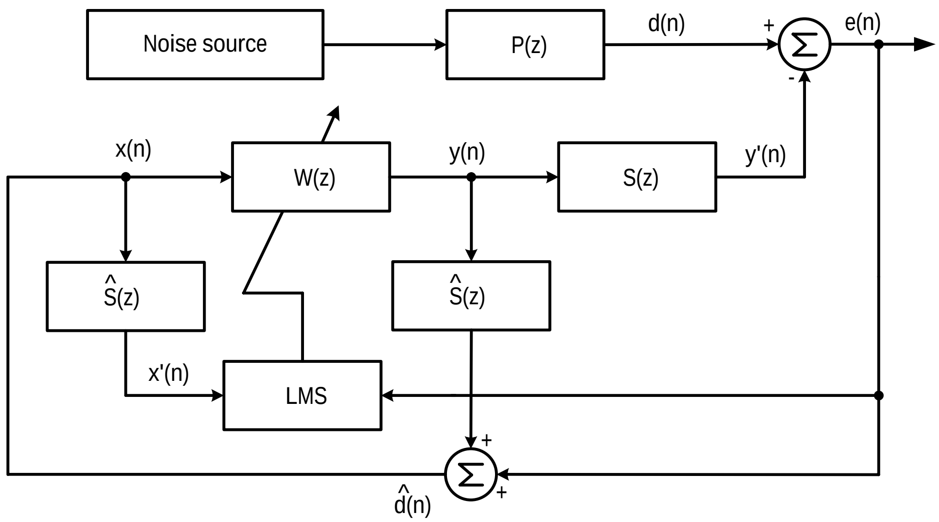

Figure 2.4 Block diagram of feedback ANC system using FxLMS algorithm reported in [11]

microphone, preamplifier, antialiasing filter, and analog-to-digital converter (ADC). The adaptive controller $W(z)$ attempts to minimize the residual error signal $e(n)$ inside the ear cup. The error sensor output is given as

$$E(z) = D(z) - S(z)Y(z) \tag{2.1}$$

$S(z)$ is approximated as $\hat{S}(z)$, and used for estimating $d(n)$ as $\hat{d}(n)$ and used as the synthesized reference signal $x(n)$. Thus

$$X(z) \equiv \hat{D}(z) = E(z) + \hat{S}(z)Y(z) \tag{2.2}$$

The secondary path transfer function $S(z)$ can be estimated using adaptive system modeling techniques using white noise [9]. The algorithm first generates the synthesized reference signal $x(n)$ and updates all the relevant coefficients of the FIR filters $\hat{S}(z)$ and *W(z)* by the filtered-x least mean square (FxLMS) algorithm. For effective cancellation, the error signal should become zero which requires the adaptive filter to converge to the optimum transfer function $W^o(z)$ [11]

$$W^o(z) = \frac{P(z)}{S(z)} \tag{2.3}$$

From above equation, the ANC system is unstable if there is a frequency ω_0 such that $S(\omega_0) = 0$. Therefore, the FXLMS algorithm works properly when the magnitude response of the secondary path is flat. The secondary path magnitude response depends on the error microphone position in the ear cup and hence we need to determine the ideal location inside the ear cup so that flat magnitude response can be achieved. The real-time implementation of ANC headphone was carried out on a DSP board based on 32-bit floating-point processor

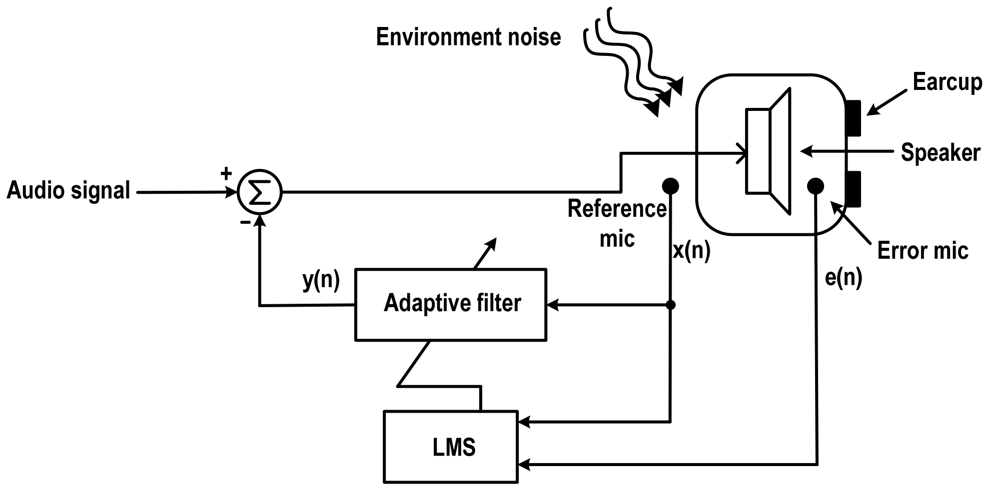

Figure 2.5 Schematic representation of the adaptive feed-forward noise canceling headphone reported in [6]

TMS320C32, 16-bit ADC and DAC on the 4 analog I/O channels. An adaptive filter of order 110 with step size of 0.3 was implemented on the digital signal processor. An attenuation of 50 dB was achieved for tonal noise of frequency up to 2 kHz and attenuation decreased as the noise frequency increased beyond 2 kHz. Digital controllers are subject to computation delay in the processing and additional delay due to the digital to analogue converters (DAC), analog to digital converters (ADC) and the phase delay of the low-pass filters [12]. The control bandwidth and attenuation level get degraded with increased delay. The delay can be reduced by using a very high sampling frequency, but it requires high cost powerful DSP processors [12].

2.2.3 Adaptive feed forward ANC

Adaptive feed forward ANC system uses a reference input coherent with the noise. A block diagram of NCH using feed-forward ANC as reported in [6] is shown in Fig. 2.5. A reference microphone is placed outside the ear cup to pick up the primary noise reference $x(n)$ and it is processed to generate the anti-noise $y(n)$. The anti-noise is added to the audio input and output through the headphone transducer. The error microphone inside the ear cup senses the acoustic signal which is considered as the residual noise $e(n)$. The LMS algorithm changes the filter weight to minimize $e(n)$.

An active noise reducing headset using feed forward ANC designed by Rafaely and Jones [13] is shown in Fig. 2.6. It consists of a headset with a circumaural ear defender, fitted with a loudspeaker and a microphone inside the shell, connected via the analog feedback control circuit. A PC based TMS320C30 DSP card was used to implement the feed-forward

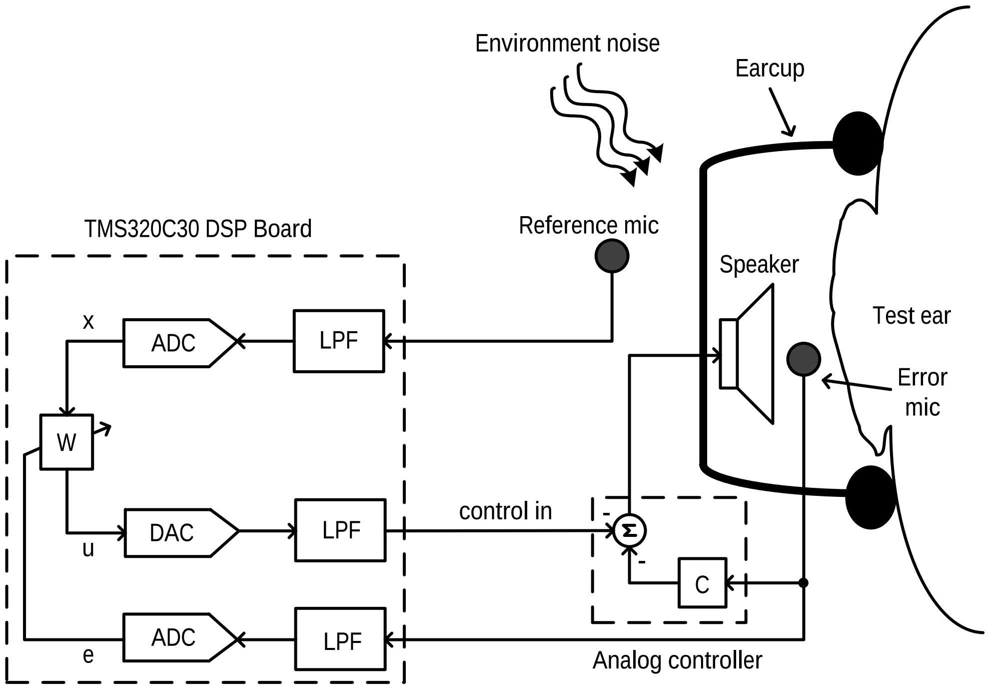

Figure 2.6 Block diagram of combined analog feedback and adaptive feed-forward ANC system reported in [13]

control system. An electret microphone positioned centrally on the outer side of the earshell provides reference input. Output of the microphone is connected to the DSP card via a preamplifier and an 8th-order anti-aliasing lowpass filter. The output of the error microphone was connected to the DSP via a low-pass filter, while the DAC output was connected to the loudspeaker via a low-pass filter and the analog control circuit. A good broadband noise cancellation can be achieved using feed forward ANC due to the primary path delay in reaching of the noise signal from outside microphone to inside microphone [13]. An attenuation of up to 15 dB was achieved by the analog feedback controller at the low frequencies and digital feed-forward controller achieved an attenuation of up to about 13 dB in the reverberant sound filed conditions. The performance will be degraded if there is an acoustic feedback from the cancelling loudspeaker to the reference microphone. The acoustic feedback can be avoided by using adaptive neutralization filter parallel with the feedback path or by using dual-microphone for obtaining reference signal [9].

2.3 Adaptive algorithms

The characteristics of the acoustic noise source and the environment may be time varying and hence we need to modify the noise cancelling filter to adapt to these variations. Adaptive filters adjust their coefficients to minimize the error signal and are realized as a finite impulse

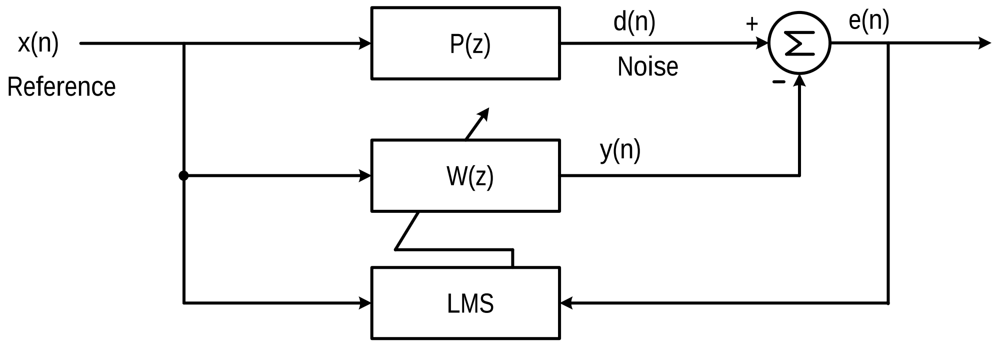

Figure 2.7 Block diagram of adaptive filter [9]

response (FIR) filter. The implementation of ANC is done using adaptive algorithms such as least mean square (LMS), normalized least mean square (NLMS) [9]. Filtered-X least mean square (FxLMS) algorithm is used to model the path transfer function existing between noise canceling speaker and error microphone [9].

2.3.1 LMS algorithm

For ANC applications, it is desired that algorithm should be computationally fast. From this consideration, LMS algorithm is the widely used adaptive algorithm [9]. A block diagram for the ANC system using LMS is shown in Fig. 2.7. In a FIR adaptive filter, the input vector $\mathbf{x}$ and the weight vector $\mathbf{w}$ at the time index n are defined as

$$\mathbf{x} = \left[x(n), x(n-1), x(n-2)....., x(n-M+1)\right]^T \tag{2.4}$$

$$\mathbf{w} = \left[w0, w1, w2....., w(M-1)\right]^T \tag{2.5}$$

where $x(n)$ is the filter input, $w(i)$ is the weight element, and M is the filter length. The filter output is obtained as

$$y(n) = \mathbf{x}^{\mathrm{T}}\mathbf{w} \tag{2.6}$$

The difference between the noise $d(n)$ and the antinoise (filter output) $y(n)$ is the error $e(n)$

$$e(n) = d(n) - y(n) \tag{2.7}$$

In the LMS algorithm, the weight vector w is updated as

$$\mathbf{w}_{\mathrm{n+1}} = \mathbf{w}_{\mathrm{n}} + \mu e(n)\mathbf{x} \tag{2.8}$$

where μ is the step-size parameter in the LMS algorithm. For the stability of the adaptive process and the convergence of the mean square error (MSE), the range of μ is given as

$$0 < \mu < \frac{2}{\mathrm{trace}[\mathbf{R}]} \tag{2.9}$$

where $\text{trace}[\mathbf{R}]$ is the trace of the input vector's autocorrelation matrix $\mathbf{R}$, given by

$$\text{trace}[\mathbf{R}] = E[\mathbf{x}^{\mathrm{T}}\mathbf{x}] \tag{2.10}$$

A large step size results in fast convergence, but mean square error after convergence, may not be small because the adapted filter may be far from an optimum filter. A small step size results in slow convergence but generally in a small error. Hence in systems with slow changes in the transmission path and requirement for low error, we should use a small step size [9].

2.3.2 Normalized least mean square (NLMS) algorithm

The normalized LMS (NLMS) [9] is known to give better convergence characteristics than the LMS, because it uses a variable step size parameter. The step size parameter is divided by the input power at every iteration. The stability of the basic NLMS is controlled by a fixed step-size constant μ, which also controls the rate of convergence, and the amount of steady-state excess mean-square error (MSE). In the NLMS algorithm, the step size parameter is given by

$$\mu_{NLMS} = \frac{\alpha}{\gamma + \mathbf{x}^{\mathrm{T}}\mathbf{x}} \tag{2.11}$$

where $\mathbf{x}^{\mathrm{T}}\mathbf{x}$ is the input vector power, and γ is a factor to avoid division by zero, and serves as a stabilization parameter. In (2.11), $\mathbf{x}^{\mathrm{T}}\mathbf{x}$ can be taken as the approximation of $\text{trace}[\mathbf{R}]$. For stable convergence in NLMS, α should be in the range of 0 to 2. The NLMS algorithm is convergent and gives better convergence characteristics than the LMS algorithm, as it can reduce the increase of the noise by dividing the step size parameter by the input vector power [9].

2.3.4 Filtered-X least mean square (FxLMS) algorithm

In the LMS algorithm for ANC system, it is assumed that the output of the adaptive filter $y(n)$ is the antinoise reaching the error microphone, In practice, the presence of the smoothing filter, power amplifier, microphone transfer function, anti-aliasing filter, and A/D converter in the path from the output of the FIR filter to the signal received as the error $e(n)$ at the input of LMS algorithm cause significant changes. There effect can be modeled as the transfer function of the secondary path $S(z)$ and it becomes necessary to compensate for its effect. One solution is to place an identical filter in the reference path for the weight updating by the LMS algorithm. This method is known as filtered-X LMS (FxLMS) algorithm, as shown in Fig. 2.8. This filter output or the secondary $y(n)$ is filtered through the secondary path $S(z)$ and combines with the primary noise to generate the residual noise $e(n)$. These

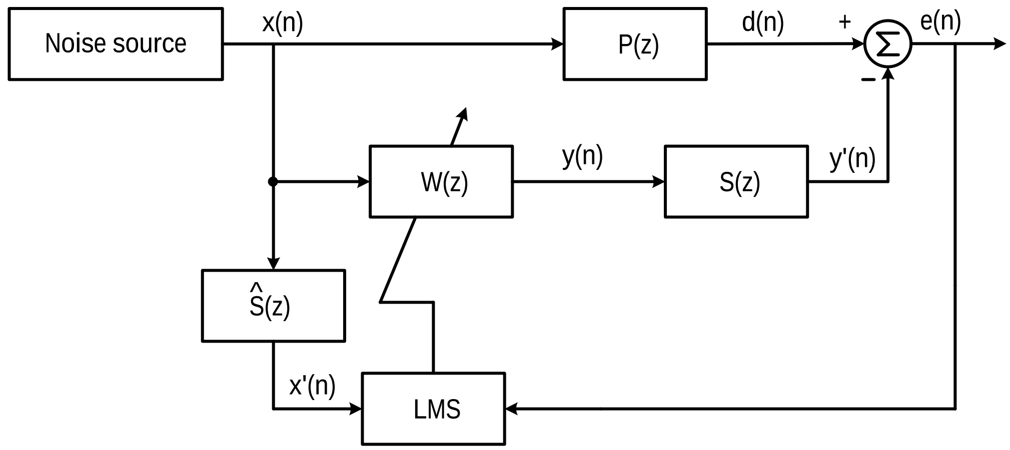

Figure 2.8 Block diagram of FxLMS algorithm for ANC [9]

operations can be expressed as

$$y'(n) = s(n) * y(n) \tag{2.12}$$

$$d(n) = p(n) * x(n) \tag{2.13}$$

$$e(n) = d(n) - y'(n) \tag{2.14}$$

where $P(z)$ is the transfer function of the primary path of the transmission of external noise $x(n)$ to the error microphone. The Fx-LMS update equation for the coefficients of $\mathbf{w}_{\mathrm{n}}$ is given as

$$\mathbf{w}_{\mathrm{n+1}} = \mathbf{w}_{\mathrm{n}} + \mu e(n)\mathbf{x}' \tag{2.15}$$

where μ is the step size and $\mathbf{x}$ is the reference vector after filtering of $\mathbf{x}$ through the secondary path model $\hat{S}(z)$.

2.4 Audiometry

Audiometry is a technique to quantify hearing sensitivity of a person. It helps in assessing the causes of the hearing impairment, so that suitable medical treatment or use of an assistive device can be prescribed. It involves presentation of systematically varying acoustic stimuli to the subject and recording the responses. The minimum intensity level to which consistent responses are obtained is taken as threshold of hearing. In audio-logical investigations, the hearing sensitivity can be tested by pure tones, speech, or other sound stimuli [2]. The electronic instrument used for measuring the hearing threshold level is called an audiometer. In pure tone audiometry, test tones of different frequencies and levels are presented and hearing thresholds are determined on the basis of patient's response. The test tones at various frequencies (125, 250, 500, 750, 1000, 1500, 2000, 3000, 4000, 6000, 8000 Hz) are presented.

The pure tone audiometer consists of an oscillator to generate pure tone sounds of various frequencies. The presentation level can be varied over 0- 110 dB HL, in steps of 5 dB [2].

To diagnose the hearing defects, a test stimulus is presented to the human ear for a short duration with long pauses. The level is varied and the threshold obtained is determined by observing the patient's responses to the presentations. In normal rooms, the ambient noise level may be high and it may affect the measured hearing thresholds [7]. Hence audiometry is generally performed in a soundproof area where the level of the ambient noise is much lower than that of the test stimulus, so that it may not cause a threshold shift. Conventional headphones provide passive attenuation of 30-40 dB, beyond that sound will be heard due to bone conduction and the reduction of noise is not uniform over the audible frequency range. Hence these headphones cannot be used without acoustically isolated rooms [7]. NCH reduces the noise to a further level using active noise canceling techniques along with PNA. The noise attenuation using an NCH may be useful in conducting audiometric tests even in normal rooms [14].

2.5 Audiometric NCH techniques

Audiometric NCH can be designed using any one of the ANC techniques described in Section2.2. Vaudrey and Saunders [5] have proposed the use of analog feedback, digital feedback, adaptive feed-forward, and adaptive feedback methods to reduce the ambient noise in adaptive feed-forward, and adaptive feedback methods to reduce the ambient noise in audiometry testing environment without affecting the test stimulus. In the patent description, various audiometric noise cancelling methods were proposed by Vaudrey and Saunders [5]. However, the real-time implementation details and the experimental results were not provided.

2.5.1 Audiometric NCH using analog and digital feedback ANC

An analog feedback control system for noise reduction in audiometry proposed by Vaudrey and Saunders [5] is shown in Fig. 2.9. An error microphone is kept inside the ear cup to sense the error signal. The error signal is amplified and applied to the speaker along with the test signal. The closed loop transfer function is a function of frequency. The error signal with the negative feedback is given as

$$E(s) = \frac{G(s)}{1+G(s)H(s)}P(s)S(s) + \frac{1}{1+G(s)H(s)}D(s) \tag{2.16}$$

where *H(s)* represents analog controller implemented using analog electronics and *G(s)* is a combination of amplifier, speaker and cavity transfer functions. For very large *H(s)*, the contribution of the acoustic noise $D(s)$ to the error signal is decreased [5]. The effect of the

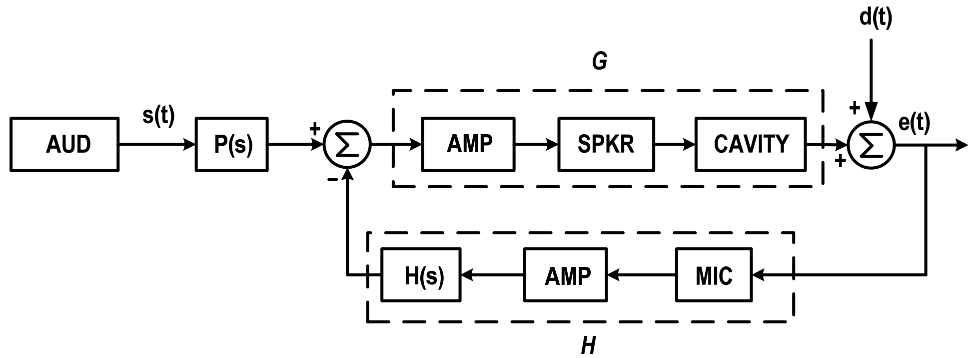

Figure 2.9 Audiometric NCH using analog feedback methods as reported in [5]

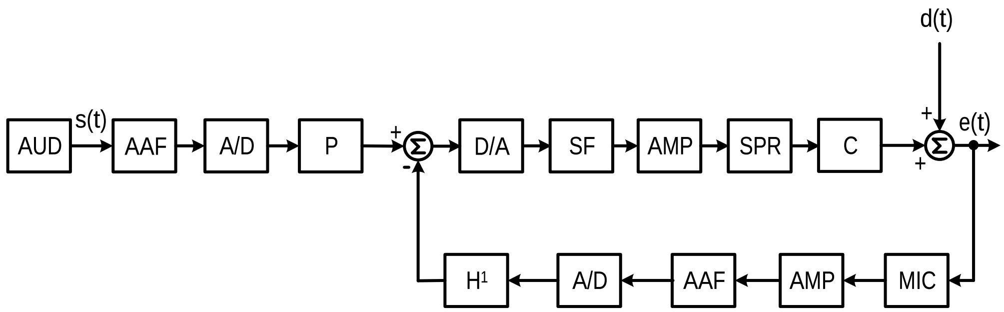

Figure 2.10 Audiometric NCH using digital feedback method as reported in [5]

control loop can be minimized on the test stimulus if the compensation filter $P(s)$ is having given by

$$P(s) = \frac{1 + G(s)H(s)}{G(s)} \tag{2.17}$$

The NCH using digital feedback proposed by Vaudrey and Saunders [5] is shown in Fig. 2.10, where $H^1$and P can be implemented using FIR or IIR filters. Digital feedback control includes additional hardware such as anti-aliasing and smoothing low pass. The performance of the feedback method is not uniform over entire audiometric frequency range due to stability constraint [5].

2.5.2 Audiometric NCH using feedback ANC with separate actuators

In order to avoid the effect of feedback on the test signal without using compensator *P*, Vaudrey and Saunders [5] proposed a new method using two actuators, one for noise control and one for test stimulus. The block diagram of the system is shown in Fig. 2.11. The insert earphone generates test stimulus and a separate actuator generates the active noise control signal. The control signal is generated using feedback ANC method. The error signal at the

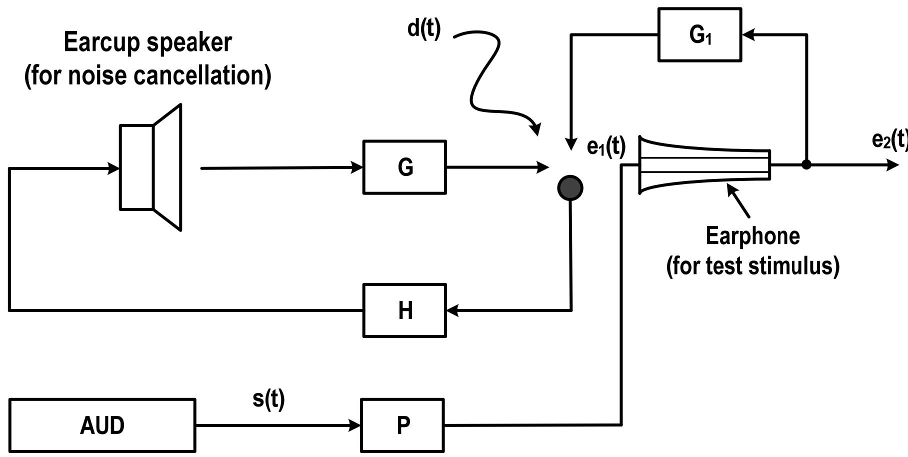

Figure 2.11 Audiometric NCH using feedback ANC with separate actuators as reported in [5]

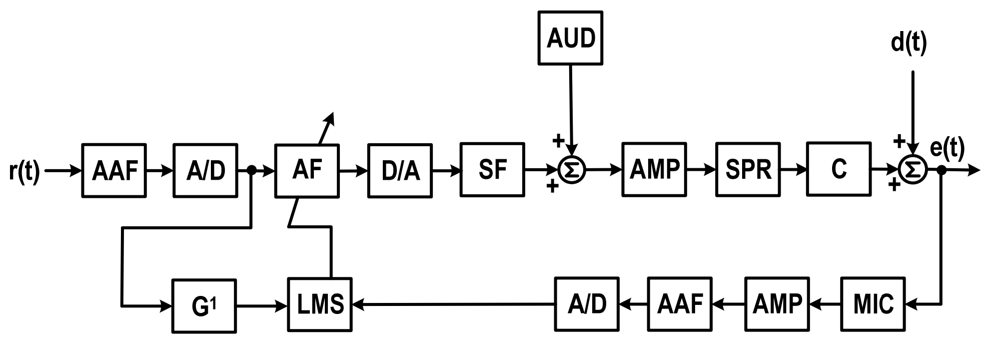

Figure 2.12 Audiometric NCH using adaptive feed-forward method as reported in [5]

eardrum is given by,

$$E_2(s) = \frac{1+G(s)H(s)}{1+G(s)H(s)+G_1(s)}P(s)S(s) + \frac{1}{1+G(s)H(s)+G_1(s)}D(s) \qquad (2.18)$$

where $G_1(s)$ is the gain of the feedback path from test signal to residual noise. From the above equation, if $G_1(s)$ is very small and open loop gain $G(s)H(s)$ is very high then the error signal becomes the product of test stimulus and the gain of the filter $P(s)$ [5]. Major advantage in using two actuators is that now compensation filter $P(s)$ is not needed, as the error signal consists of test stimulus only if $G_1(s)$ is small [5].

2.5.3 Audiometric NCH using adaptive feed forward ANC

The adaptive feed-forward ANC control system proposed by Vaudrey and Saunders [5] is shown in Fig. 2.12. Feed-forward ANC is a method of canceling noise by using a reference input coherent with noise. The reference noise outside the ear cup is obtained using reference

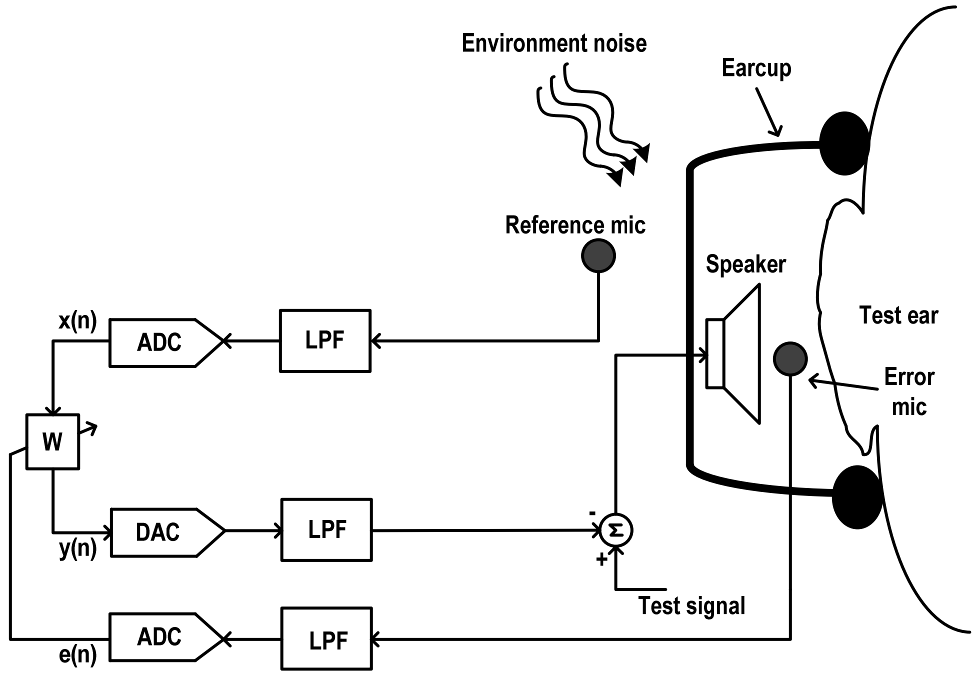

Figure 2.13 Audiometric earphone using adaptive feed-forward method as reported in [7]

microphone and error signal inside the ear cup is obtained using an error microphone. The adaptive FIR filter coefficients are modified based on error signal using LMS algorithm. Anti-noise generated by the adaptive filter using reference signal is added to the test stimuli and input to the ear-cup speaker. Inside the ear-cup, acoustic superposition of the anti-noise with the transmitted noise results in cancellation of ambient noise and thus only test signal presented in the ear-cup remains. In Fig. 2.12, $G^1(s)$ is the secondary path compensating filter. This method is effective for reducing tonal noises since the correlation between reference and error signal is highest for sinusoidal waveforms [5].

Rafaely and Furst [7] designed a NCH with active noise cancellation using feed-forward method. The block diagram of the earphone is shown in Fig 2.13. It consists of reference microphone, error microphone, and speaker in the plugged ear canal connected via low pass filters (LPF), analog-to-digital converters (ADC), digital-to-analog converters (DAC) to the digital controller $W(z)$. The ambient noise produced is attenuated inside the ear canal to form a zone of silence. An attenuation of 30 dB was achieved for noise of tone 500 Hz. Rafaely concluded that the proposed system was not practical for broadband noise attenuation as the earphone's error path group delay consisting of electronics and transducer was about 3 ms which was much longer than the primary path group delay of 100 μs. Thus broadband noise attenuation can be achieved by reducing the group delay of error path by using improved transducers, high sampling frequency and a powerful processor.

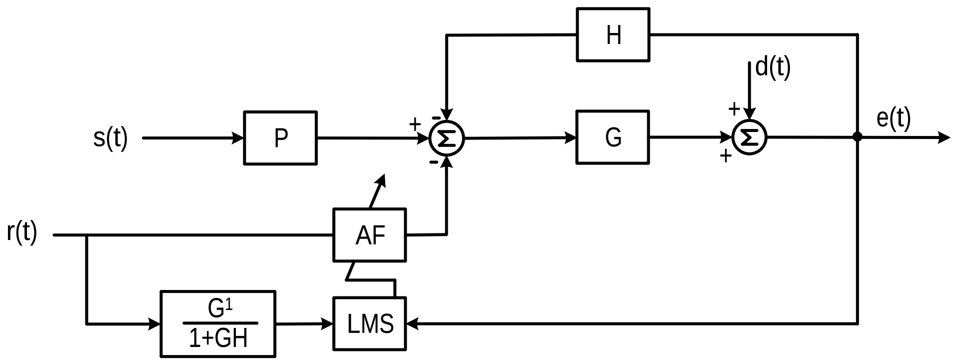

Figure 2.14 Audiometric NCH using hybrid methods as reported in [5]

2.5.4 Audiometric NCH using Hybrid ANC

A combination of feedback and feed-forward control for NCH in audiometry proposed by Vaudrey and Saunders [5] is shown in Fig. 2.14. The feedback control is analog implementation and the feed-forward controller is digital implementation. As mentioned earlier, the feedback control affects the test stimulus and the compensation has to be made through a filter *P*. The feedback control tends to perform better for broadband noise fields while feed-forward control performs better for tonal noise fields and thus combination provides good broadband noise cancellation [5].

2.5.5 Audiometric NCH using stimulus controlled adaptive feed-forward ANC

The adaptive feedback and feed-forward methods are based on continuous adaptation of the filter coefficients with respect to the error response in the ear-cup. The test stimulus is generally much larger than the ambient noise and it gets affected by continuous adaption of filter coefficients, as the error signal also contains the test signal. Narahari [14] proposed a modified adaptive feed-forward method in which the filter coefficients were continuously adapted when the stimulus was not being presented and the adaptation was suspended during the stimulus presentation. This will reduce the noise without affecting the test signal because the test stimuli in audiometry are presented for short durations with relatively long inter-stimulus pauses. The ANC feed-forward method for audiometry proposed by Narahari [14] is shown in Fig. 2.15. Two microphones are used in this method. The error signal inside the ear-cup is picked up by the error microphone and the reference signal sensed by the reference microphone is input to adaptive filter. The LMS algorithm is used to adjust the coefficients of the adaptive filter for minimizing the mean square error. The anti-noise generated by adaptive filter and test stimulus signal is output to the headphone transducer. Audiometer gives an “adapt/pause” control to the LMS algorithm and adaptation in paused during the stimulus presentation. Since the stimulus does not contribute to the adaptation, it

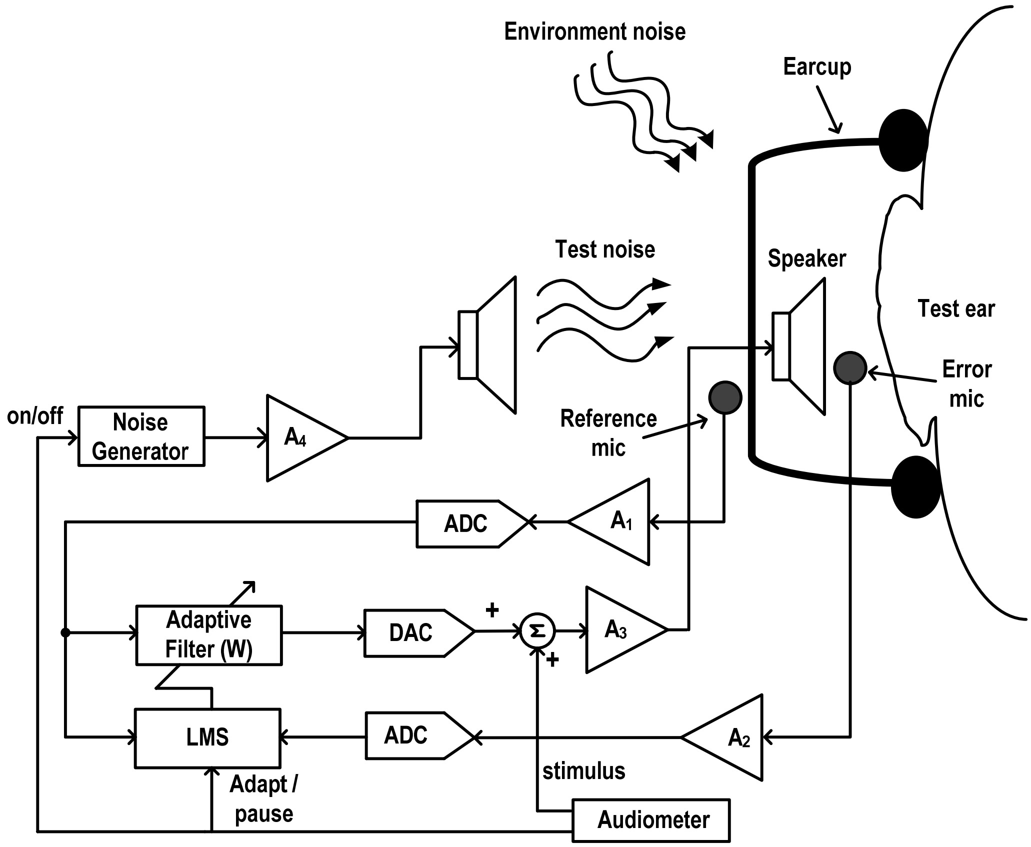

Figure 2.15 Block diagram of adaptive feed-forward system as proposed in [14]

was not affected by adaptation. Real-time implementation of ANC was carried out using ADSP BF33 (16-bit, fixed point processor from Analog devices) based DSP board Blackfin 533 EZ Kit Lite. LMS and FXLMS algorithms were implemented. Adaptive filter of order 48 was used with the sampling frequency of 48 kHz. Noise reduction of about 25 dB was achieved for tone swept over 200 Hz to 1.5 kHz. Broadband noise cancellation could not be achieved as the error path group delay of 1.5 ms was much longer than the primary path group delay (estimated as 100 μs). It was concluded that broadband noise cancellation can be achieved by reducing the error path group delay, by using DSP processor with high sampling rate and processing speed. It was also concluded that the filter order needed to be increased.

Chapter 3
THE PROPOSED NCH METHOD

Ambient noise in audiometry clinics is broadband and generally not concentrated at a single frequency. An earlier study [14] has shown that real-time implementation of LMS-based adaptive filter for broad-band noise cancellation is not practical. Hence a method is proposed to use a fixed high order FIR filter for broad-band noise cancellation. An LMS based adaptation is used to obtain the magnitude and phase response of the required broadband filter by using a swept sine wave as the noise source. Subsequently this magnitude and phase response is used to realize the fixed FIR filter for cancellation of broad-band noise. Simulation of the broad-band noise cancellation is carried out using Matlab. Simulation of the noise cancellation for various noises and their results are discussed in the subsequent sections.

3.1 Proposed NCH method for audiometry

In a modified adaptive feed forward method proposed by Narahari [14], the filter coefficients were continuously adapted during the inter-stimulus silence duration and the adaptation was suspended during the presentation of the stimululus in the ear-cup. The objective was to avoid any effect of ANC on the stimulus. The method was found to be effective in cancellation of the tonal noise, but ineffective in cancelling the broadband noise. The error path group delay (delay in ADC, DAC, anti-aliasing filter, reconstruction filter, FIR filter) of about 1.5 ms was much longer than the primary path group delay (delay in the path of the noise from outside microphone to inside microphone) of 100 μs. It was concluded that broadband noise cancellation can be achieved by reducing the error path group delay using DSP processor with high sampling rate and processing speed. It was also concluded that broadband noise cancellation will be effective if higher filter order is used.

When the error path delay was longer than the primary path delay, the noise cancelling system becomes non-causal for broadband noise. However active noise cancellation was effective for tones of all frequencies as the LMS based adaptation was able to track the sinusoidal tones by matching the phase shift. Hence we can obtain the magnitude and phase response of the noise cancelling filter for all the tonal frequencies. If the relative position of the reference microphone and error microphone is fixed then a fixed FIR filter can be used for broadband noise cancellation. In the proposed method, a fixed FIR filter for broadband noise cancellation is designed using the frequency sampling method, whose magnitude and phase response for entire frequency range is obtained by use of adaptive filter

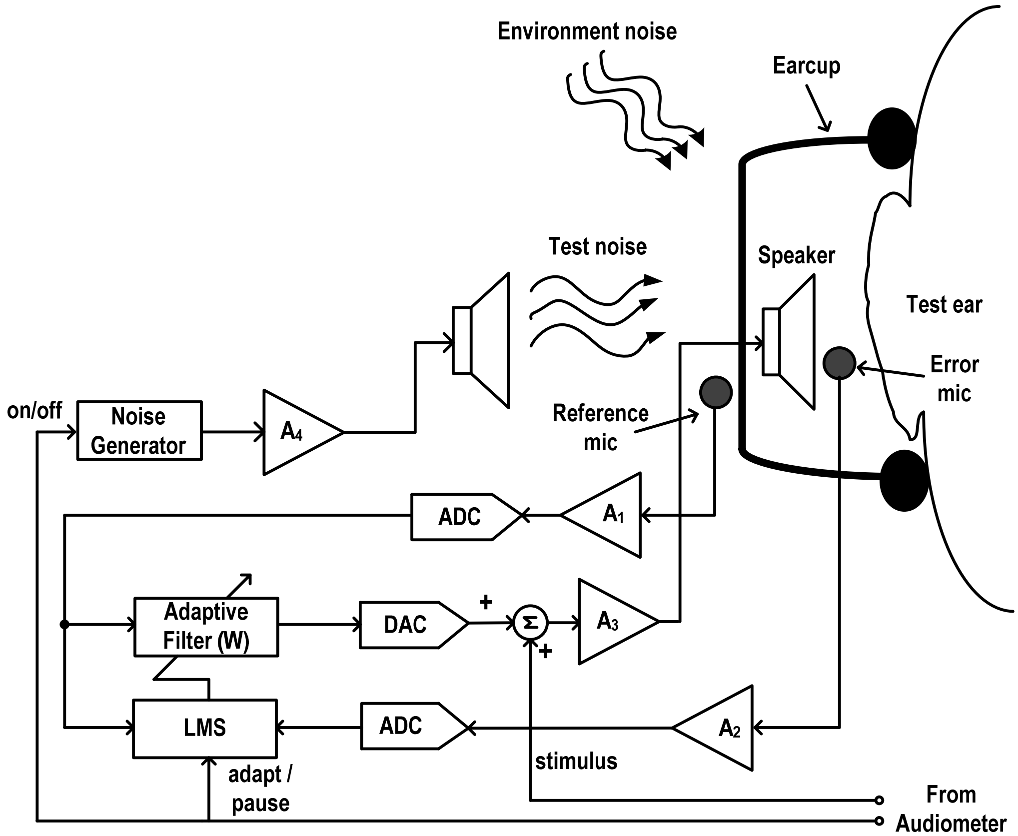

Figure 3.1 Setup of the proposed NCH

for cancellation of a swept sine wave as a noise source. The NCH setup used to obtain the frequency response of the FIR filter is shown in Fig. 3.1. It uses two microphones, one for reference noise and the other for error sensor. LMS based adaptive feed-forward method is used for active noise cancellation. The outputs of the reference microphone and the error microphone are used to adjust the adaptive filter using LMS algorithm. The noise inside the ear-cup is picked by the error microphone and is given as input to the adaptive filter. An LMS algorithm adjusts the filter coefficients to reduce the mean square error. No stimulus signal is presented to the headphone. A sinusoidal signal is used as the ambient noise. Once the adaptation is complete, magnitude and phase response of the adapted filter for the corresponding frequency of the tonal noise are obtained from the filter coefficients. The process is followed to obtain the magnitude and phase at different frequencies by varying, in discrete steps, the frequency of the sinusoidal tone presented as the ambient noise. Thus we get a sampled version of the frequency response over the frequency band of interest. An FIR filter for broad-band noise cancellation is obtained using frequency sampling method. After adaptation is completed, the adapted FIR filter is used for broad-band noise cancellation. The error sensing microphone may be used for monitoring the noise cancellation. The adaptive

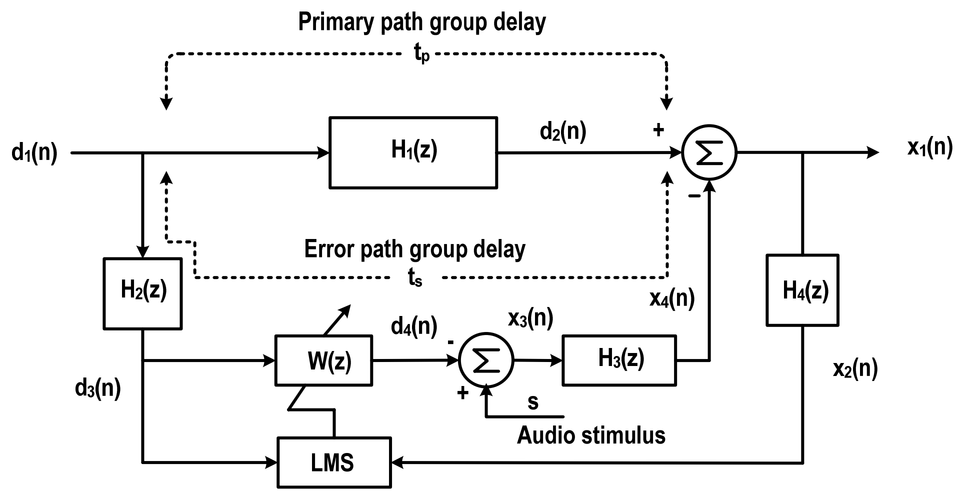

Figure 3.2 Signal flow diagram of NCH

process by sweeping the frequency of the external noise source is completed everytime a patient puts on the headphone for audiometric test. Once the coefficients of the adapted FIR filter have been found, the filter is then onwards used as the noise cancelling headphone. In case the headphone is adjusted, the adaptation may need to be carried out once again.

3.2 Simulation and results

Initially the non-causal behavior of the noise cancelling system for broadband noise cancellation as reported earlier by Narahari [14] was simulated. Next simulation of the noise cancellation using the proposed method was carried out. In order to obtain the magnitude and phase response of the FIR filter for broadband noise cancellation, the LMS algorithm for sinusoidal signals of frequency varied in discrete steps was simulated. Further, this fixed FIR filter was used to cancel different broadband noises. Results are plotted and analyzed in the subsequent sections for various noises. All simulations were carried out using Matlab.

3.2.1 Non-causal behavior of ANC for broadband noise

A model of the noise cancellation system during adaptation is shown in Fig. 3.2. A test noise $d_1(n)$ is picked by reference microphone. The reference microphone output $d_3(n)$ is input to the adaptive filter. Reference noise transmits through the headphone modeled by transfer function $H_1(z)$. Residual noise is picked by the error microphone. The LMS algorithm is used to update the coefficients vector $\mathbf{w}_n$ of the adaptive filter so as to minimize the mean square error. Anti-noise $d_4(n)$ produced by the adaptive filter is added to the transmitted noise to simulate acoustic superposition. The transfer functions of the microphones and speaker are assumed to be unity for simulation. The test stimulus was assumed to be zero during the adaptation process. Simulation equations in z-domain are,

$$D_3(z) = D_1(z) \tag{3.1}$$

$$D_2(z) = D_1(z)H_1(z) \tag{3.2}$$

$$D_4(z) = D_3(z)W(z) \tag{3.3}$$

$$X_2(z) = X_1(z) \tag{3.4}$$

$$X_3(z) = S(z) - D_4(z) \tag{3.5}$$

$$X_4(z) = X_3(z) \tag{3.6}$$

$$X_1(z) = X_4(z) + D_2(z) \tag{3.7}$$

Sampling frequency of 24 kHz, step-size of 0.0005 and filter order of 400 is used in the simulation. The step size for LMS adaptation was set to 0.1/[signal power x filter order]. The plant transfer function $H_1(z)$ is assumed to be 2nd order Butterworth low pass filter with cutoff frequency of 500 Hz cascaded with a primary delay. $H_3(z)$ represents the secondary path transfer function cascaded with secondary path delay. The primary path delay t_p and secondary path delay t_s measured from TMS320C5515 processor based NCH setup, as described later in chapter 4, were 375 µs and 1.875 ms respectively.

In order to observe the effect of ANC on broadband noise, simulation was carried out with white Gaussian noise as ambient noise. Initially simulation was carried out with secondary path delay assumed to be zero which is less than primary path group delay. The waveforms for the noise inside the ear-cup, with and without ANC for zero secondary path delay, are shown in Fig. 3.3. The power spectral density with ANC was lower than -60 dB. Thus it is observed that the white Gaussian noise is cancelled effectively. Similarly the simulation was carried out for white Gaussian noise with secondary path delay set as1.875 ms. The waveforms and power spectral density for the noise inside the ear-cup, with and without ANC are shown in Fig. 3.3. It can be observed that broadband noise cancellation is ineffective if the secondary path delay is longer than the primary path delay.

3.2.2 Estimation of filter coefficients for broadband noise cancellation

Active noise cancellation for tonal noise of different frequencies was simulated using same simulation parameters as described in section 3.2.1. The waveforms and power spectral density for the sinusoidal signal of frequency 1 kHz as noise inside the ear-cup, with and without ANC are shown in Fig. 3.4. In Fig. 3.4, power spectral density for the noise inside the ear cup with ANC is below -60 dB. It can be seen that noise cancellation is effective for tonal signal of 1 kHz. It was also observed that ANC is effective for all the tonal frequencies even

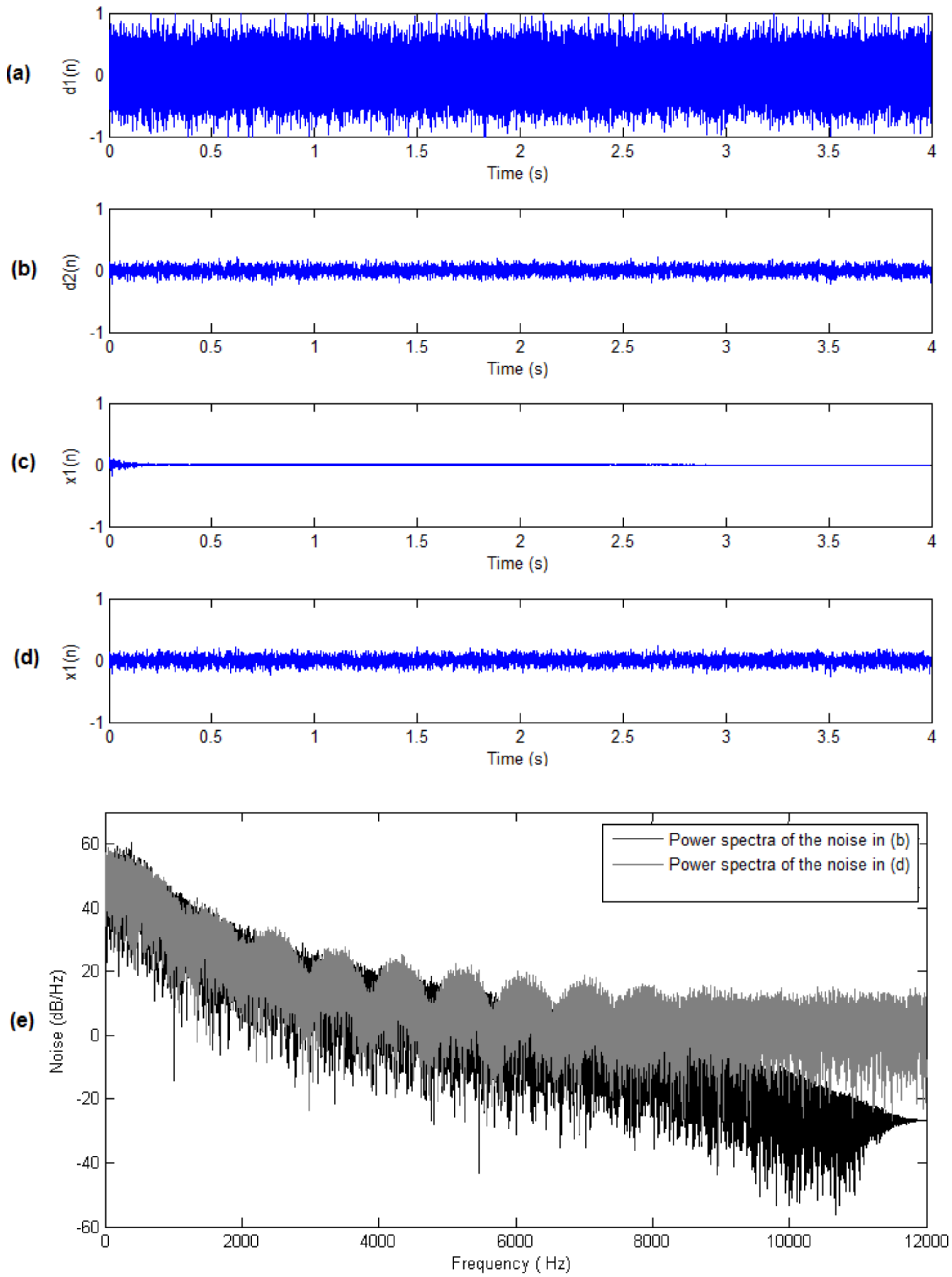

Figure 3.3. Example of noise cancellation by setup in Fig. 3.2 for white Gaussian noise: (a) noise outside the ear cup (output of the reference mic.); (b) noise transmitted to the inside of the ear cup(output of the error mic. without ANC); (c) noise inside the ear cup with ANC, t_p = 375 µs, t_s = 0 s; (d) noise inside the ear cup with ANC, t_p = 375 µs, t_s = 1.875 ms; (e) Power spectra of the noise in (b) and (d).

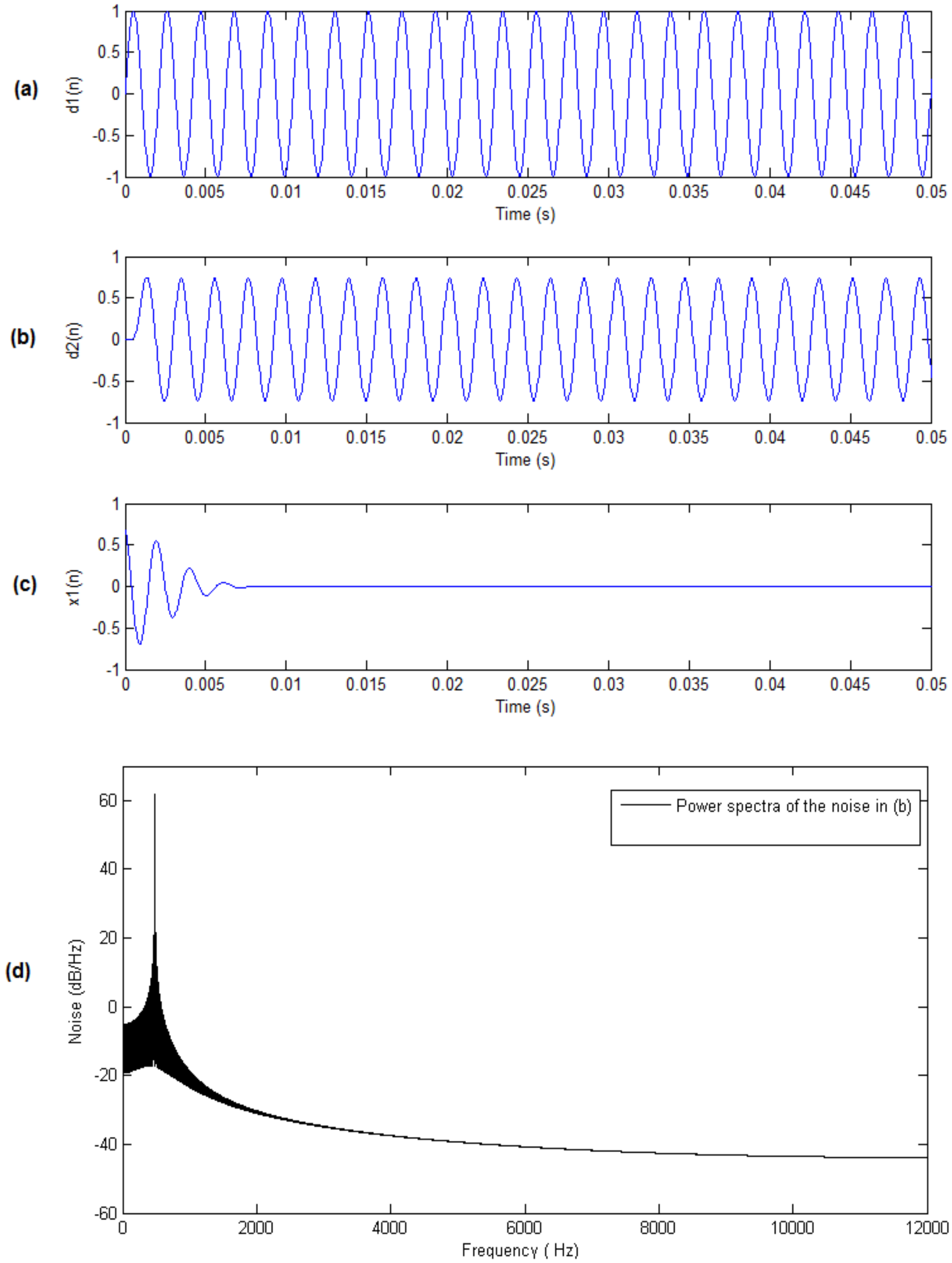

Figure 3.4. Example of noise cancellation by the setup in Fig. 3.2 for tone of 1 kHz noise: (a) noise outside the ear cup (output of the reference mic.); (b) noise transmitted to the inside of the ear cup (output of the error mic. without ANC); (c) noise inside the ear cup with ANC, t_p = 375 µs, t_s = 1.875 ms; (d) Power spectra of the noise in (b) and (c).

though the secondary path delay was much longer than the primary path delay. The simulation was carried out for sinusoidal signals of frequencies from 0-12 kHz in steps of 10 Hz. The magnitude and phase response of the adapted filter are obtained at each tonal frequency. This resulted in the frequency response uniformly sampled at 2400 points, with frequency samples given at,

$$\omega_k = \frac{2\pi}{2400}k \qquad k = 0, 1, 2, \ldots\ldots, 1200 \tag{3.8}$$

The frequency response [22] is described as,

$$H(k) = H_d(\omega)\Big|_{\omega=\omega_k} \qquad k = 0, 1, 2, \ldots\ldots, 1200 \tag{3.9}$$

$$H(k) = H^*(2400-k) \qquad k = 1201, 1202, \ldots\ldots, 2399 \tag{3.10}$$

The response $H(k)$ thus obtained is considered as the 2400-point discrete Fourier transform (DFT) of the impulse response of the desired noise cancelling filter. The impulse response is obtained by taking the inverse Fourier transforms of $H(k)$ as

$$h(n) = \frac{1}{2400}\sum_{k=0}^{2400} H(k) e^{j2\pi kn/2400} \qquad n = 0, 1, 2, \ldots\ldots, 2399 \tag{3.11}$$

The impulse response is used for realizing the FIR filter. It may be noted that as the filter is obtained by IDFT, the impulse response may have errors due to aliasing and iterative design methods may be needed.

3.2.3 Results for various noises

The fixed FIR filter for broadband noise cancellation designed as described above is used to cancel various broadband noises such as music, white Gaussian noise, air-conditioner noise, helicopter noise and train noise. Sampling frequency of 24 kHz and fixed FIR filter order of 2400 are used in the simulation. The plant transfer function $H_1(z)$ was assumed to be 2nd order Butterworth low pass filter with cutoff frequency of 500 Hz cascaded with primary path delay. The LMS adaptation used filter order of 400 and step-size of 0.0005 with noise power of 0.5.

The waveforms for the various noises are shown in the Fig. 3.5 - 3.9. Plots of power spectral density of the noise inside the ear-cup, with and without ANC are also shown. From Fig. 3.10, it can be observed that the test stimulus is not affected by music. In order to check the effect of the fixed FIR filter on the test stimulus, a tone of 240 Hz was used as the ambient noise. It can be observed from Fig. 3.11 that the test stimulus of 500 Hz tone was not affected by the tonal noise of 240 Hz tone. Table 3.2 shows the average noise reduction for the various broadband noises and it is observed that the designed fixed FIR filter is effective for broadband noise cancellation.

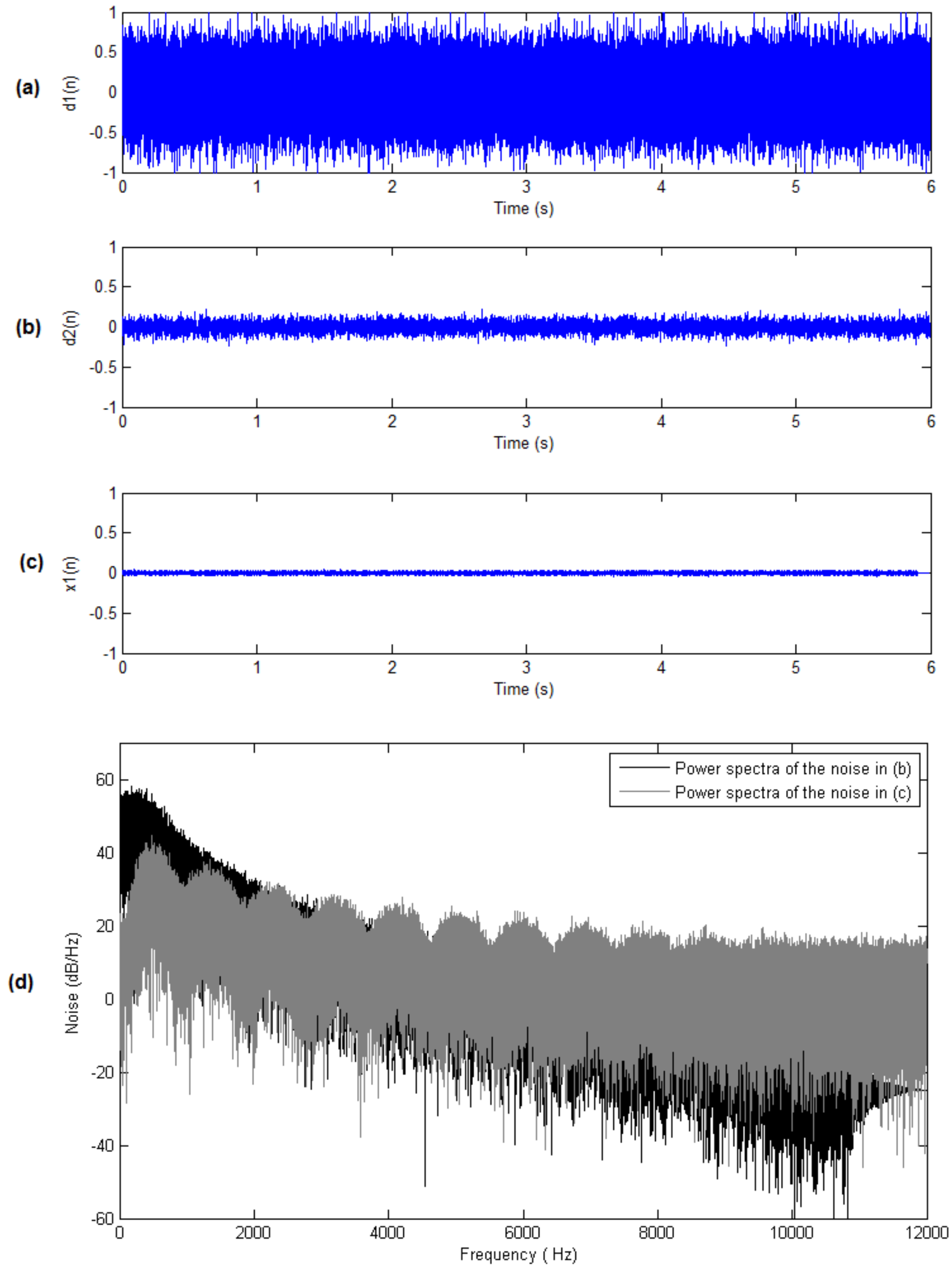

Figure 3.5. ANC using fixed FIR filter for white Gaussian noise with t_p = 375 μs, t_s = 1.875 ms: (a) noise outside the ear cup (output of the reference mic.); (b) noise transmitted to the inside of the ear cup (output of the error mic. without ANC); (c) noise inside the ear cup with ANC; (d) Power spectra of the noise in (b) and (c).

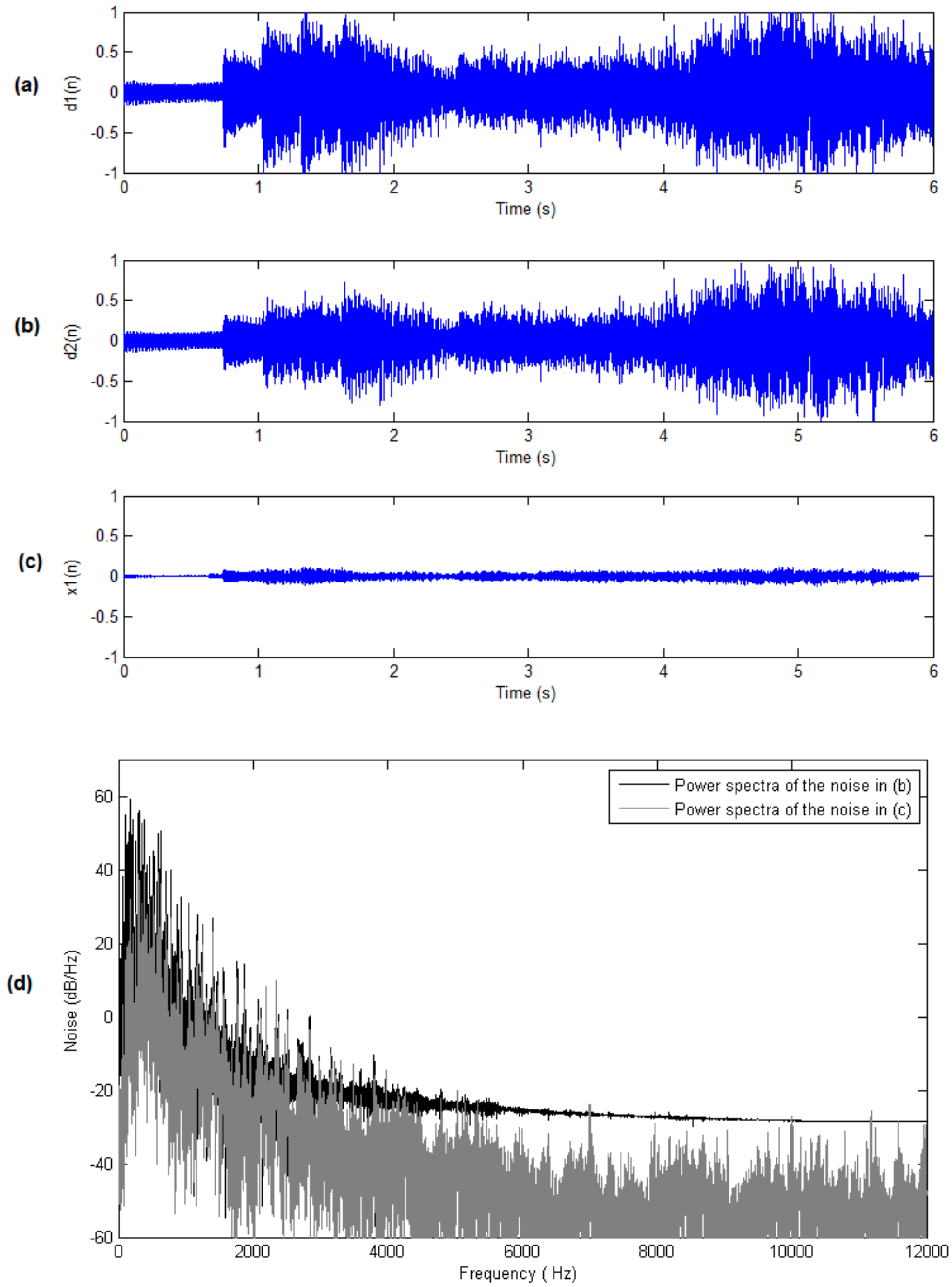

Figure 3.6. ANC using fixed FIR filter for music with t_p = 375 μs, t_s = 1.875 ms: (a) noise outside the ear cup (output of the reference mic.); (b) noise transmitted to the inside of the ear cup (output of the error mic. without ANC); (c) noise inside the ear cup with ANC; (d) Power spectra of the noise in (b) and (c).

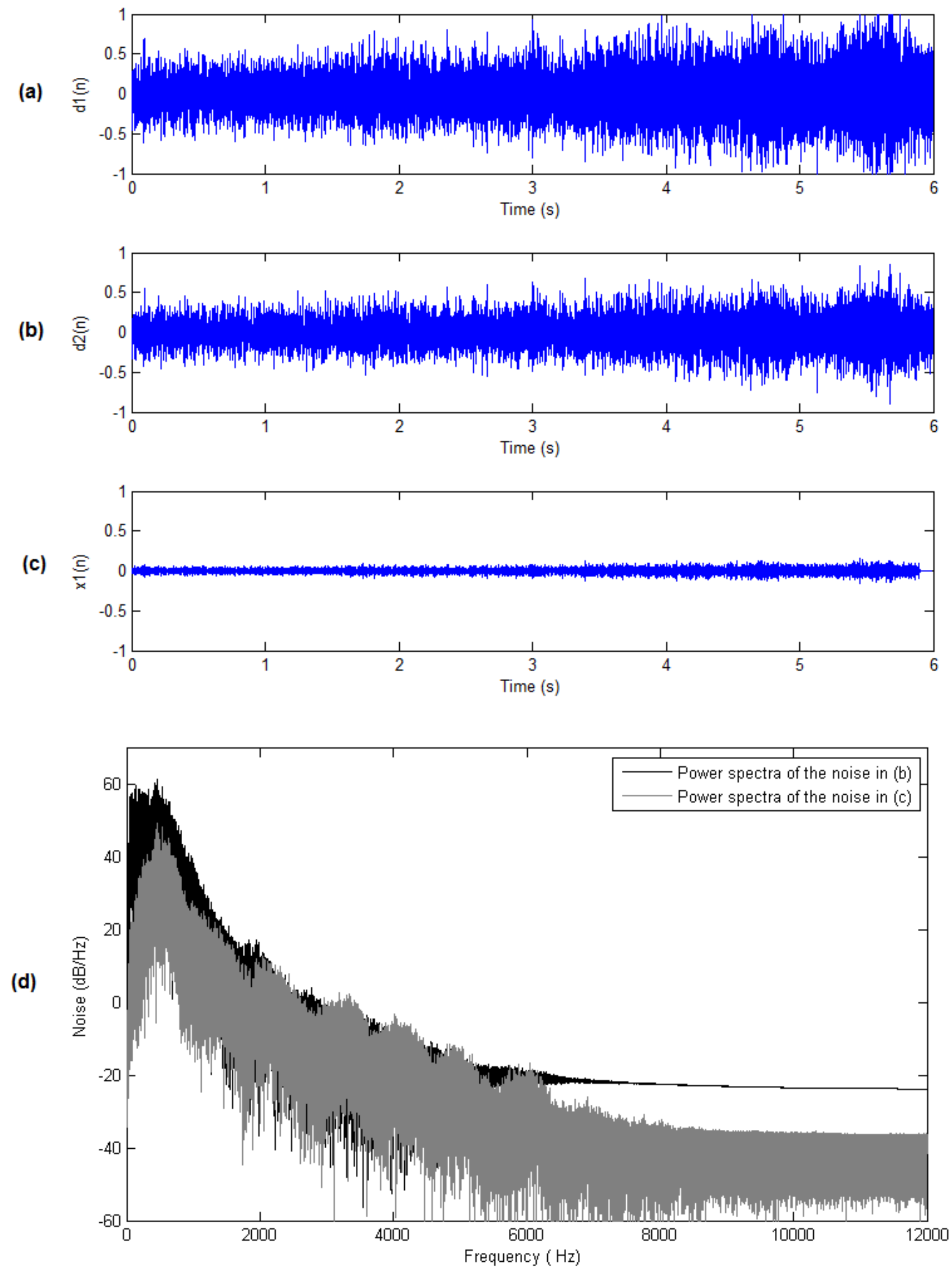

Figure 3.7. ANC using fixed FIR filter for train noise with t_p = 375 µs, t_s = 1.875 ms: (a) noise outside the ear cup (output of the reference mic.); (b) noise transmitted to the inside of the ear cup (output of the error mic. without ANC); (c) noise inside the ear cup with ANC; (d) Power spectra of the noise in (b) and (c).

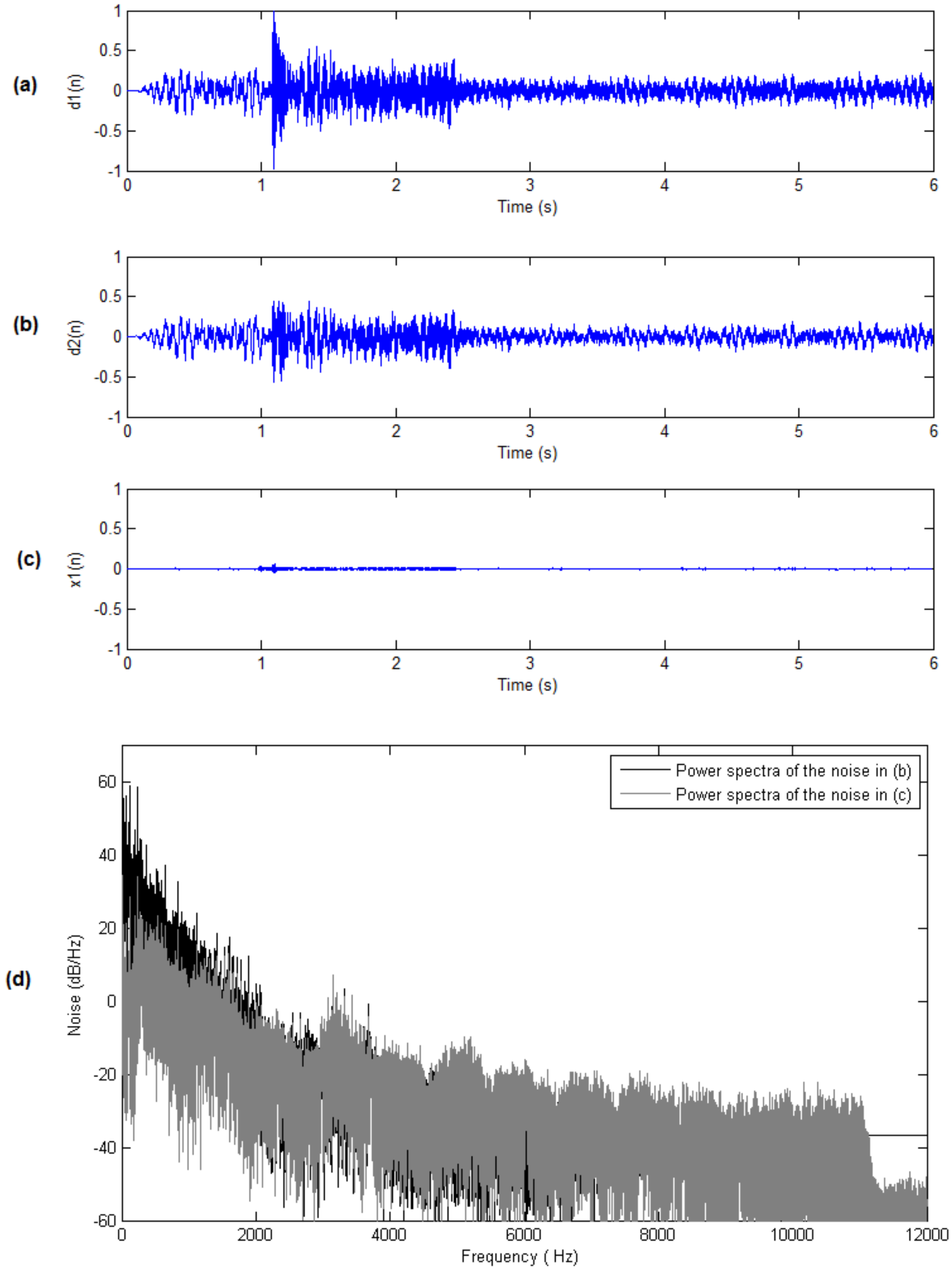

Figure 3.8. ANC using fixed FIR filter for air-conditioner noise with t_p = 375 μs, t_s = 1.875 ms: (a) noise outside the ear cup (output of the reference mic.); (b) noise transmitted to the inside of the ear cup (output of the error mic. without ANC); (c) noise inside the ear cup with ANC; (d) Power spectra of the noise in (b) and (c).

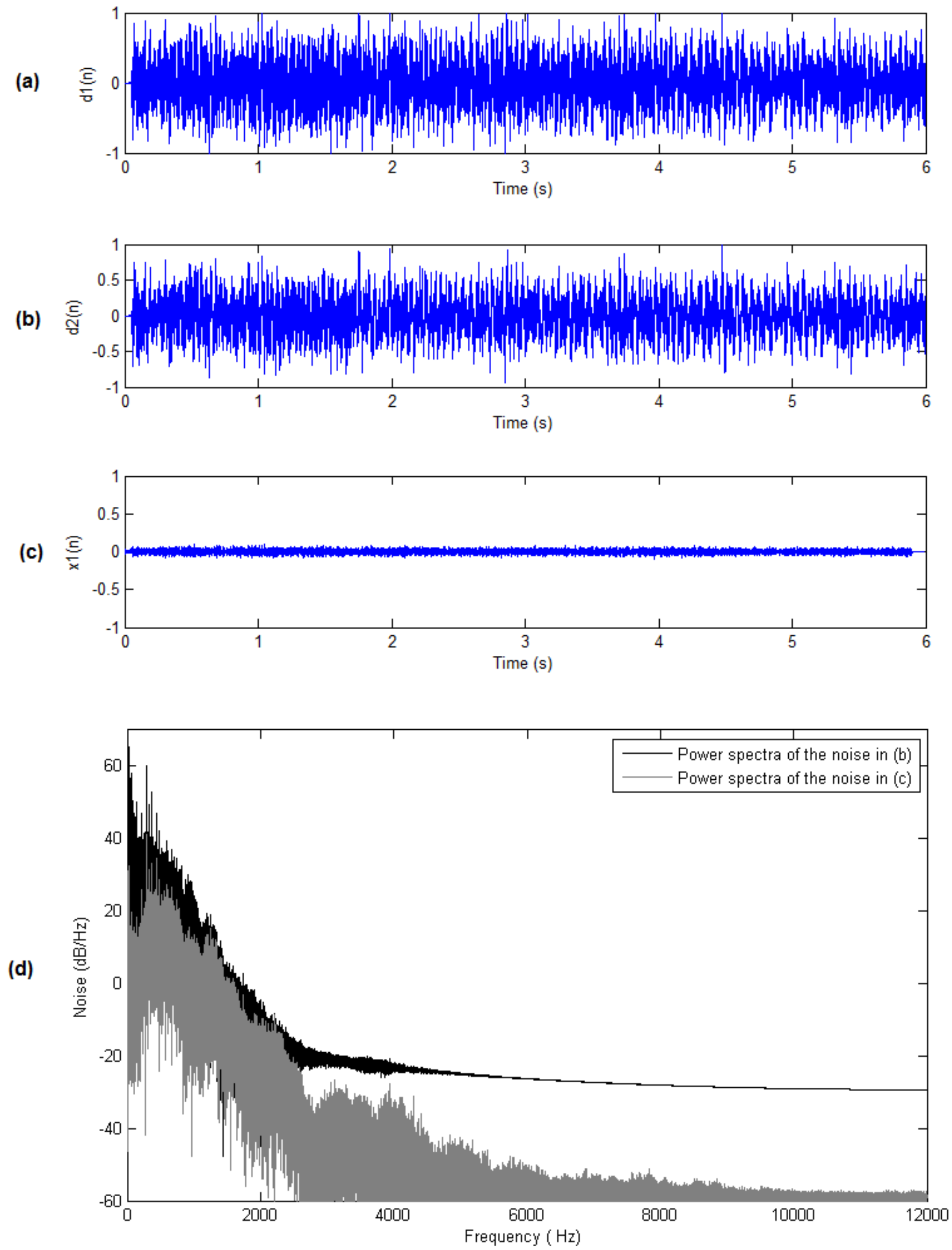

Figure 3.9. ANC using fixed FIR filter for helicopter noise with t_p = 375 μs, t_s = 1.875 ms: (a) noise outside the ear cup (output of the reference mic.); (b) noise transmitted to the inside of the ear cup (output of the error mic. without ANC); (c) noise inside the ear cup with ANC; (d) Power spectra of the noise in (b) and (c).

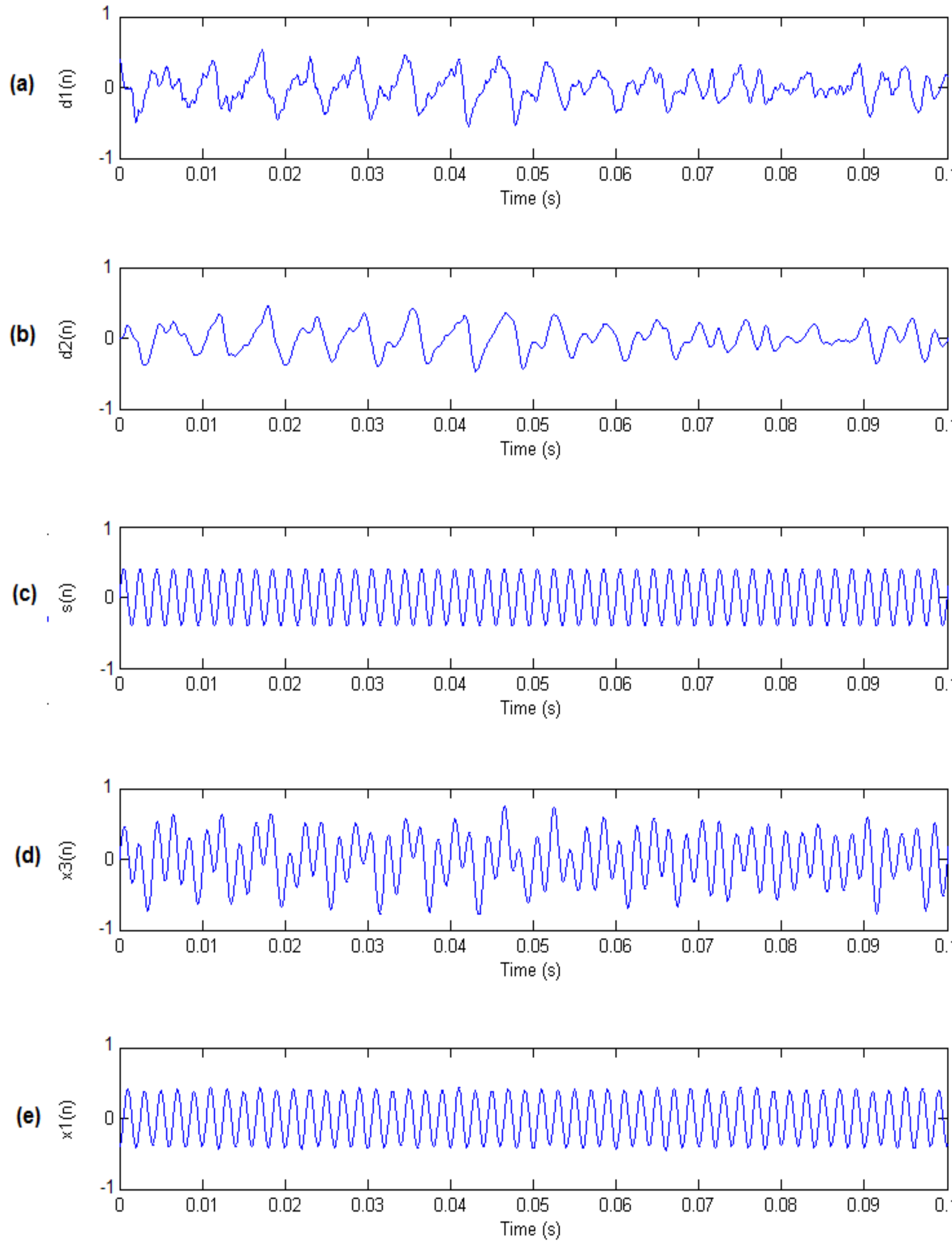

Figure 3.10. Waveforms of the signal at various points of NCH, for test signal of 500 Hz tone and music as noise: (a) noise outside the ear cup; (b) transmitted noise inside the ear cup; (c) test signal; (d) signal inside the ear cup, without NCH; (e) signal inside the ear cup, with NCH.

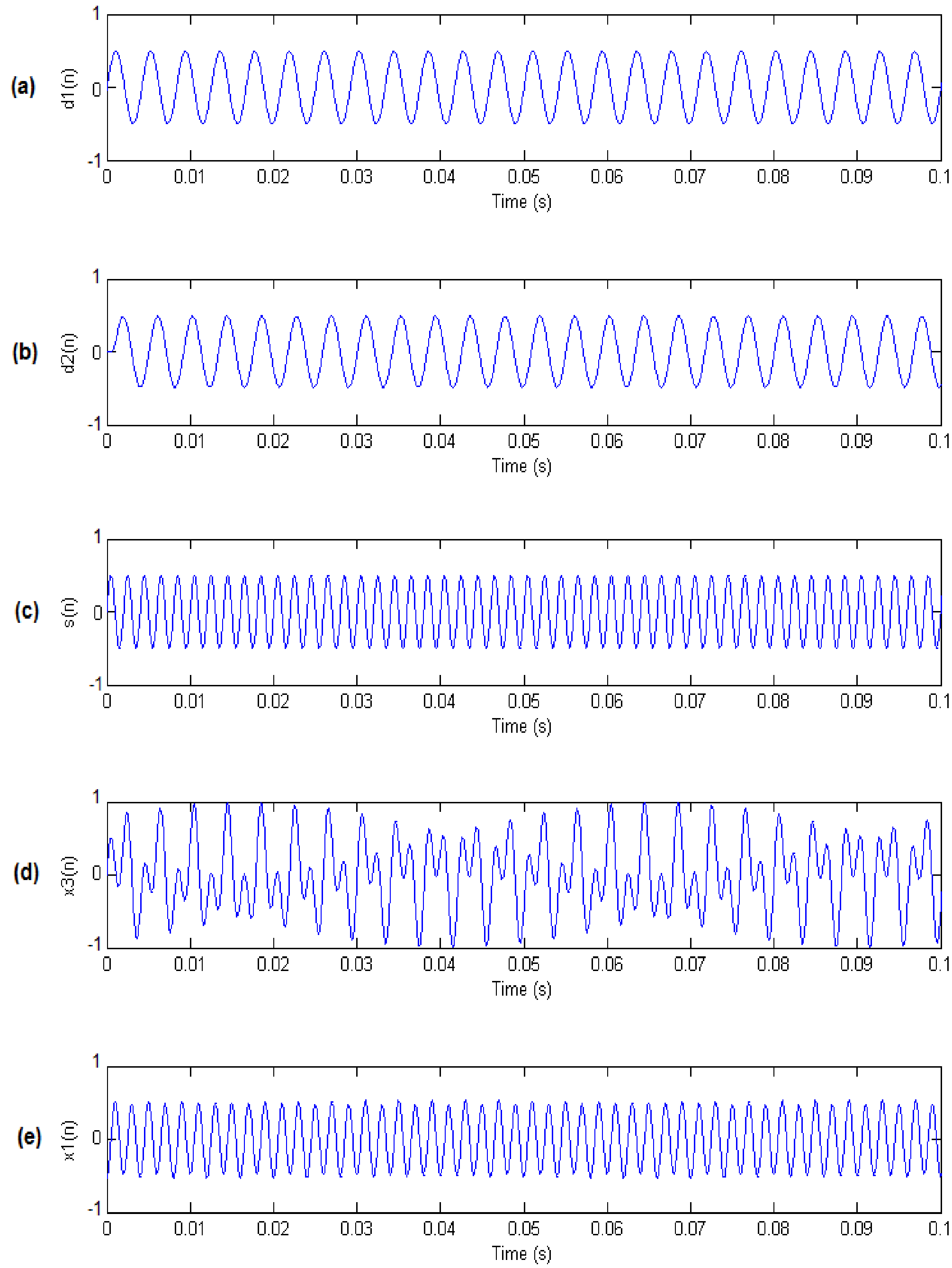

Figure 3.11. Waveforms of the signal at various points of NCH, for test signal of 500 Hz tone and noise is a tone of 240 Hz: (a) noise outside the ear cup; (b) transmitted noise inside the ear cup; (c) test signal; (d) signal inside the ear cup, without NCH; (e) signal inside the ear cup, with NCH.

Table 3.1 Noise attenuation, during LMS adaptation, as a function of step size (noise = 400 Hz tone, noise power = 0.5, filter order = 400, t_p = 375 μs, t_s = 1.875 ms, PNA = 1.5 dB, Fs = 24 kHz)

Step size	Attenuation due to ANC (dB)
.0050	84.5
.0049	115.3
.0048	143.0
.0047	170.7
.0046	199.0
.0045	228.3
.0044	258.6
.0043	272.3
.0042	272.7
.0041	273.0
.0040	273.2
.0039	273.4
.0038	273.6

Table 3.2 Noise attenuation (dB) due to ANC (using fixed FIR filter), for different types of noise (Filter order = 2400, t_p = 375 μs, t_s = 1.875 ms, Sampling frequency = 24 kHz)

Noise type	Noise attenuation (dB)		
	due to PNA	due to PNA+ANC	due to ANC
White Gaussian noise	23.4	38.1	14.7
Music	18.3	37.6	19.3
Train noise	17.1	29.7	12.6
Air-conditioner noise	33.0	37.6	4.6
Helicopter noise	2.8	30.1	27.3

3.2.4 Effect of step-size on the noise reduction

In order to study the effect of step-size on the noise reduction, simulations were carried out with different step-size for tonal noise of 400 Hz. For simulation, adaptive filter order of 400, primary path delay of 375 μs and secondary path delay of 1.875 ms were used. The maximum step-size was set to 0.1/[signal power x filter order]. The tonal noise is chosen in the range of [-1, 1] for simulation. From Table 3.1, it can be observed that as the step-size decreases the noise reduction increases up to a certain step-size, and after that the noise reduction remains constant.

3.2.5 Effect of filter order on the noise reduction

In order to study the effect of filter order on the noise reduction, simulations were carried out with different filter order for music as a broadband noise with PNA is 18.3 dB. From Table 3.3, it can be observed that as the filter order increases the noise reduction remains almost constant.

Table 3.3 Noise reduction due to ANC as a function of filter order (Music as a noise source, PNA = 18.3 dB, Fs = 24 kHz, Noise power = 0.0398)

Filter order	Noise Attenuation(dB)	
	Attenuation due to ANC	Attenuation due to PNA+ANC
400	17.2	35.5
800	15.1	33.4
1200	16.4	34.7
1600	15.6	33.9
2000	17.4	35.7
2400	19.3	37.6
2800	18.3	36.6
3200	19.2	37.5
3600	19.2	37.5
4000	17.5	35.8
4400	15.1	33.4
4800	19.5	37.8

Chapter 4
REAL TIME IMPLEMENTATION USING PROCESSOR dsPIC33FJ128GP802

The real-time implementation of ANC was first attempted using the low-cost digital signal controller dsPIC33FJ128GP802 from Microchip. The main feature of this processor is that it can be used for realizing an NCH without external peripherals. This chapter gives a description of the experimental setup and investigations to realize the NCH using this processor. The speed and memory of the processor were found to be inadequate. The noise reduction was effective only for lower audiometric frequencies, as it could not be operated at higher sampling frequency. To overcome this problem, it was later decided to use TI TMS320C5515 as the processor. These investigations will be presented in the next chapter.

4.1 Setup for ANC system

The experimental setup uses a wooden slab shown in Fig. 4.1, as used earlier in [14]. It has elliptical depression with a small hole for placing a microphone. A headphone is placed around the wooden box so that the ear cup entirely covers the elliptical depression. Two microphones are used, one is placed inside the ear cup to pick-up the error and the other one is placed outside the ear cup to pick-up the reference noise.

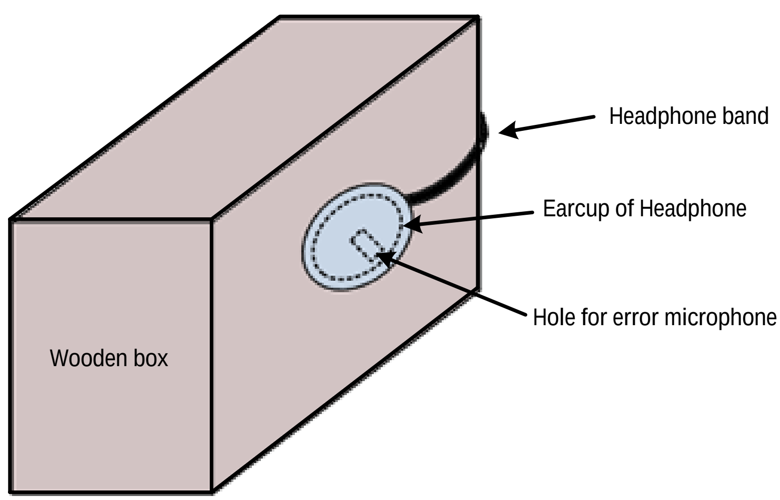

Figure 4.1 Wooden slab for the ANC experimental setup

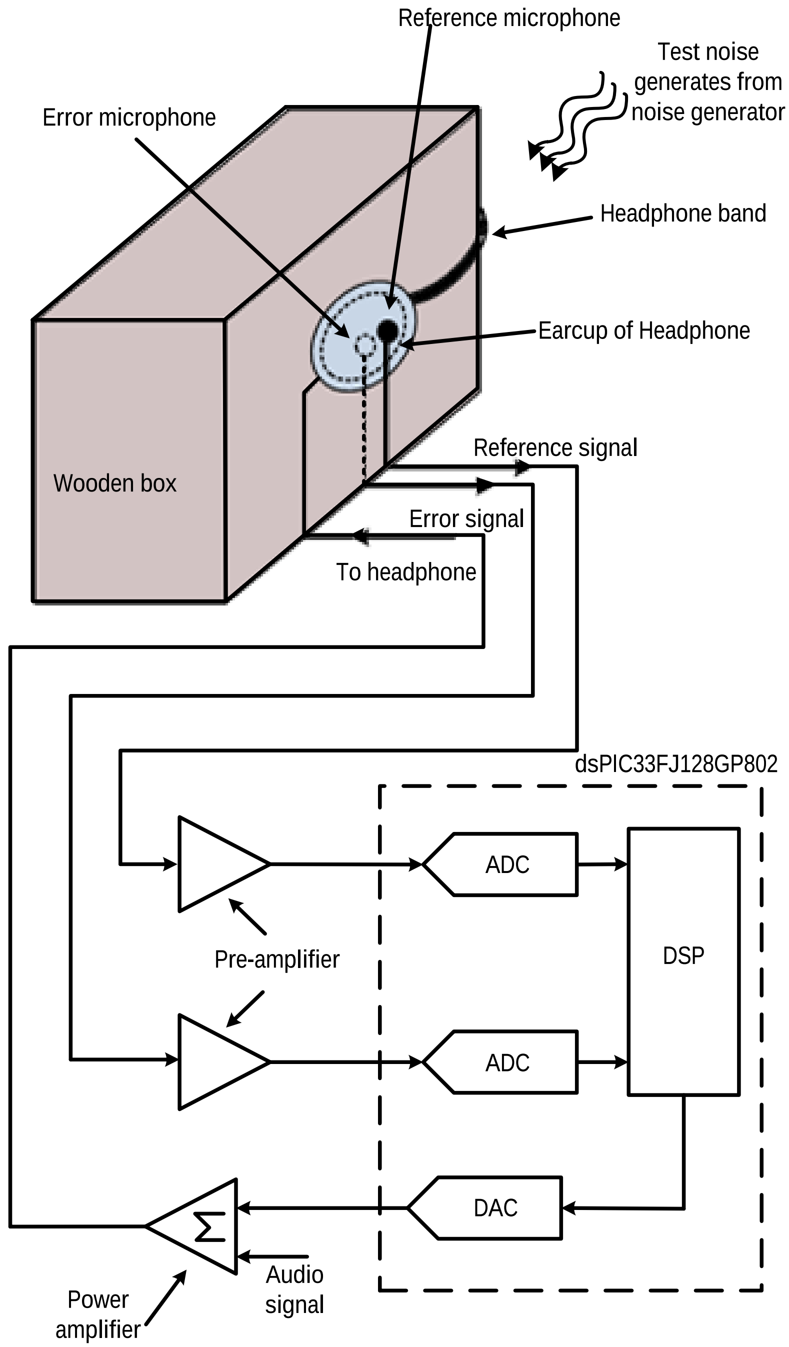

Figure 4.2 Experimental setup for ANC system using dsPIC33FJ128GP802

The block diagram of the experimental setup for the ANC system is shown in Fig. 4.2. The low level (0.1-100 mV) signal from the microphone [15] is amplified by the pre-amplifier to the required level (0-3.3 V) for processing. The outputs of the pre-amplifiers are then simultaneously sampled and digitized by the ADCs. The digitized signal is used to update

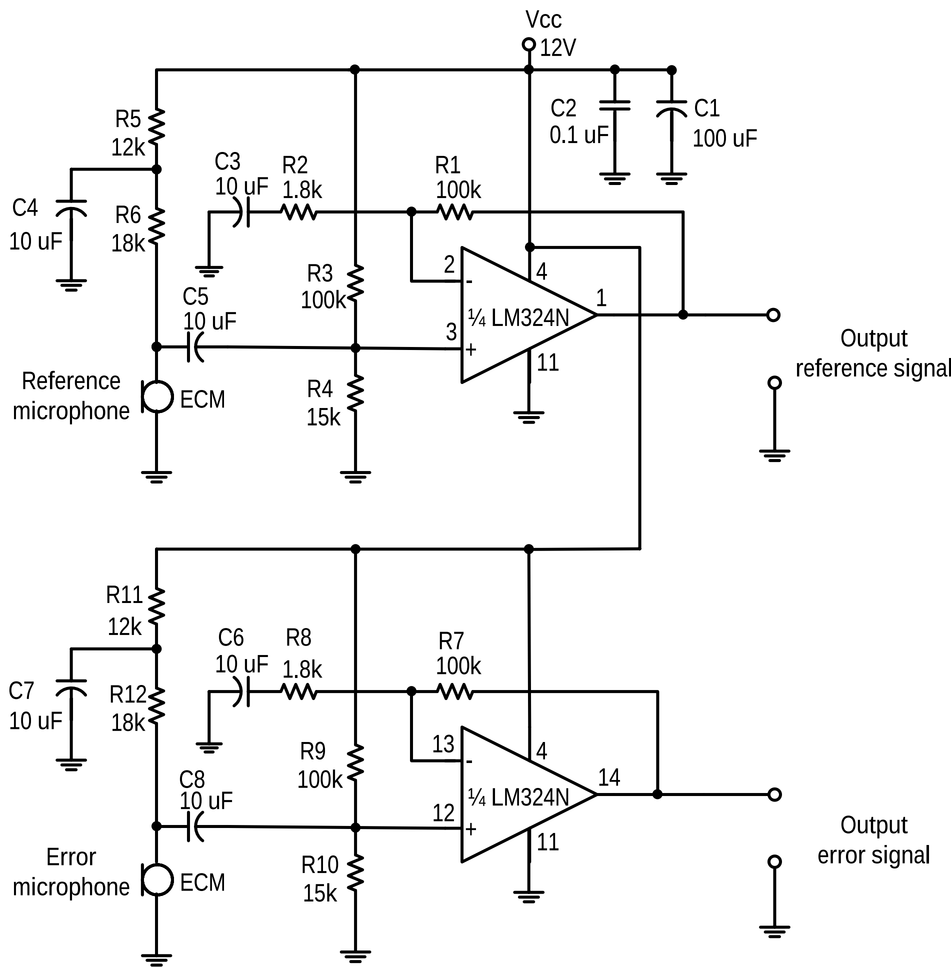

Figure 4.3 Circuit diagram of pre-amplifier

the adaptive filter coefficients using LMS algorithm. Anti-noise digital signal is generated as a result of adaptation process in the digital signal processor. This digital anti-noise signal is converted back to the analog signal using DAC. The output of DAC is added to the test stimulus and amplified by the power amplifier for driving the ear cup speaker.

The microphones used for NCH are electret condenser microphones (ECMs). It consists of a pre-charged non-conductive membrane, placed between moving plate and static plate which forms the capacitor [15]. Movement of the plate changes the capacitance value, which results in change in the output voltage. An ECM has an inbuilt high impedance buffer using a JFET. The main benefits of this type of ECM are its small size, low cost and relatively low noise. ECMs have very small output range (0.1-100 mV) [15], it requires significant pre-amplification before giving it as input to ADCs. The pre-amplifier circuit is shown in Fig. 4.3. Pre-amplifier circuit is designed using LM324 IC which have large output voltage swing (0 V to Vcc-1.5 V) [16] and it is powered by 12 V dc supply. The biasing is done through a resistor

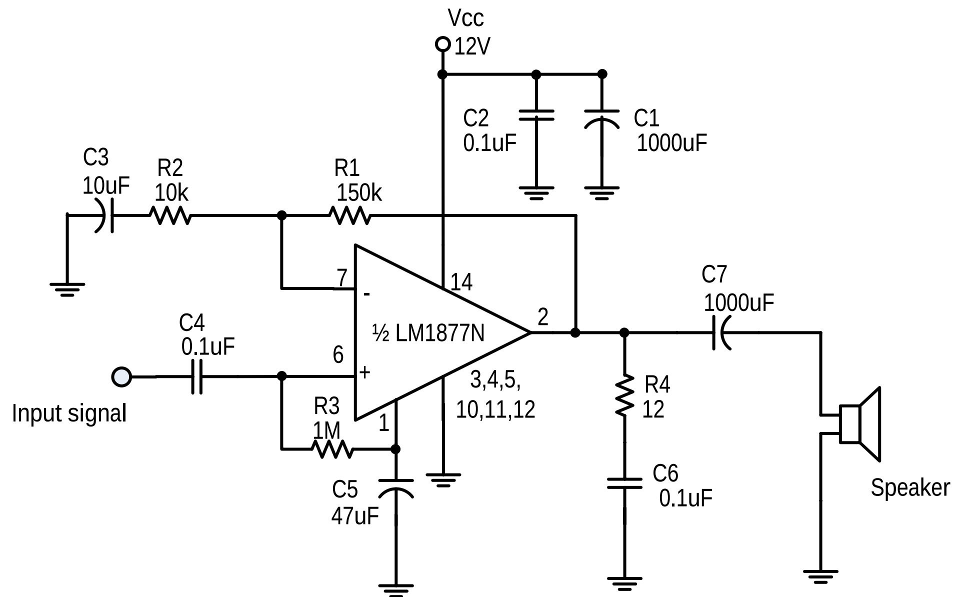

Figure 4.4 Circuit diagram of power-amplifier

and a series capacitor. An offset of 1.6 V is added to the input signal using R3, R4 and R9, R10 resistors to keep the signal in the ADC input voltage range of 0-3.3 V. The gain of the amplifier can be changed by varying resistors R1, R2 and R7, R8. It is operated in non-inverting mode with a gain of 55.55 and an offset of 1.6 V.

The output signals from the DAC are power amplified to drive the headphones. Power amplifier circuit is designed using LM1877 IC. It is a monolithic dual power amplifier so that one single IC can be used for driving two acoustic transducers. It can deliver 2 W powers per channel continuously into 8 ohm load [17]. It has wide supply range of 6V-24V, low cross-over distortion, AC short circuit protection and channel separation refers to output is -65 dB [17]. Power amplifier circuit for left headphone is shown in Fig. 4.4. The circuit is operated at 12 V supply. An LM1877 is operated in non-inverting mode with gain of 15. The gain can be adjusted by using different values of resistors R1 and R2.

4.2 DSP processor for ANC

NCH is a real-time embedded system, in which the ANC algorithm is implemented using a DSP processor. The suitable DSP is selected on the basis of operating speed, flexibility, cost and architecture optimized for adaptive signal processing. The DSP board should contain at least two analog input signals and one analog output signal. There are several processors and boards available from different manufacturers such as Microchip, Texas Instruments, Analog Devices, and Freescale Semiconductors. We selected the 16-bit fixed-point digital signal controller Microchip dsPIC33FJ128GP802. It has inbuilt ADC, DAC and DSP processor and

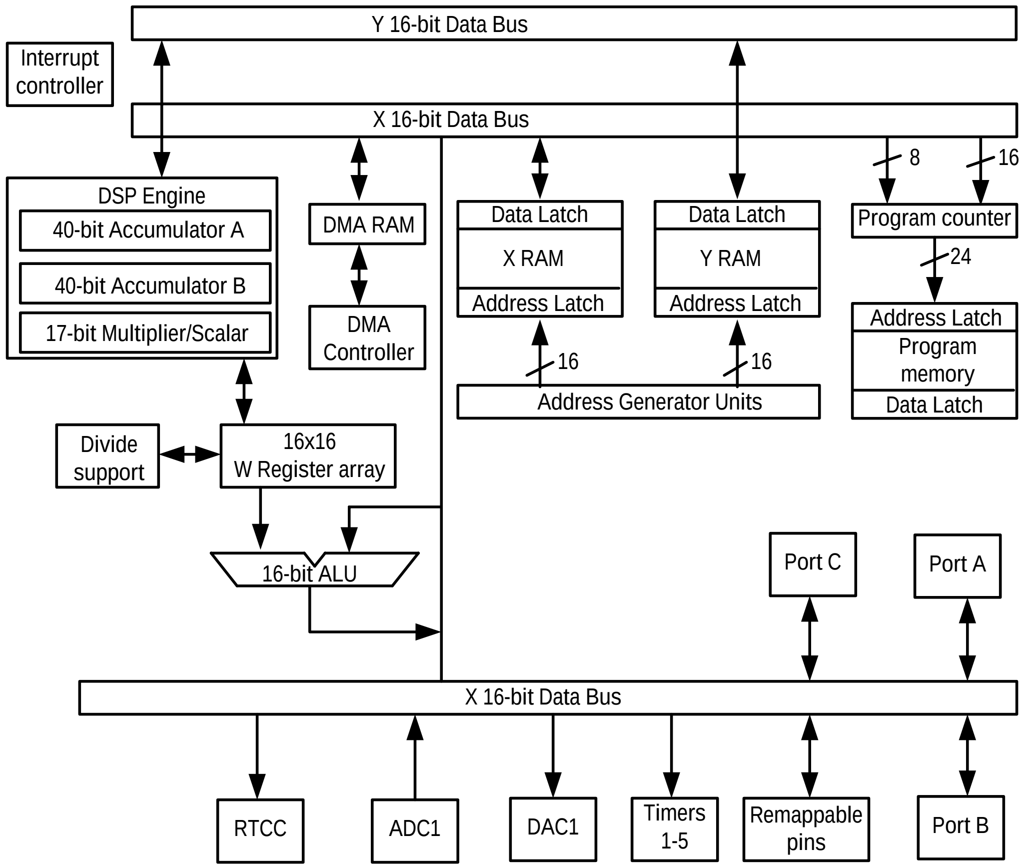

Figure 4.5 Simplified schematic of the architecture of Microchip dsPIC33FJ128GP802 [18]

it is supported by MPLAB IDE tools and C30 compiler/debugger [18]. It is a low cost digital signal controller with 40 MHz clock speed, on-chip program memory of 128 KB, data memory of 16 KB including DMA memory of 2 KB and on-chip ADC and DAC modules [18]. The on-chip I/O modules of dsPIC33FJ128GP802 are used for signal acquisition. Signal acquisition unit consists of on-chip ADC, DAC, and digital signal processor. The input analog signals are amplified and applied to input of the respective ADC channel. The ADC converts the analog signal into digital signal. The DSP sends the processed signal to DAC and the data is converted to analog voltages by their respective sigma-delta DACs comprised of a digital interpolation filter and a digital modulator.

A block diagram of dsPIC33FJ128GP802 architecture with the resources needed for adaptive algorithm implementation is shown in Fig. 4.5.The chip has inbuilt fast RC (FRC) oscillator which can be configured using PLL settings to provide instruction clock up to 40 MHz. It consists of 10-bit ADC which can sample 4 channels simultaneously with a conversion speeds up to 500 kHz. The conversion results from the ADC are stored in a single-word result buffer ADC1BUF0. The dsPIC33FJ128GP802 consists of 16-bit dual channel

DAC module with 128-tap FIR reconstruction filter, 256x over-sampling ratio and sampling rate of up to 100 kHz [18]. A 4 word FIFO array DAC1RDAT buffers the data for each channel. The chip has ADC input range of 0.0 - 3.3 V and DAC output range of 1.125 - 2.235 V [18]. The chip has five 16-bit timers which can be combined to form two 32-bit timers. It also has 49 interrupt sources, 3 external interrupts and 35 programmable digital I/O pins. It supports 16-bit wide data, 24-bit wide instruction, 16x16 fractional/integer multiplication operation, two 40-bit accumulators with rounding and saturation options, single-cycle multiply and accumulate.

The experimental set up for real-time implementation of ANC using dsPIC33FJ128GP802 is shown in Fig. 4.2. ANC system hardware includes microphones, pre-amplifier, headphone, digital signal controller, and noise generator. A tonal noise is generated through a speaker using PC sound card. A reference microphone kept on the top of the ear cup picks up the noise presented outside the headphone. Noise transmitted inside the ear cup is picked up by an error microphone kept near the noise cancelling speaker. Reference signal and error signal from pre-amplifiers are sampled at 20 kHz using on-chip ADC module. ADC module sequentially converts the two analog signals into digital signals. An antinoise signal to cancel the ambient noise inside the ear cup is obtained using the LMS algorithm based on the reference and error signal. The digital antinoise signal thus estimated is input to DAC module. The analog signal from DAC is amplified by a power amplifier to drive the headphone speaker. The headphone speaker generates acoustic sound in the ear cup. The anti-noise reduces noise present inside the ear cup by acoustical superposition. The error signal, present in the ear cup, is sensed by error microphone and used to updates adaptive filter coefficients.

4.3 Software Implementation

Software of real-time ANC includes A/D and D/A conversion of input and output signals, LMS algorithm, and FIR filtering. The FRC oscillator was configured to operate at 40 MIPS by setting the PLL value. Two analog input port pins are configured for reference and error signals. ADC was configured to operate in 10-bit signed fraction mode with sampling rate of 20 kHz. DAC was configured to operate in 16-bit signed fraction mode. Sampling rate for DAC was set by clock divider and left channel was selected for output. ADC was configured to interrupt the processor after completion of conversion of sample data. The two analog channels are sampled simultaneously but conversion was done sequentially so when first ADC interrupts occurs, sample value from ADC buffer was stored to circular buffer A and when second ADC interrupt occurs, sample value from ADC buffer was stored to RAM memory. In the interrupt service routine the acquired data from the ADC were processed by LMS algorithm and output was sent to DAC.

The LMS algorithm sub-routine, used to update the coefficients of the adaptive filter is written in assembly language. For efficient computation the algorithm was implemented using 16-bit fixed-point arithmetic. For 16-bit word length, the fixed-point number has the range -2^{15} to $2^{15}-1$. The Q1.15 fraction format is used for computation. It has the range [-1, 0.9999] so the multiplication of two fraction gives results in a number smaller than one and hence there is no overflow during multiplication. But when large number of accumulation operations are performed then it is possible that the results may exceed beyond the range [-1, 0.9999]. Saturation logic may be enabled to avoid overflow. But results may get clipped if the saturation logic is enabled. The saturation problems can be solved by scaling the input signal before computation. All the equations are implemented with appropriate scaling of intermediate results, to keep them within the 16-bit range. The processor has a 40-bit accumulator and special multiply-accumulate instruction (MAC). The saturation flag is set whenever the computation result in the accumulator exceeds 32-bit. All the digital signals and variables, which are used for implementing the LMS algorithms, are in 16-bit fractional format. The signed integer variable can be changed to fractional format by dividing the integer value with 2^{15} so the variable has the value within the range (-1 to 0.9999). The scaling operations are performed using right shifting. For LMS algorithm implementation, all the discrete signals and filter coefficients are in Q1.15 fractional format as shown in Table 4.1.

Table 4.1 Q1.15 fractional format representation

Bit	15	14	13	12	11	9	8	….	0
Value	S	Q14	Q13	Q12	Q11	Q9	Q8	…..	Q0

The S bit is the sign bit and the rest 15 bits contain the 2's complement fractional format number. The finest fractional resolution is 2^{-15}. Floating point value can be represented by Q1.15 format by multiplying it with 2^{15}.

4.3.1 Computations involved in the DSP implementation

Assuming $d_1(n)$ and $x_1(n)$ to be in the range [-1, 1], step size μ is selected empirically in the range 0-0.0125, for filter order M=250. The adaptive filter output d_4 is given as

$$d_4(n) = \left[\sum_{k=0}^{M-1} d_1(n-k) w_n(k) \right] \tag{4.1}$$

where M = order of the adaptive filter (selected as 250), and $w_n(k)$ are the filter coefficients. The filter coefficients are assumed to be in the range {-1, 1} and initialized as zeros. These are updated using

$$w_{n+1}(k) = w_n(k) + \mu x_1(n) d_1(n-k) \tag{4.2}$$

We use scaling factor $\alpha = 2^{15}$, and hence the scaled step size is given as

$$\mu_s = \alpha\mu \tag{4.3}$$

The reference inputs $D_1(n)$, error inputs $X_1(n)$ and filter coefficients $W_n(k)$ are in Q1.15 fractional format and can be considered on being

$$D_1(n) = \alpha d_1(n) \tag{4.4}$$

$$X_1(n) = \alpha x_1(n) \tag{4.5}$$

$$W_n(k) = \alpha w_n(k) \tag{4.6}$$

The adaptive filter output $D_4(n)$ in Q1.15 format is related to $d_4(n)$ as

$$D_4(n) = \alpha d_4(n) \tag{4.7}$$

and hence is computed by using

$$D_4(n) = \frac{1}{\alpha}\left[\sum_{k=0}^{M-1} D_1(n-k) W_n(k)\right] \tag{4.8}$$

The filter coefficient update equation, in the fractional format, is given as

$$W_{n+1}(k) = W_n(k) + \frac{1}{\alpha}\left\{\mu_s \frac{1}{\alpha}\left[\left(X_1(n) D_1(n-k)\right)\right]\right\} \tag{4.9}$$

4.3.2 Simulation results

An LMS algorithm is simulated using Microchip MPLAB simulator. MPLAB simulator has a provision to calculate number of instruction cycles consumed by the algorithm using linear profiling. During simulation overhead due to interrupts was not considered. For the filter order of 250, step-size of .0013 and sampling frequency of 20 kHz, the total number of instruction cycles taken by the LMS algorithm was observed to be 1850. Hence the execution time required is 462.5 µs (as the instruction cycle time of dsPIC33FJ128GP802 is 250 ns). Simulation was carried out by taking a tone of 1000 Hz as an ambient noise. Headphone is modeled by 2nd order Butterworth low-pass filter with cut off frequency of 500 Hz. The transmitted noise and reference noise were stored in buffer. The LMS algorithm was simulated using MPLAB simulator and error signal was stored in error buffer array. It can be observed from Fig. 4.6, the noise reduction for 1000 Hz tonal noise was 35.0 dB.

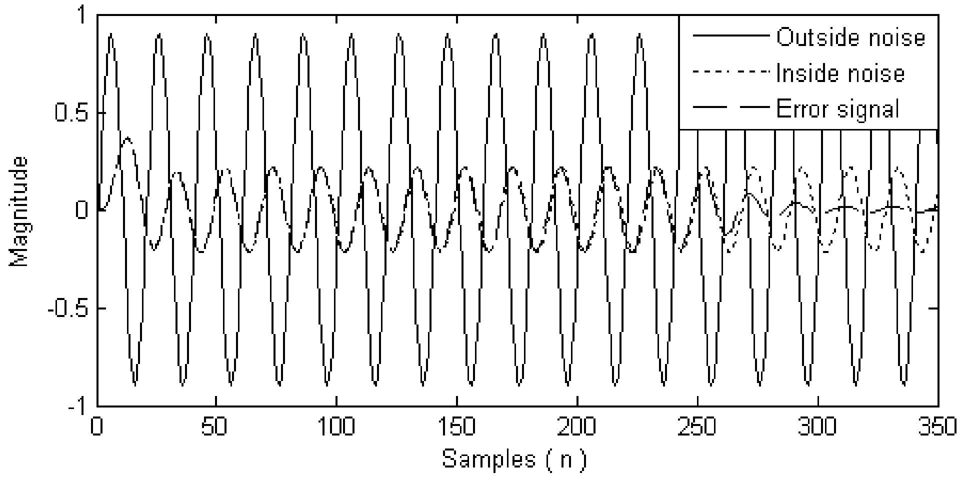

Figure 4.6 Plot of noise with and without ANC using MPLAB simulator

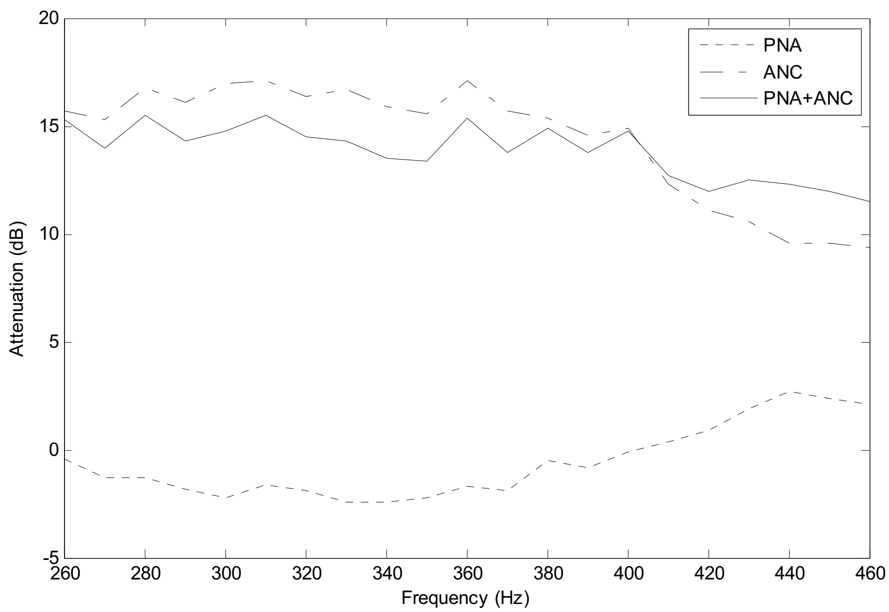

Figure 4.7 ANC result: Attenuation of tonal noise as a function of frequency (Filter order = 250, Step-size = 0.0013, and Sampling frequency = 20 kHz)

4.4 Results and Discussion

Experiments were carried out with tonal noise of different frequencies. For sampling rate of 20 kHz, the maximum FIR filter order permitted by the code execution speed was 250. The step-size set to 0.0013 with respect to full range of 16-bit register. The plot of noise reduction as a function of frequency of tonal noise is shown in Fig. 4.7. The tonal noise used is incremented in steps of 10 Hz and it is observed that the adaption process converges to minimum error from 260 Hz to 460 Hz. Fig. 4.8 – 4.11 shows the waveforms of error signal with and without adaption for various noises. It can be observed that the noise reduction is different for tonal noises of different frequencies. The noise reduction is maximum (15.5 dB) at a frequency of 310 and 360 Hz. An average noise reduction of 13.8 dB was observed for frequencies up to 460 Hz. Beyond the 460 Hz tonal noise, the adaption process does not converge to minimum error due to low processing speed and sampling rate limitation.

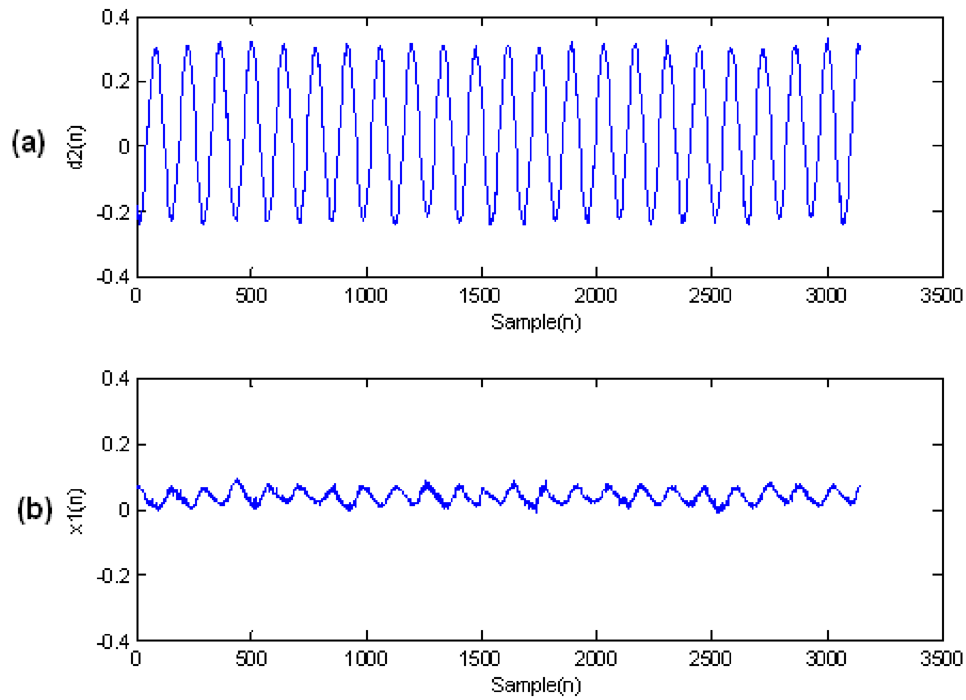

Figure 4.8 ANC of a tone of 280 Hz noise: (a) noise inside the ear cup without ANC; (b) noise inside the ear cup with ANC.

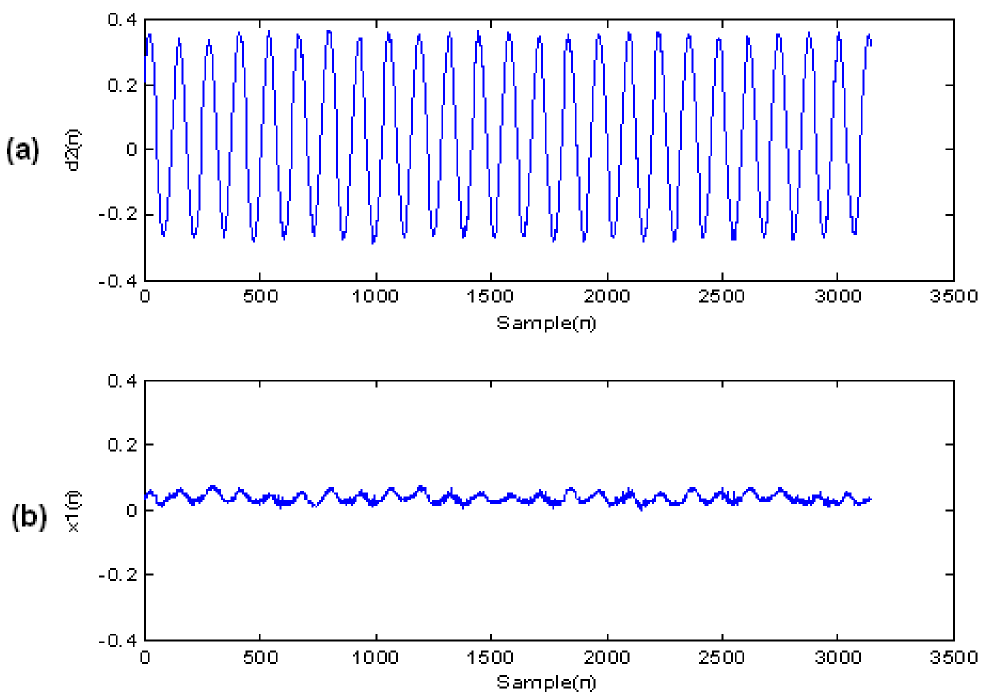

Figure 4.9 ANC of a tone of 300 Hz noise: (a) noise inside the ear cup without ANC; (b) noise inside the ear cup with ANC.

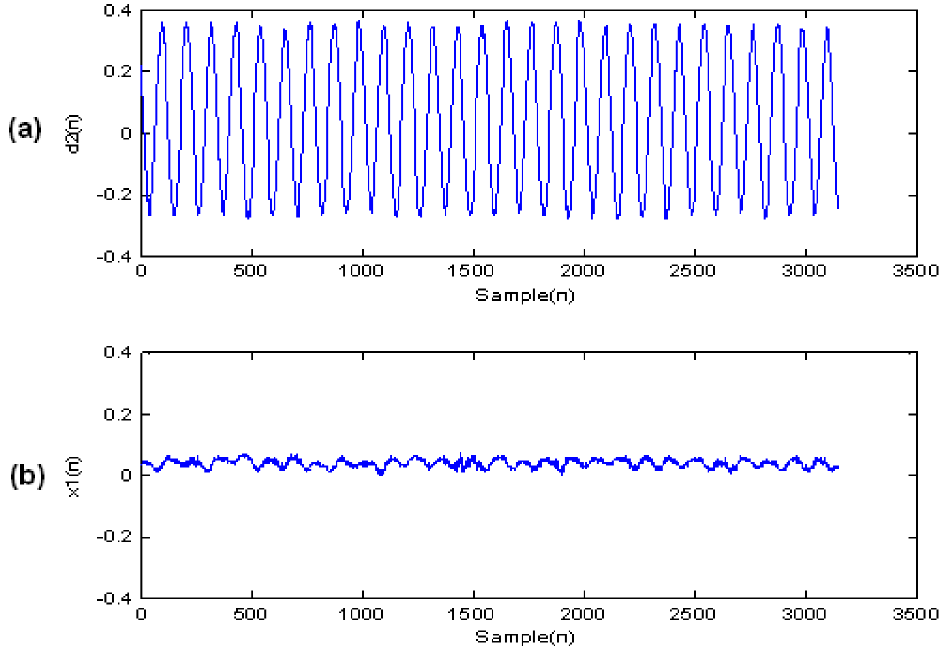

Figure 4.10 ANC of a tone of 350 Hz noise: (a) noise inside the ear cup without ANC; (b) noise inside the ear cup with ANC.

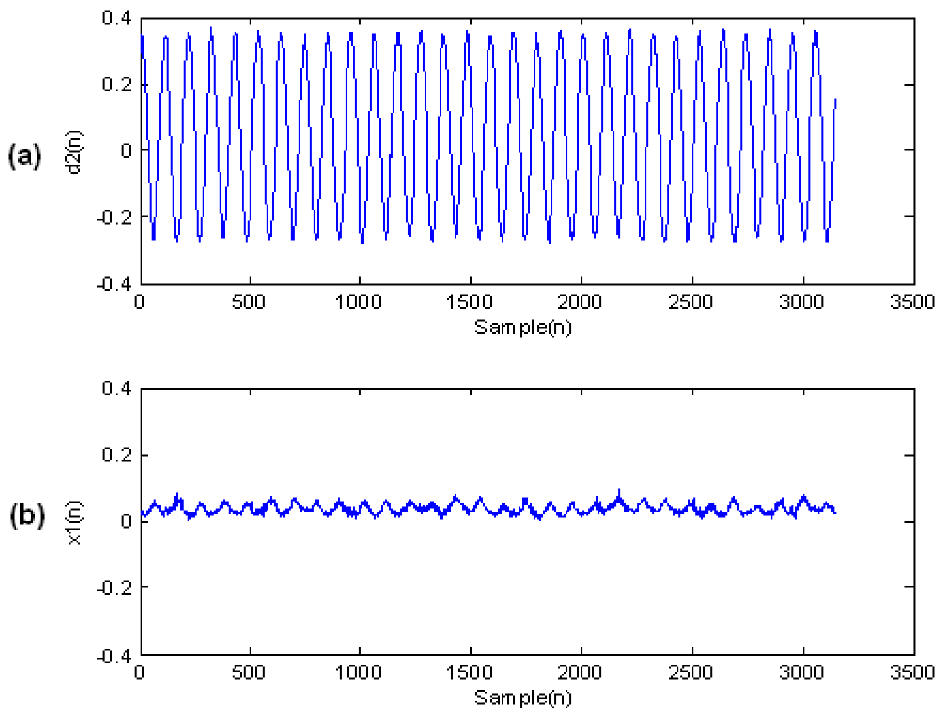

Figure 4.11 ANC of a tone of 370 Hz noise: (a) noise inside the ear cup without ANC; (b) noise inside the ear cup with ANC.

Chapter 5
REAL-TIME IMPLEMENTATION OF ANC USING TMS320C5515

The noise reduction using dsPIC33FJ128GP802 processor was effective only for tonal noise for frequencies up to 460 Hz. The processing speed and sampling rate found to be inadequate for cancellation at higher frequencies. To overcome this problem, it was decided to use Texas Instruments TMS320C5515 processor having a clock rate of 120 MHz and on-chip RAM of 320 KB for real-time implementation of ANC algorithm. An FIR filter for broad-band noise cancellation was designed using magnitude and phase response of noise cancelling filter obtained for all tonal frequencies. Subsequently the fixed FIR filter is used to cancel the broad-band noise. Implementation using TMS320C5515 eZdsp USB stick and the results are described in subsequent sections.

5.1 Overview of TMS320C5515 eZdsp USB Stick Kit

The block diagram of the TMS320C5515 eZdsp USB stick is shown in Fig. 5.1. It consists of digital signal processor TMS320C5515, stereo codec TLV320AIC3204, USB 2.0 interface to C5515 processor, 32 Mb NOR flash, embedded USB XDS100 JTAG emulator and it is

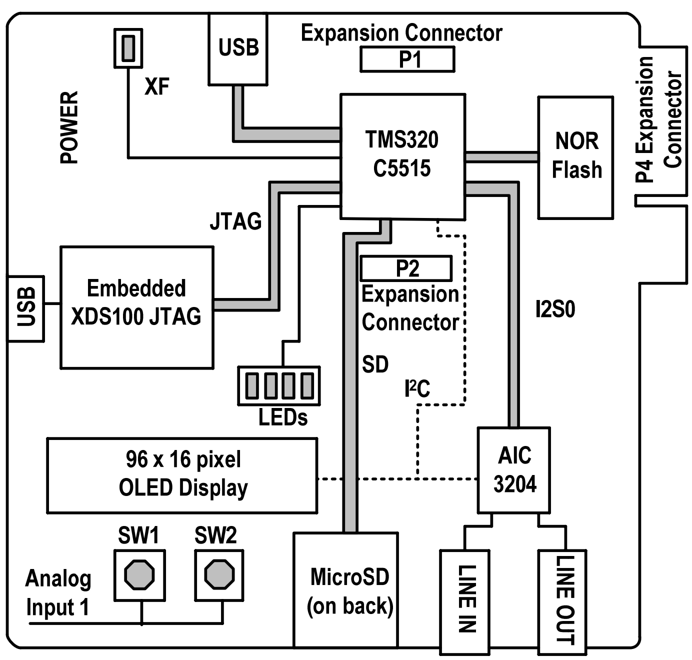

Figure 5.1 Block Diagram of TMS320C5515 eZdsp USB Stick [20]

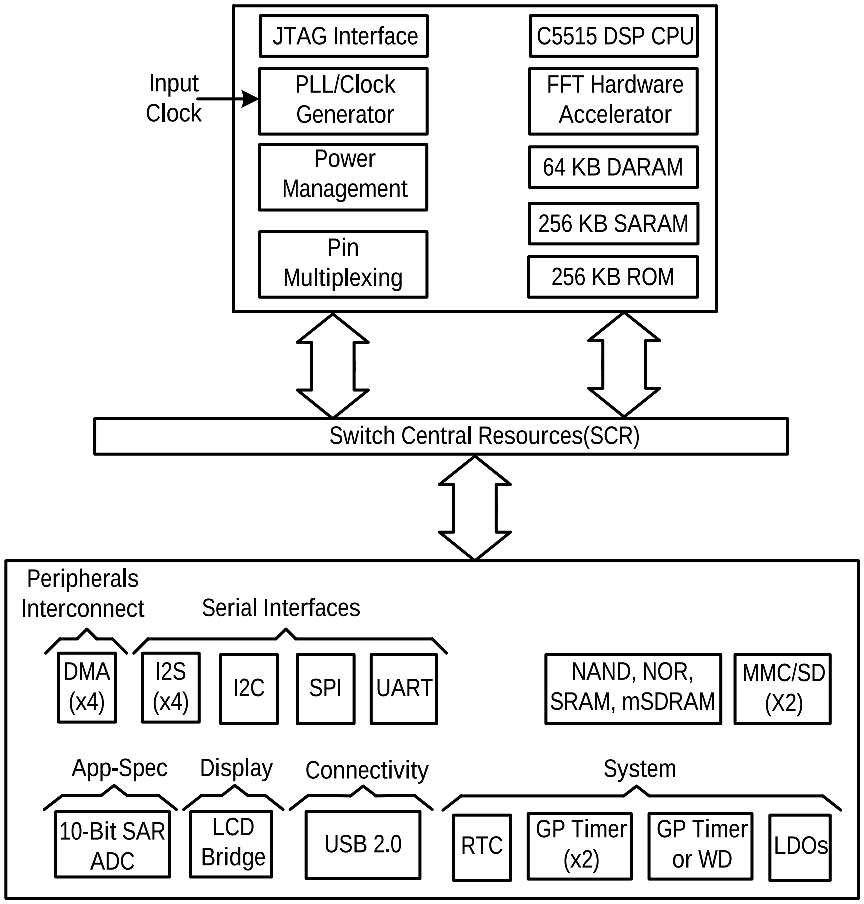

Figure 5.2. Functional Block Diagram of TMS320C5515 [23]

compatible with Texas Instruments Code Composer Studio v4. The TMS320C5515 eZdsp USB Stick provides an evaluation suite of the Code Composer Studio development platform, including a complete Integrated Development Environment (IDE) [20].

5.1.1 TMS320C5515 Digital signal processor

The TMS320C5515 has a high speed and flexible architecture optimized for audio processing. The functional block diagram of the TMS320C5515 is shown in Fig. 5.2. It can execute an instruction in as little as 100 ns. It consists of a CPU with associated memory, FFT hardware accelerator, 4 DMA controllers, external memory interface, power management module, and a set of I/O peripherals that includes I2S, I2C, SPI, UART, Timers, EMIF, 10-bit SAR ADC, LCD controller, and USB 2.0 [23]. It supports a unified 16 MB memory map consisting of the on-chip and external memory. The on-chip memory consists of 320 KB of RAM and 128 KB of ROM. The on-chip RAM of 320 KB consists of 64 KB of dual-access RAM (DARAM) and 256 KB of single-access RAM (SARAM). It has 8 blocks of 8 KB of DARAM. Each DARAM block can perform two accesses per cycle (two reads, two writes, or a read and a write). The DSP has 32 blocks of 8 KB of SARAM. Each SARAM block can perform one access per cycle (one read or one write). The system clock is set to 100 MHz using real-time clock (RTC) oscillator and PLL. A central 40-bit arithmetic logic unit (D- unit ALU) is supported by an additional 16-bit arithmetic logic unit (A-unit ALU). The CPU provides two multiply-accumulate (MAC) units, each capable of 17-bit x 17-bit multiplication (fractional or integer) and a 40-bit addition or subtraction with optional 32/40-bit saturation in a single cycle.

5.1.2 TLV320AIC3204 Codec description

The block diagram of TLV320AIC3204 codec is shown in Fig. 5.3. The TLV320AIC3204 consists of low voltage stereo audio ADC, stereo audio DAC, programmable inputs and outputs, signal processing blocks and integrated PLL [21]. The internal clock required for TLV320AIC3204 can be derived from internal PLL (phase locked loop). There are six analog inputs channels which can be configured as either 3 stereo single ended pairs or 3 fully differential pairs. An analog programmable gain amplifier (PGA) is used as pre-amplifier. It has flexibility to choose, input impedance of PGA among 10 kΩ, 20 kΩ and 40 kΩ, pre-amplifier gain from 0 dB to 47.5 dB for single-ended inputs or 6 dB to 53.5 dB for fully-differential inputs, common mode value among 0.75 V and 0.9 V. The ADC supports sampling rates from 8 kHz to 192 kHz. The ADCs uses a delta sigma modulator with a programmable oversampling ratio, followed by digital decimation filter with -73 dB stop-band attenuation and linear phase response, operating at an oversampling ratio of 128 or 64. The TLV320AIC3204 integrates 2^{nd} order analog anti-aliasing filter with 28 dB attenuation at 6 MHz [21]. The TLV320AIC3204 has four DAC channels arranged as two independent stereo pairs. The DAC supports data rates from 8 kHz to 192 kHz. Each channel of the stereo audio DAC consists of fixed processing blocks, a digital interpolation filter and an analog reconstruction filter. The oversampling rate configured over a range from 1 to 1024 and -65 dB stop-band attenuation of interpolation filter. The sampling rate, resolution, gain of PGA, gain of headphone amplifier, and attenuation filter selection of ADC and DAC modules can be programmed. ADCs and DACs of TLV320AIC3204 can be configured to set the resolution of 32, 24, 20, or 16 bits. A serial peripheral interface (SPI) port is included to adjust codec parameters.

The codec can be programmed using SPI in I2S mode. The I2S bus is used for communication between processor and codec. Data on the I2S0_RX pin of processor is shifted serially into the receive shift register and then copied into the receive buffer register. The data is then copied to I2S0 receive left/right data register. For each channel (left and right), these registers can be accessed as two 16-bit registers by the CPU. Similarly, the CPU writes the transmit data to the I2S0 transmit left/right data register which is then copied to the

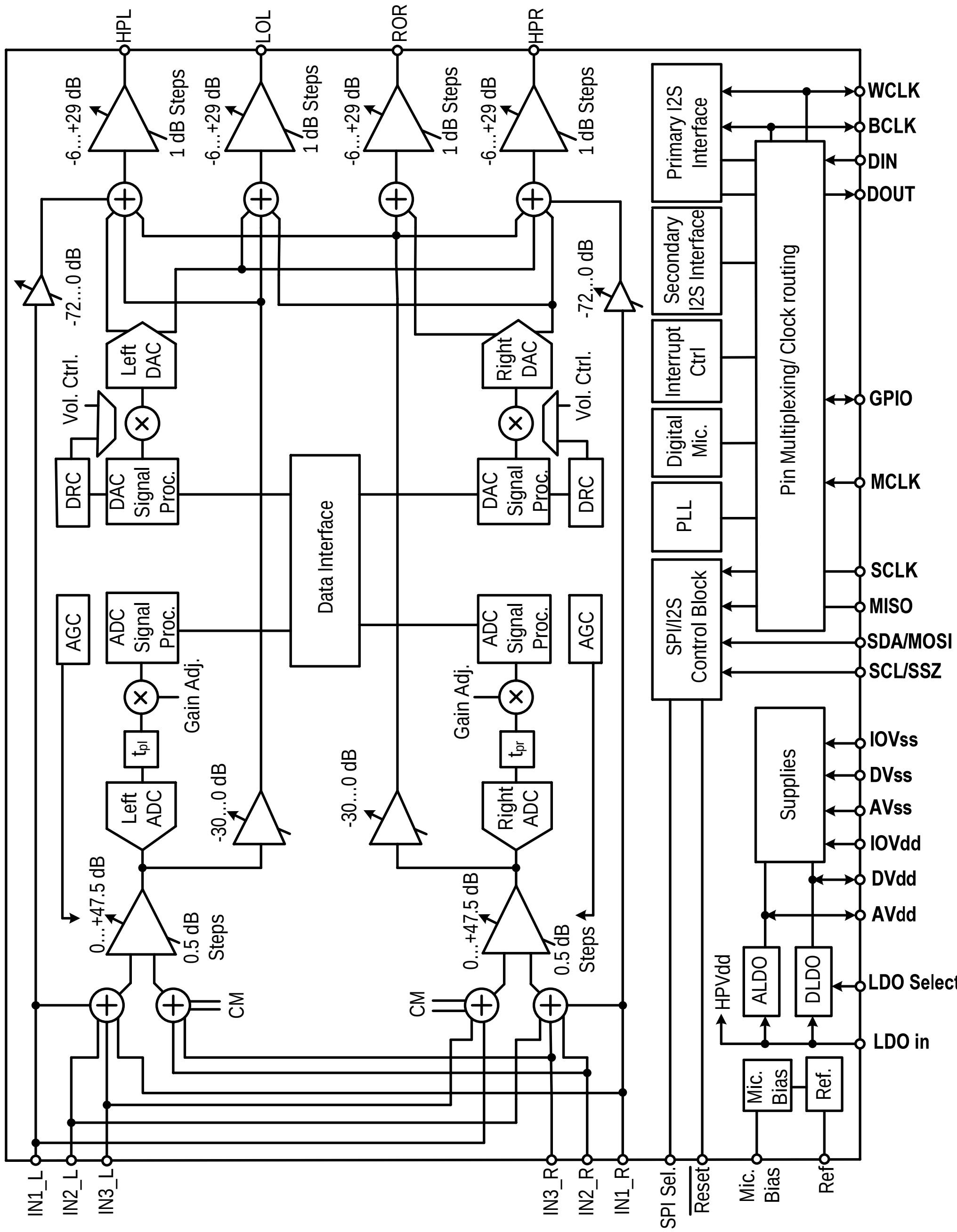

Figure 5.3. Simplified Block Diagram of TLV320AIC3204 codec [21]

transmit shift register through the transmit buffer register and shifted serially out to I2S0_TX pin.

5.2 Experimental setup for real-time implementation

The block diagram of the experimental setup for the ANC system using TMS320C5515 eZdsp USB stick is shown in Fig. 5.4. The low level (0.1-100 mV) signal from the microphone [15] is amplified by the pre-amplifier to the required level (0-1.95 V) for

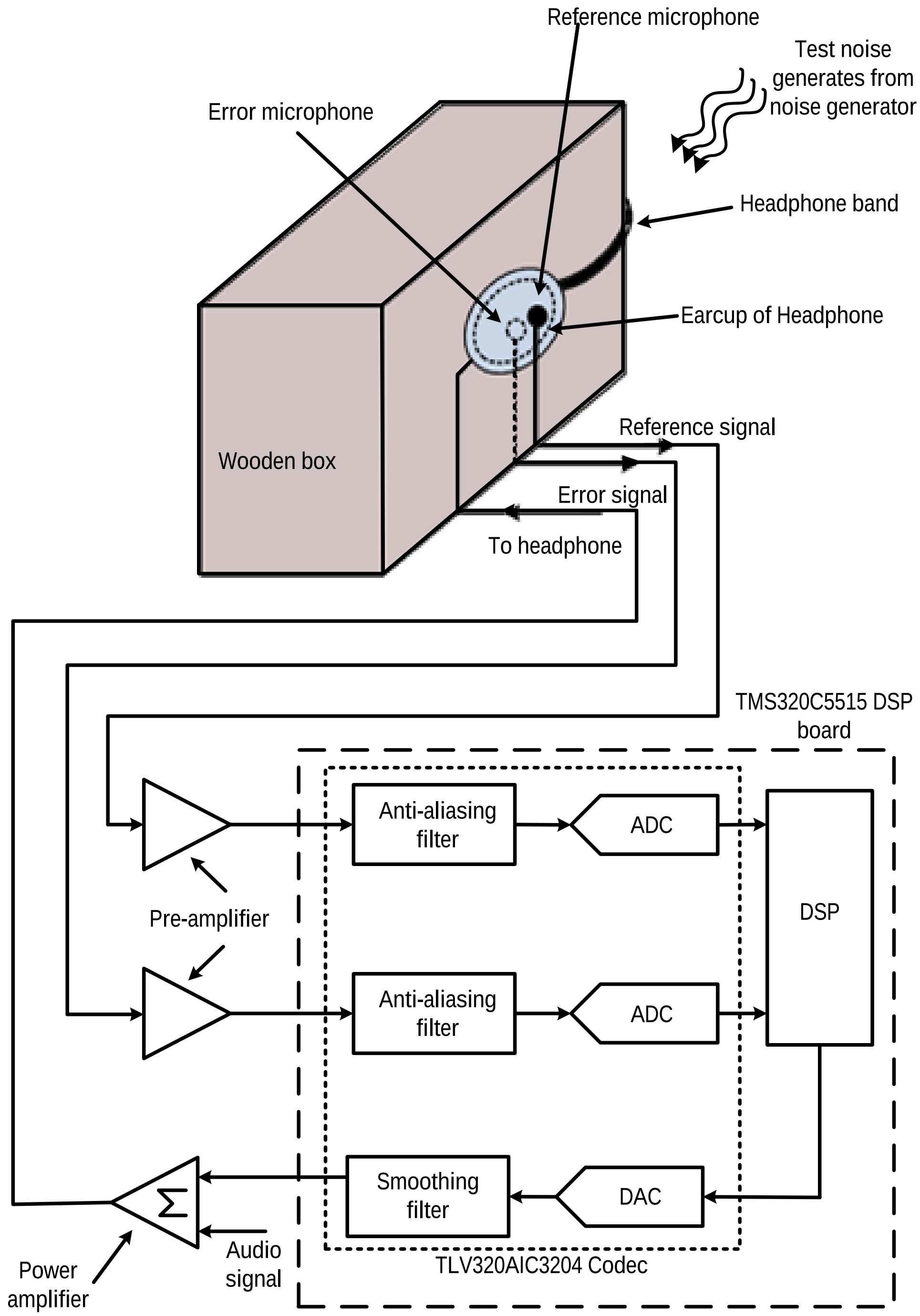

Figure 5.4 Experimental setup for ANC system using TMS320C5515 processor board

processing. To remove the effect of aliasing during sampling, the amplified signal is passed through an anti-aliasing filter with cut-off frequency of 10.56 kHz, pass band (0 – 9.36 kHz) gain of 0.062 dB and stop band (13.2 kHz – 24 kHz) gain of -73 dB. The outputs of the two anti-aliasing filters are then simultaneously sampled and digitized by the ADCs. The digitized signal is used to update the adaptive filter coefficients using LMS algorithm. Anti-noise digital signal is generated as a result of adaptation process in the digital signal processor. This digital anti-noise signal is converted back to the analog signal using DAC, which is then passed through the smoothening filter with cut-off frequency 12 kHz. Smoothening filter have pass band (0 - 10.8 kHz) gain is 0.015 dB and stop band (13.2 kHz – 24 kHz) gain is -65 dB. The output of smoothening filter is added to the test stimulus and amplified by the power amplifier for driving the ear cup speaker.

Initially ANC was carried out using tonal noise to obtain the frequency response of the desired filter. During this experiment, no test signal is given to headphone transducer. Tonal noises of different frequency are stored in WAV format in the PC. A tonal noise is generated through a speaker using PC sound card. A reference microphone kept on the top of the ear cup, picks up the noise presented outside the headphone. Noise transmitted inside the ear cup is picked up by an error microphone kept near the noise cancelling speaker. Reference signal and error signal from pre-amplifiers are given to stereo audio input ports of DSP board. An anti-noise signal to cancel the ambient noise inside the ear cup is obtained using the LMS algorithm based on the reference and error signal. The digital anti-noise signal thus estimated is given to stereo audio output ports of DSP board. The analog signal from DAC is amplified by a power amplifier to drive the headphone speaker. The headphone speaker generates acoustic sound in the ear cup. The anti-noise reduces noise present inside the ear cup by acoustical superposition. The error signal, present in the ear cup, is sensed by error microphone and used to update the adaptive filter coefficients. Once the adaptive filter converges to the minimum error, coefficients of the filter are stored in the memory and then transferred to PC. The magnitude and phase response of the filter for the corresponding tone frequency are obtained from the filter coefficients. Similarly the magnitude and phase response values are obtained for all the tonal frequencies.

An FIR filter was designed from the measured magnitude and phase response of the noise cancelling filter using frequency sampling method. Then this fixed FIR filter is used for broad-band noise cancellation. During ANC for broadband noise cancellation, only the reference noise is sampled and given as input to the fixed FIR filter. Anti-noise generated as an output of the FIR filter is mixed with the test signal and then given to transducer of the headphone. The anti-noise reduces noise present inside the ear cup by acoustical superposition.

5.3 Software Implementation

Software of real-time ANC consists of A/D and D/A conversion of input and output signals, LMS algorithm, and FIR filtering. The internal oscillator (RTC) was configured to operate at 100 MHz by setting the PLL value. After that the SPI is configured to initialize the codec to set the parameters like number of analog input and output channels, sampling rate, resolution of ADC and DAC, PGA gain, and processing block for anti-aliasing filter and reconstruction filter. Left channel of stereo audio ADC was configured for reference signal and right channel of stereo audio ADC was configured for error signal with 16-bit resolution with a sampling frequency of 24 kHz. The data from the codec is copied to the I2S0 receive data register and an interrupt is generated. When the interrupt occurs, the data from I2S0 receive data register is copied to RAM. Right channel of the DAC was configured for anti-noise signal. The data to be sent on DAC is copied to I2S0 transmit data register.

The LMS algorithm sub-routine, used to update the coefficients of the adaptive filter is written in assembly language. For efficient computation the algorithm is implemented using 16-bit fixed-point arithmetic. To reduce the adaptation time, the weight vector is initialized with a vector having only one non-zero element. The position of the non-zero element which gives minimum error was obtained by shifting the non-zero element for the entire length of the weight vector. The non-zero value was empirically obtained as 0.8. For 16-bit word length, the fixed-point number has the range -2^{15} to $2^{15}-1$. The Q1.15 fraction format is used for computation. It has the range (-1 to 0.9999) so the multiplication of two fraction give the results less than one and hence there is no overflow during multiplication. But when large number of accumulation operations are performed then it is possible that the results may be exceed beyond the range (-1 to 0.9999). Saturation logic may be enabled to avoid overflow. But results may get clipped if the saturation logic is enabled. The saturation problems can be solved by scaling the input signal before computation. All the equations were implemented with appropriate scaling of intermediate results, to keep them within the 16-bit range. The processor has a 40-bit accumulator and special multiply-accumulate instruction (MAC). The saturation flag is set whenever the computation results in accumulator exceed 32-bit. All the digital signals and variables, which are used for implementing the LMS algorithms, are in 16-bit fractional format. The signed integer variable can be changed to fractional format by dividing the integer value with 2^{15} so the variable has the value within the range (-1 to 0.9999). The scaling operations are performed using right shifting. For LMS algorithm implementation, all the discrete signals and filter coefficients are in Q1.15 fractional format as shown in Table 5.1.

Table 5.1 Q1.15 fractional format representation

Bit	15	14	13	12	11	9	8	….	0
Value	S	Q14	Q13	Q12	Q11	Q9	Q8	…..	Q0

The S bit is represents sign bit and rest 15 bits contain the 2's complement fractional format number. The finest fractional resolution is 2^{-15}. A fractional number can be represented by Q1.15 format by multiplying it with 2^{15}.

5.3.1 Computations involved in the DSP implementation

The reference input $d_1(n)$ and error input $x_1(n)$ are in the range {-1, 1}. The step size μ is selected empirically in the range 0-0.0125. The adaptive filter output d_4 as

$$d_4(n) = \left[\sum_{k=0}^{M-1} d_1(n-k) w_n(k) \right] \tag{5.1}$$

where M = filter order, selected as 400, and $w_n(k)$ are the filter coefficients assumed to be in the range {-1, 1}. These are updated using

$$w_{n+1}(k) = w_n(k) + \mu x_1(n) d_1(n-k) \tag{5.2}$$

Since step size μ is a fractional number, we use $\alpha = 2^{15}$ as a scaling factor. The scaled step-size compatible with Q1.15 format is given as

$$\mu_s = \alpha\mu \tag{5.3}$$

The reference inputs $D_1(n)$, error inputs $X_1(n)$ and filter coefficients $W_n(k)$ in Q1.15 fractional format are given as

$$D_1(n) = \alpha d_1(n) \tag{5.4}$$

$$X_1(n) = \alpha x_1(n) \tag{5.5}$$

$$W_n(k) = \alpha w_n(k) \tag{5.6}$$

The adaptive filter output in Q1.15 format is computed as

$$D_4(n) = \frac{1}{\alpha} \sum_{k=0}^{M-1} D_1(n-k) W_n(k) \tag{5.7}$$

The filter coefficient update equation, in the fractional format, is given as

$$W_{n+1}(k) = W_n(k) + \frac{1}{\alpha} \left\{ \mu_s \frac{1}{\alpha} \left[\left(X_1(n) D_1(n-k) \right) \right] \right\} \tag{5.8}$$

Thus the reference input, error input, step size, filter coefficients and output are all in Q1.15 fractional format.

5.3.2 Simulation results

An LMS algorithm is simulated using Microchip Code Composer Studio (CCStudio) simulator. CCStudio simulator has a provision to calculate number of instruction cycles consumed by the algorithm using linear profiling. During simulation overhead due to interrupts was not considered. For the filter order of 400, step-size of 0.003, and sampling rate

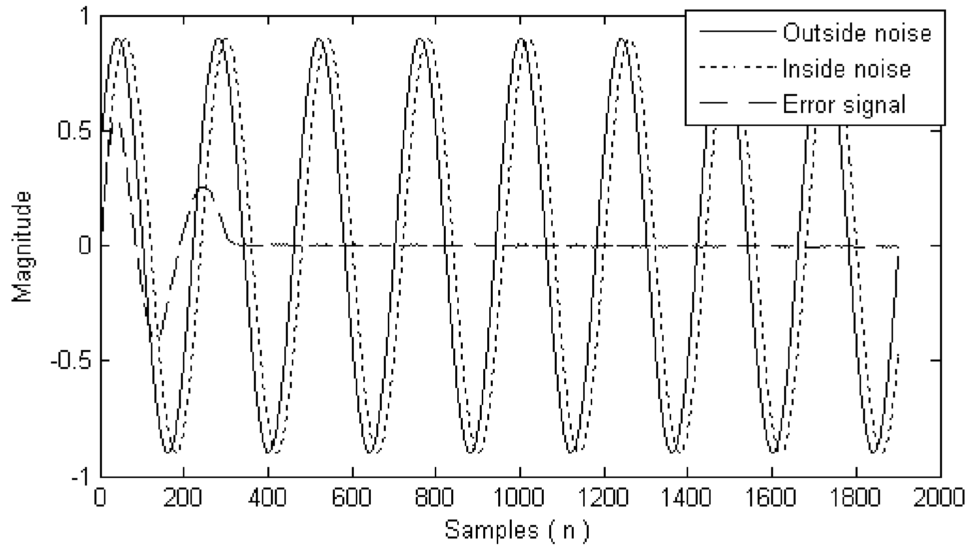

Figure 5.5 Plot of noise with and without ANC using CCStudio simulator

of 24 kHz, the total number of instruction cycles taken by the LMS algorithm was observed to be 2120. Hence the execution time required is 212 μs (as the instruction cycle time of TMS320C5515 is 100 ns). Simulation was carried out by taking a tone of 100 Hz as an ambient noise. Headphone is modeled by 2nd order Butterworth low-pass filter with cut off frequency of 500 Hz. The transmitted noise and reference noise were stored in buffer. The LMS algorithm was simulated using CCStudio simulator and error signal was stored in error buffer array. It can be observed from Fig. 5.5, the noise reduction for 100 Hz tonal noise was 42.1 dB.

5.4 Test and Results

5.4.1 Measurement of primary and secondary path delays

A tonal noise is generated through a speaker using PC sound card. During this measurement adaptation was not carried out. Reference signal and error signal from the pre-amplifier output were observed on the digital storage oscilloscope (DSO). The frequency of the tonal noise is varied till the reference signal and error signal coincide with each other. It was found that at 200 Hz, reference signal and error signal coincide with each other indicating integer cycle delay between the two signals. Again the frequency of the tonal noise is increased till the next time reference signal and error signal coincide with each other. This frequency was found to be at 3 kHz. Primary path delay t_p was estimated as,

$$t_p = \frac{1}{f_2 - f_1} \tag{5.9}$$

The primary path delay was found to be 375 μs. For secondary path delay measurement the error signal is fed back to DAC and the delay was measured with respect to the power amplified signal. The frequency of the error signal is varied till the error signal coincides with the power amplifier output signal for two subsequent measurements. These frequencies were found to be 280 Hz and 820 Hz respectively. The secondary path delay t_s was estimated as,

$$t_s = \frac{1}{f_2 - f_1} \tag{5.10}$$

The secondary path delay was found to be 1.875 ms.

5.4.2 Estimation of filter coefficients for broad-band noise cancellation

Initially experiments are conducted with the tonal noise of different frequencies. Sampling rate of 24 kHz, step-size of 0.003 and FIR filter order 400 is used for real-time implementation of ANC. From Fig. 5.4., it uses two microphones, one for reference noise and the other for error sensor. LMS based adaptive feed-forward method is used for active noise cancellation. The outputs of the reference microphone and the error microphone are used to adjust the adaptive filter using LMS algorithm. The noise inside the ear-cup is picked by the error microphone and is given as input to the adaptive filter. An LMS algorithm adjusts the filter coefficients to reduce the mean square error. No stimulus signal is presented to the headphone. A sinusoidal signal is used as the ambient noise. Once the adaptation is complete, magnitude and phase response of the adapted filter for the corresponding frequency of the tonal noise are obtained from the filter coefficients. The process is followed to obtain the magnitude and phase at different frequencies by varying, in discrete steps, the frequency of the sinusoidal tone presented as the ambient noise. Fig. 5.6 – 5.10 shows the waveform of error signal with and without adaption for various noises. It can be observed from the plot that noise reduction is different for different tonal frequency. The tonal noise used is incremented in steps of 10 Hz till 800 Hz. Noise reduction as a function of the tonal frequency of noise is shown in Fig. 5.11. An average noise reduction of 20.2 dB was observed till 800 Hz.

Magnitude and phase response values of the noise cancelling filter are obtained for each of the tonal noise. Thus we get a sampled version of the frequency response over the frequency band of 200 – 800 Hz. An FIR filter for broad-band noise cancellation is obtained using frequency sampling method. The frequency response uniformly sampled at 2400 points, with frequency sampled given at,

$$\omega_k = \frac{2\pi}{2400} k \qquad k = 0, 1, 2, \ldots\ldots, 1200 \tag{5.11}$$

The desired frequency response is given as,

$$H(k) = 0 \qquad k = 0, 1, 2, \ldots\ldots, 19 \tag{5.12}$$

$$H(k) = H_d(\omega)\Big|_{\omega=\omega_k} \qquad k = 20, 21, 22, \ldots\ldots, 80 \qquad (5.13)$$

$$H(k) = 0 \qquad k = 81, 82, \ldots\ldots, 1200 \qquad (5.14)$$

$$H(k) = H^*(2400 - k) \qquad k = 1201, 1202, \ldots\ldots, 2399 \qquad (5.15)$$

The $H(k)$ thus obtained is considered as the 2400-point discrete Fourier transform (DFT) of the impulse response of the desired noise cancelling filter. The impulse response is obtained by taking the inverse Fourier transforms of $H(k)$ obtained by simulation.

$$h(n) = \frac{1}{2400}\sum_{k=0}^{2400} H(k) e^{j2\pi kn/2400} \qquad n = 0, 1, 2, \ldots\ldots, 2399 \qquad (5.16)$$

The impulse response is used for realizing the FIR filter for broad-band noise cancellation.

5.4.3 Results for tonal noise cancellation using fixed FIR filter

An FIR filter was designed using the magnitude and phase response values for frequency range from 200 Hz to 800 Hz. The frequency response of the desired FIR filter and approximated FIR filter is shown in Fig. 5.12. It can be observed that the magnitude response of approximated FIR filter matches with that of the desired FIR filter magnitude response. The fixed FIR filter was used to cancel tonal noise of different frequencies to test the performance of FIR filter designed. Noise reduction for tonal noise for different frequencies using fixed FIR filter are shown in Fig. 5.13-5.15. It is observed that noise reduction is significant for frequencies 200 Hz to 800 Hz. Noise reduction as a function of the tonal frequency of noise is shown in Fig. 5.16. An average noise reduction of 10.4 dB was observed till 800 Hz. Power spectral densities for swept tonal noise and band-pass filtered white Gaussian noise in the range of 200 – 800 Hz with and without ANC is shown in Fig. 5.17. It is observed that an average noise reduction for swept tonal noise was 6.5 dB and filtered band-pass white Gaussian noise was 2.3 dB. The low noise reduction may be due to the small number of samples and phase response values. More number of samples of magnitude and phase response needs to be taken for improving the noise cancellation.

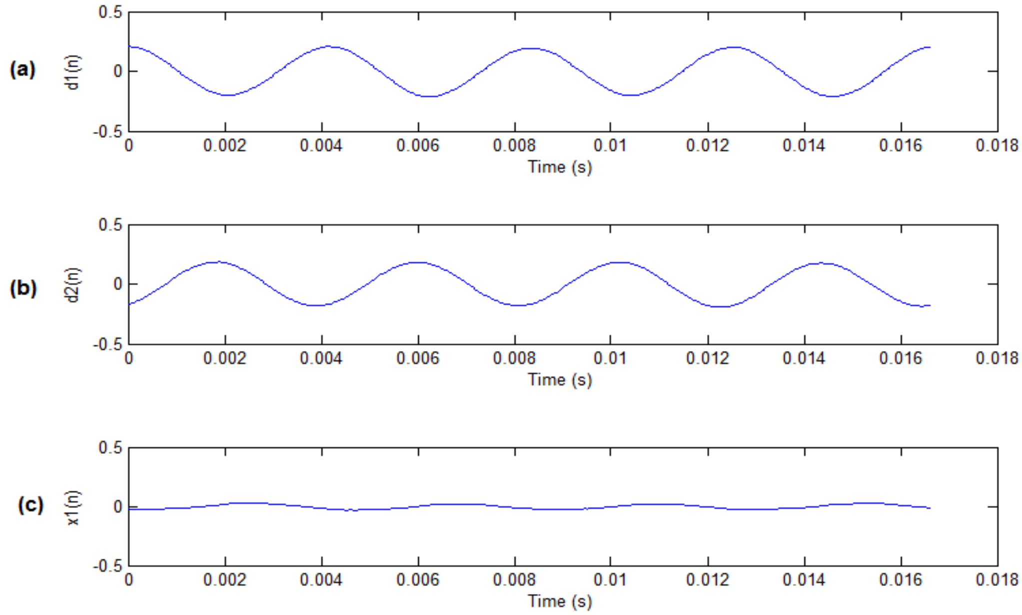

Figure 5.6 Plots of a tone of 240 Hz noise: (a) noise outside the ear cup; (b) transmitted noise inside the ear cup without ANC; (c) noise inside the ear cup with ANC.

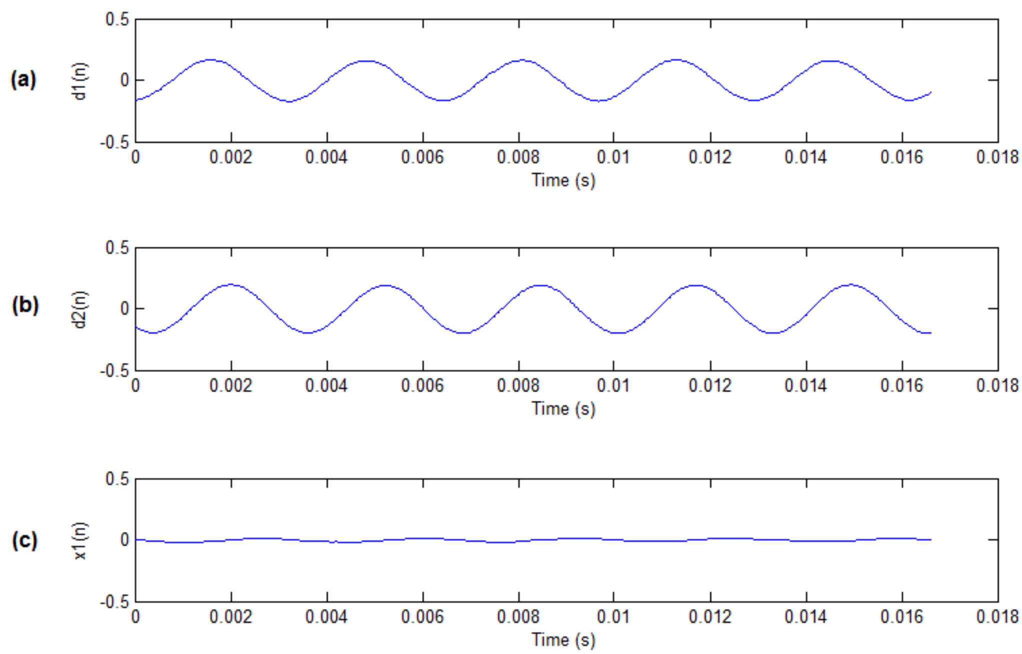

Figure 5.7 Plots of a tone of 310 Hz noise: (a) noise outside the ear cup; (b) transmitted noise inside the ear cup without ANC; (c) noise inside the ear cup with ANC.

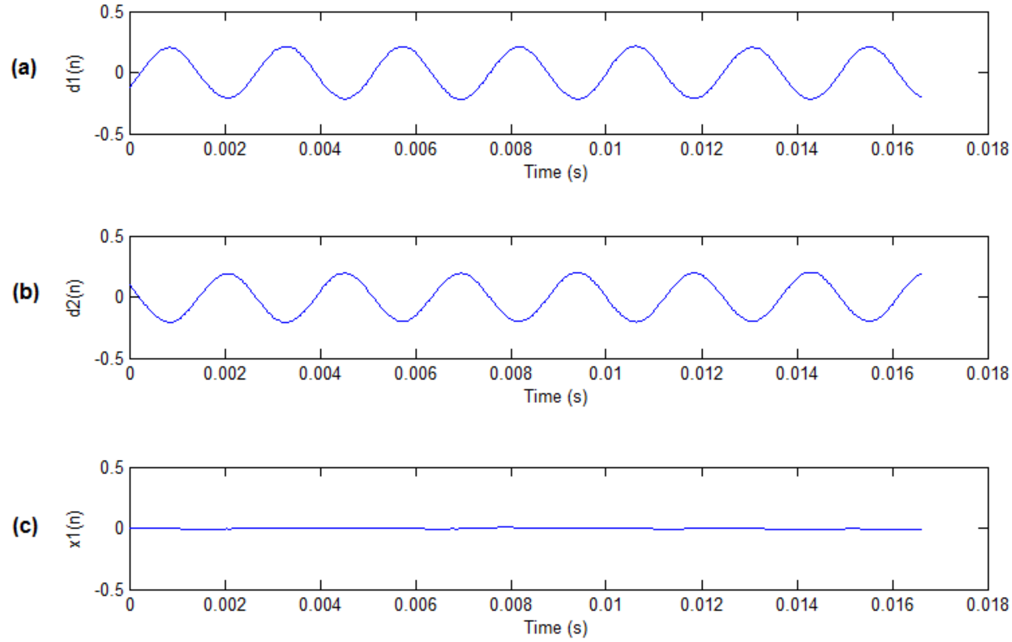

Figure 5.8 Plots of a tone of 410 Hz noise: (a) noise outside the ear cup; (b) transmitted noise inside the ear cup without ANC; (c) noise inside the ear cup with ANC.

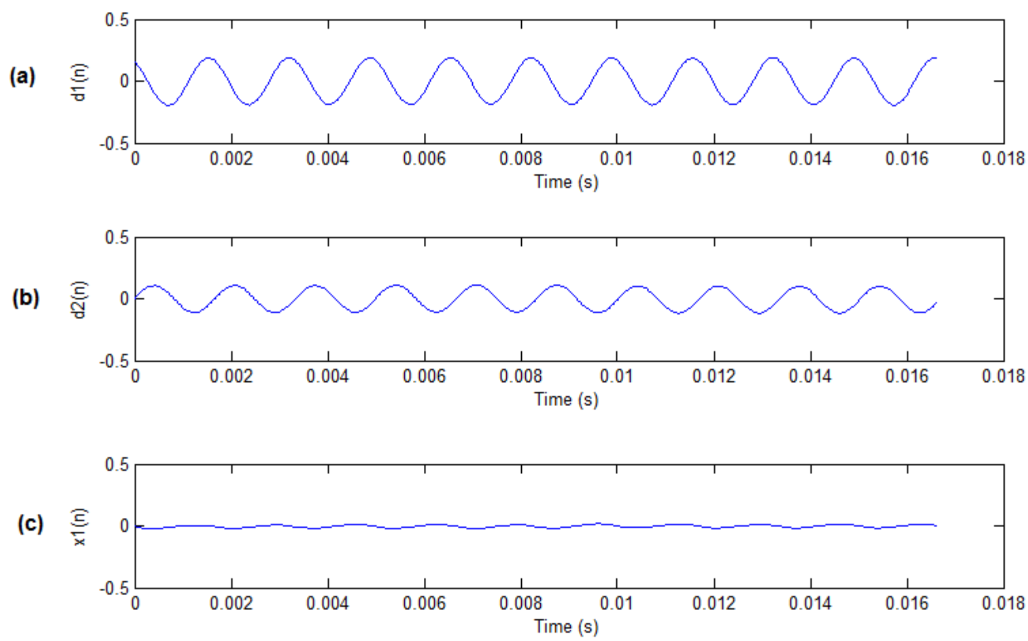

Figure 5.9 Plots of a tone of 600 Hz noise: (a) noise outside the ear cup; (b) transmitted noise inside the ear cup without ANC; (c) noise inside the ear cup with ANC.

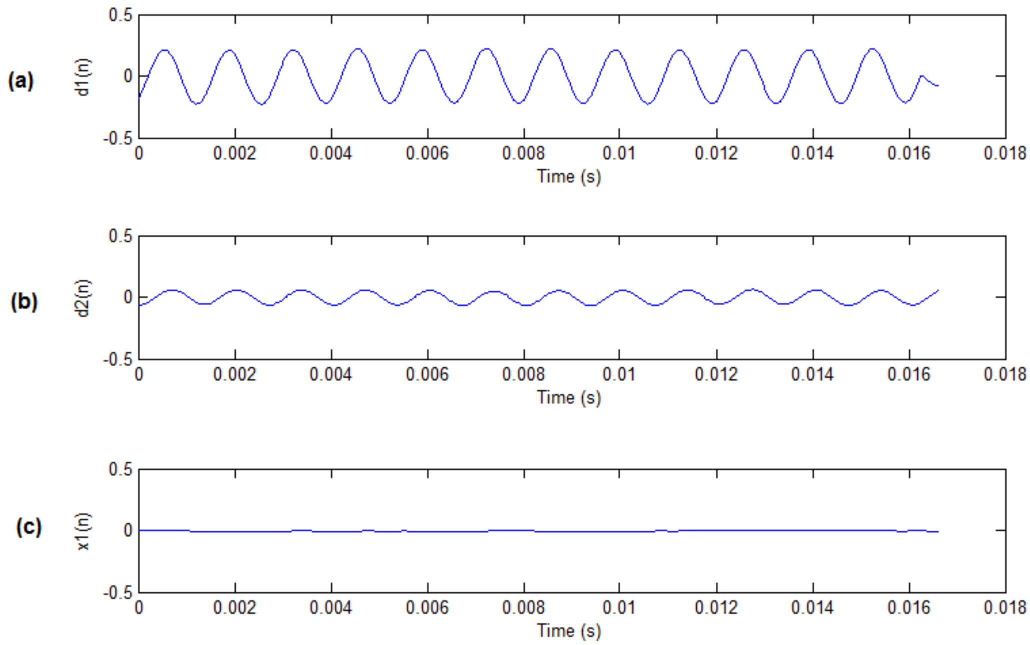

Figure 5.10 Plots of a tone of 750 Hz noise: (a) noise outside the ear cup; (b) transmitted noise inside the ear cup without ANC; (c) noise inside the ear cup with ANC.

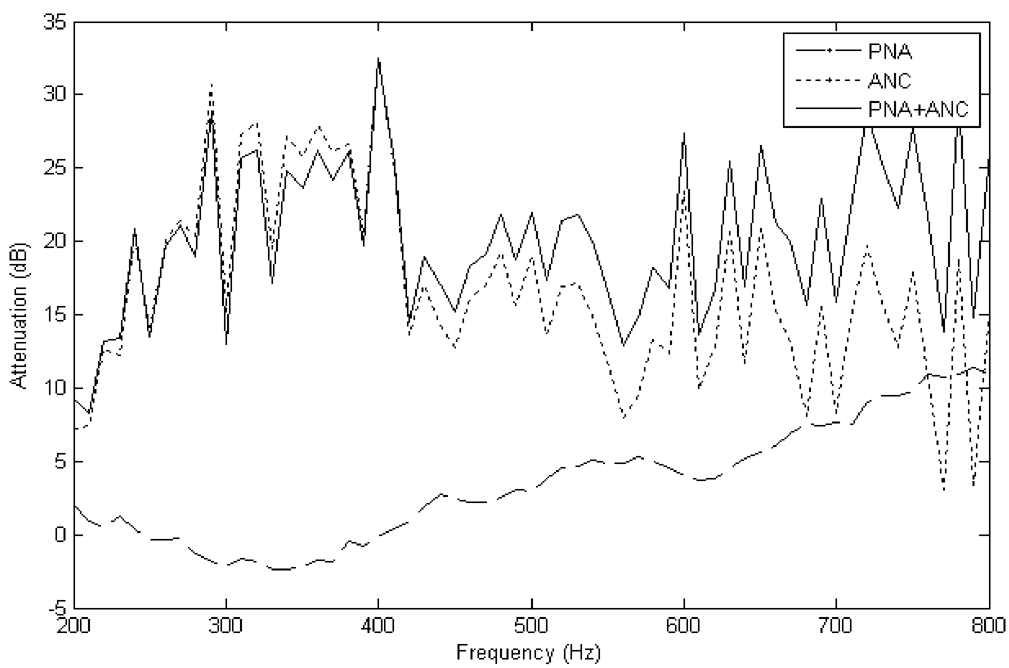

Figure 5.11 Attenuation of tonal noise as a function of frequency (Step size = 0.003, filter order 400, and tonal noise as a background noise)

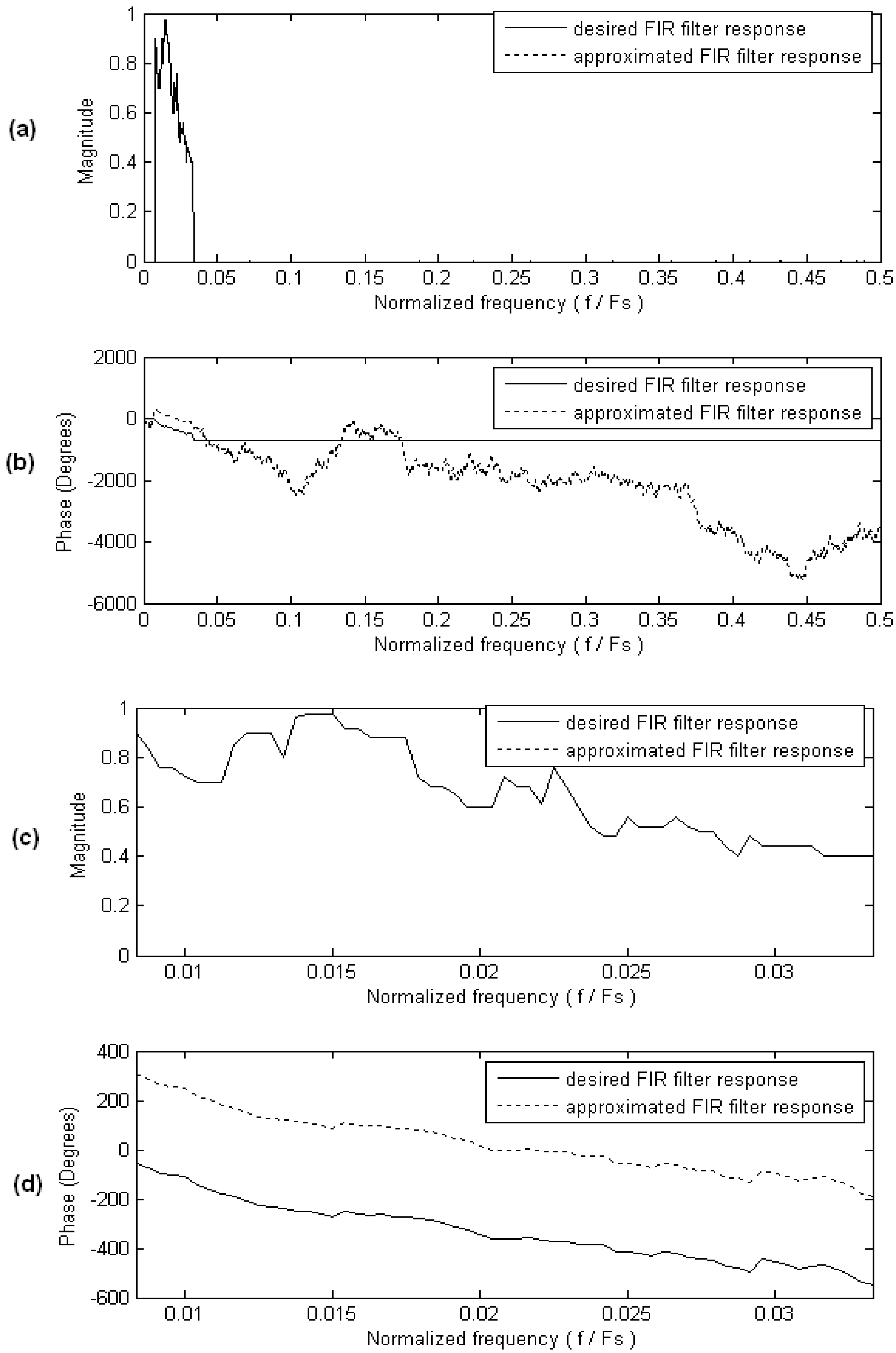

Figure 5.12 Frequency responses of fixed FIR filter: (a) desired magnitude response and approximated magnitude response; (b) desired phase response and approximated phase response; (c) desired magnitude response and approximated magnitude response over a range of 200 - 800 Hz; (d) desired phase response and approximated phase response over a range of 200 - 800 Hz.

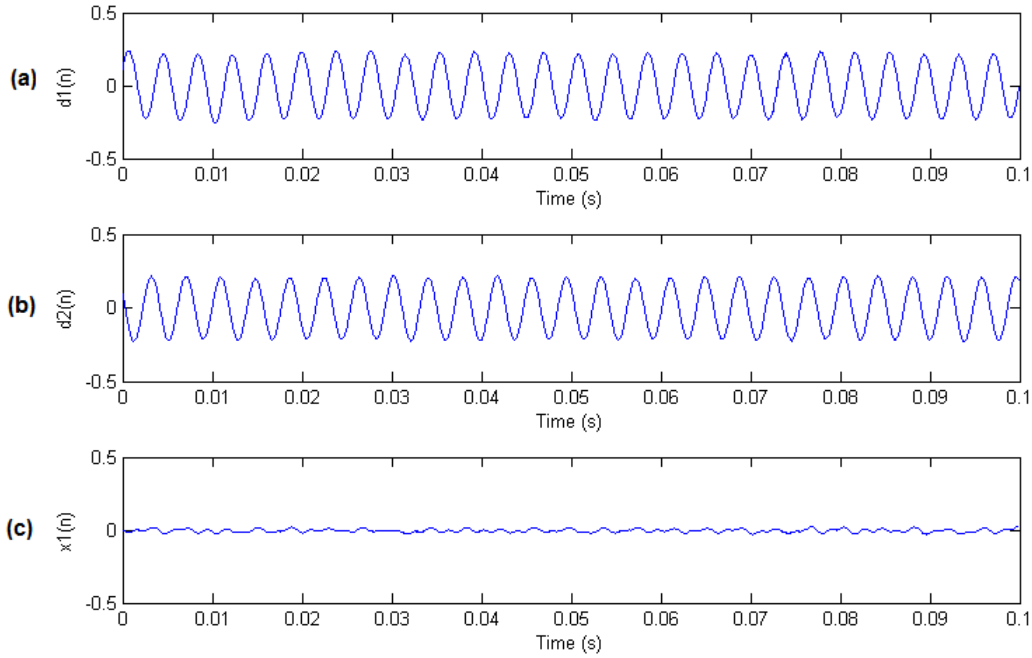

Figure 5.13 Plots of a tone of 260 Hz noise: (a) noise outside the ear cup (b) transmitted noise inside the ear cup without ANC; (c) noise inside the ear cup with ANC (using fixed FIR filter).

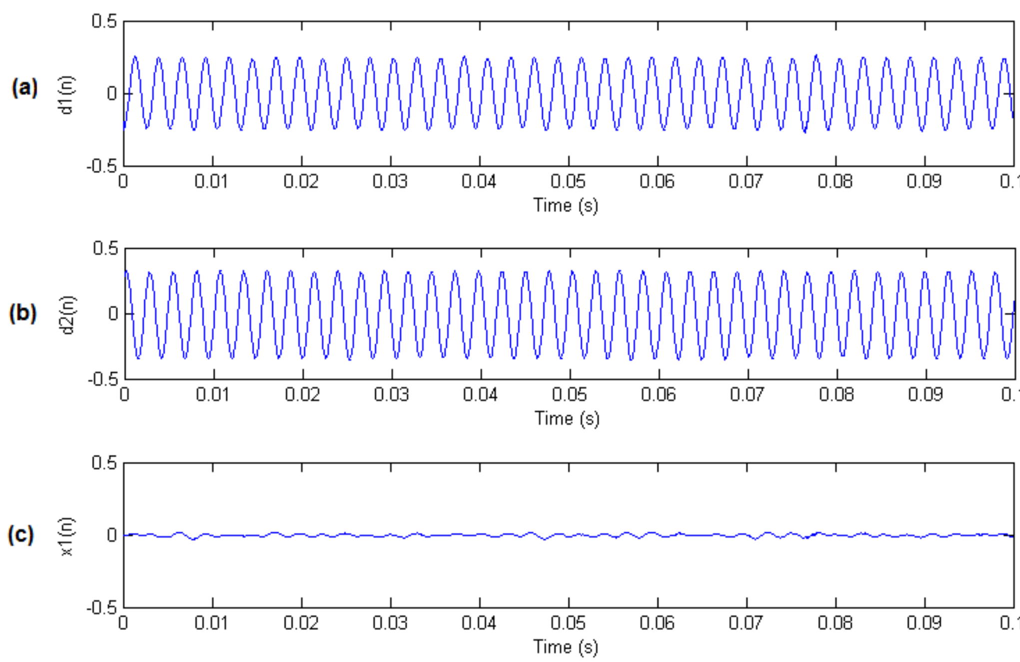

Figure 5.14 Plots of a tone of 380 Hz noise: (a) noise outside the ear cup; (b) transmitted noise inside the ear cup without ANC; (c) noise inside the ear cup with ANC (using fixed FIR filter).

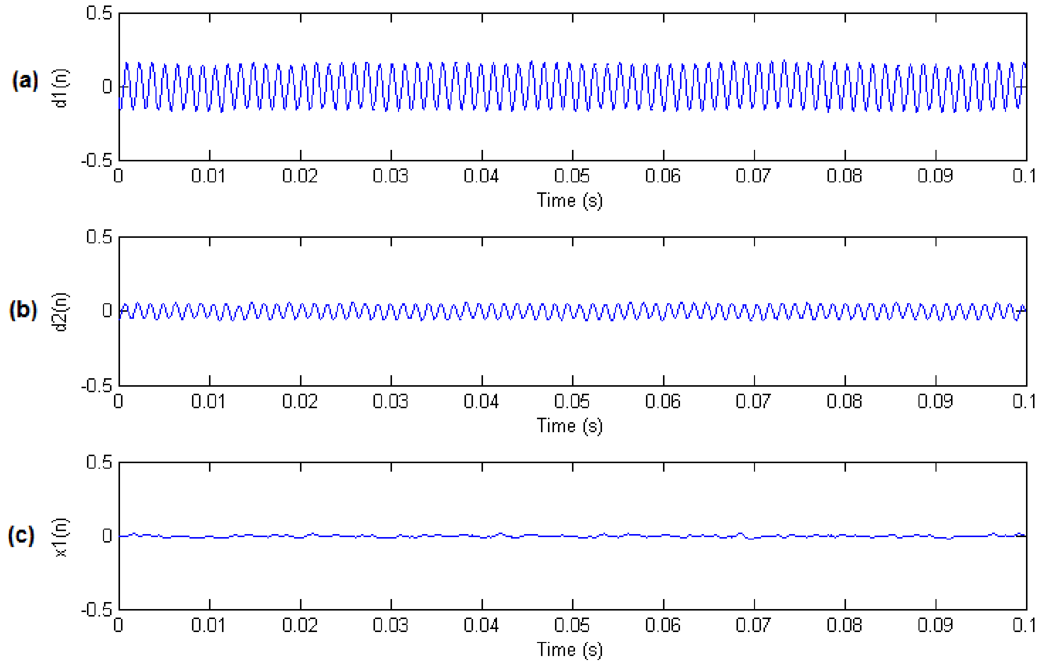

Figure 5.15 Plots of a tone of 720 Hz noise: (a) noise outside the ear cup; (b) transmitted noise inside the ear cup without ANC; (c) noise inside the ear cup with ANC (using fixed FIR filter).

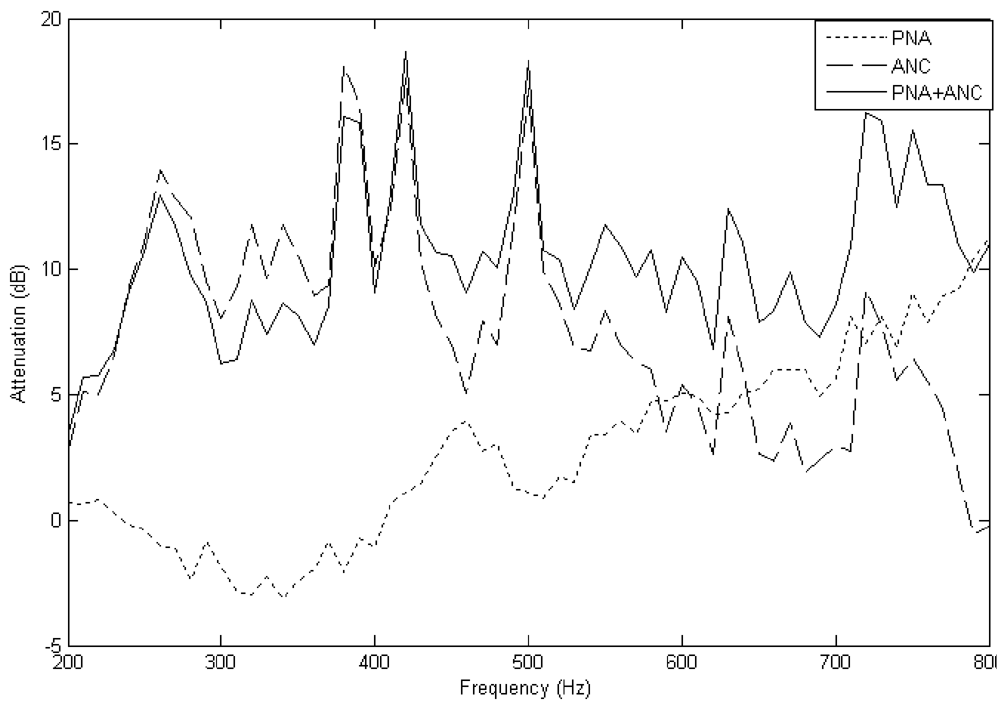

Figure 5.16 Attenuation of tonal noise as a function of frequency using designed fixed FIR filter.

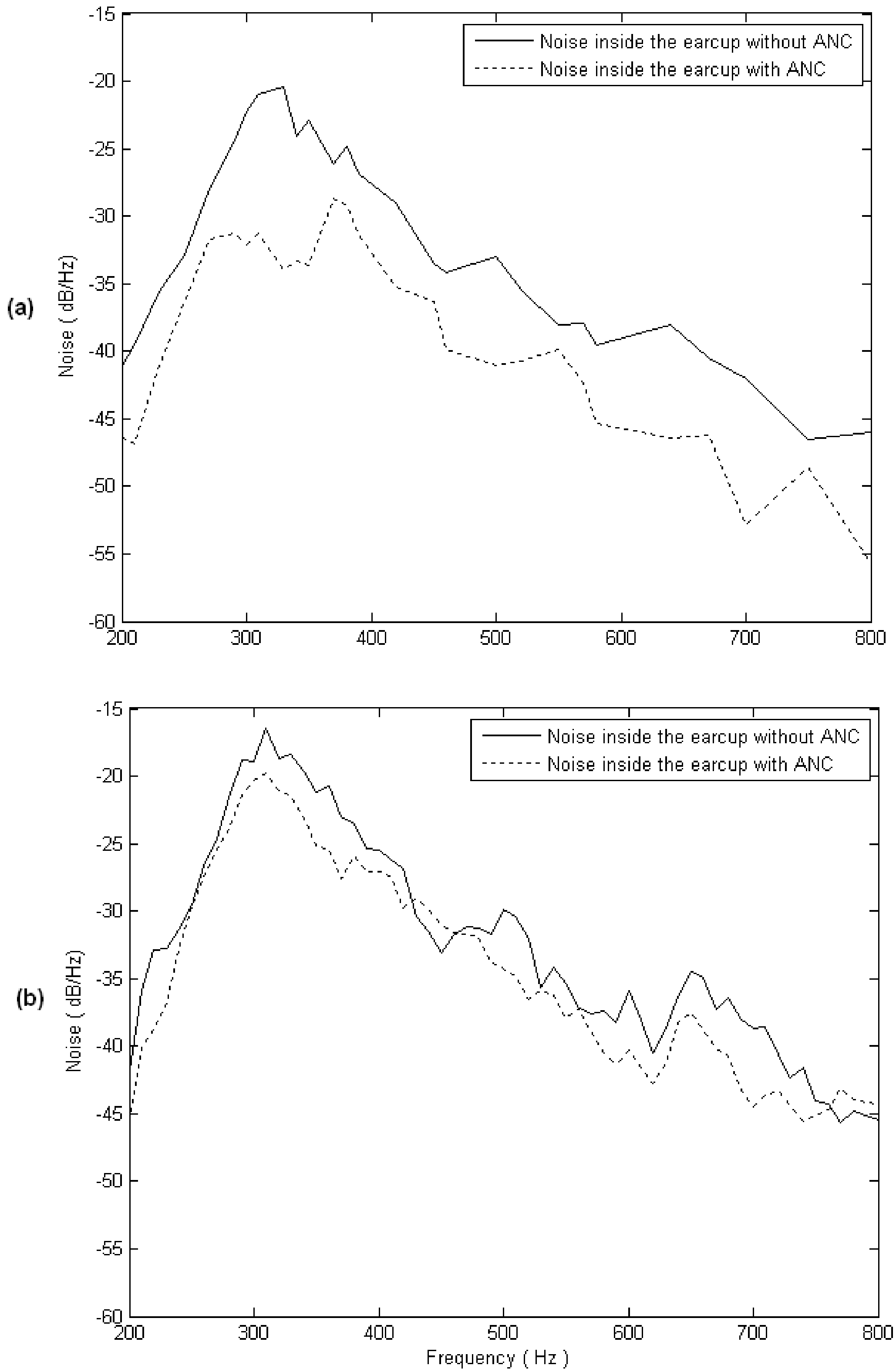

Figure 5.17 Power spectral density of: (a) swept tonal noise in the range of 200 – 800 Hz; (b) band-pass filtered (200 – 800 Hz) white Gaussian noise.

Chapter 6
SUMMARY AND SUGGESTIONS FOR FUTURE WORK

6.1 Summary

An effective broadband noise cancellation is reduction of the ambient noise needed for conducting audiometric test. In order to conduct these tests without using an acoustically isolated cabin, the noise reduction in the ear cup of the headphone should be around 40 dB over the frequency range of 125 Hz to 8 kHz.

An earlier study has shown that real-time implementation of LMS-based adaptive feed-forward filter for broad-band noise cancellation is not practical, since the secondary path delay was longer than the primary path delay. Hence a method is proposed to use a fixed high order FIR filter for broad-band noise cancellation. An LMS based adaptation is used to obtain the magnitude and phase response of the required filter for broad-band noise cancellation by using a swept sine wave as the noise source. Subsequently this magnitude and phase response is used to realize the fixed FIR filter using frequency sampling method for cancellation of broad-band noise.

Simulations were carried out using LMS based adaptation for tonal noise of different frequencies. It was observed that noise cancellation was ineffective for broad-band noise when the secondary path delay is larger than the primary path delay. However ANC was effective for tones of all frequencies as the LMS based adaptation was able to track the sinusoidal tones by matching the phase shift. Simulations were carried out with various broad-band noise such as white Gaussian noise, music, air-conditioner noise, train noise and helicopter noise as ambient noise, using fixed FIR filter assuming the secondary path delay to be larger than the primary path delay. An average noise reduction of 34.6 dB was observed.

In a real-time implementation, the processing speed and on-chip memory limit the sampling frequency and filter order to be used. Real-time implementations were carried out using two processors. The implementation using dsPIC33FJ128GP802 with 40 MHz clock speed and 16 KB on-chip memory was carried out with sampling frequency of 20 kHz and filter order of 250. Average noise reduction of 13.9 dB was observed for tones over a frequency range of 260 Hz to 460 Hz. To improve the performance, TI TMS320C5515 processor with 120 MHz clock rate and 320 KB on-chip RAM was used for real-time implementation with sampling frequency of 24 kHz and filter order of 400. Average noise reduction of 20.2 dB was observed for tone frequency range of 200-800 Hz. A fixed FIR filter was designed using samples of magnitude and phase response of noise cancelling filter. An average noise reduction for tonal noise swept over the frequency range of 200-800 Hz was 6.5 dB and filtered band-pass white Gaussian noise was 2.3 dB. The low noise reduction may be due to the small number of samples and phase response values. It was observed that noise cancelling was not effective for broad-band noise. Further investigations with real-time implementations are needed to examine various issues involved in the cancellation of broad-band noise.

6.2 Suggestions for future work

FIR filter needs to be designed using a larger number of samples of magnitude and phase response of noise cancelling filter over the entire frequency range of 125 Hz to 8 kHz. Broad-band noise cancellation needs to be tested by increasing the sampling rate and filter order.

APPENDIX

Noise cancelling headphones developed by various manufactures are listed in the following table.

Sr. No.	Manufacture	Model	Cost	Specification and features
1	Sennheiser	PXC 350	$340	Passive noise attenuation up to 32 dB and active noise reduction up to 18 dB (<1000 Hz)
2	Sennheiser	PXC 310	$300	PNA up to 26 dB ANR up to 15 dB (<1000 Hz)
3	JVC	HA-NC250	$200	Up to 85 % ambient noise reduction (more than 18 dB at 150 Hz)
4	Denon	AH-NC732	$300	Reduce low frequency noise up to 18 dB
5	Sony	MDR-NC500D	$400	Total noise reduction up to 20 dB
6	Sony	MDR-NC60	$200	Up to 85 % ambient noise reduction (16.5 dB at 200 Hz)
7	Audio-Technica	ATH-ANC7b QuietPoint	$220	Active noise reduction up to 20 dB
8	Bose	QuietComfort 15	$390	Not Specified
9	Bose	Quiet Comfort 3	$497	Not Specified
10	Creative	Aurvana X-Fi	$200	Noise reduction up to 20 dB
11	Plane Quiet	Platinum NCH	$100	Noise reduction up to 10 dB between 150 - 400 Hz
12	Able Planet	Clear Harmony NCH	$350	Not Specified
13	Panasonic	RP-HC500	$200	Reduces outside noise by 22 dB at 200 Hz

REFERENCES

[1] S. J. Elliott and P. A. Nelson, "Active noise control," *IEEE Signal Process. Mag.*, vol. 10, no. 10, pp. 12-35, 1993.

[2] A. Biswas, *Clinical Audio - Vestibulometery for Otologists and Neurologists.* Mumbai: Bhalani, pp. 1-17, 2nd Ed, 1995.

[3] E. H. Berger and M. C. Killion, "Comparison of the noise attenuation of three audiometric earphones, with additional data on masking near threshold," *J. Acoust. Soc. Amer.,* vol. 86, no. 4, pp. 1392-1403, 1989.

[4] R. Sapiejewski, "Supra-aural headphone noise reducing," US Patent 0,269,090, Nov. 30, 2006.

[5] M. A. Vaudrey and W. R. Saunders, "Active noise reduction for audiometry," US Patent 6,396,930, May 28, 2002.

[6] C. Moy, Active Noise Reduction Headphone Systems, 2010, [Online] Available: http://gilmore2. chem.northwestern .edu/tech/anr_ tech.htm.

[7] B. Rafaely and M. Furst, "Audiometric ear canal probe with active ambient noise control," *IEEE Trans. Speech Audio. Process.*, vol. 4, no. 3, pp. 224-230, 1996.

[8] A. G. Bose, "Feedback control," US Patent 4,494,074, Jan. 15, 1985.

[9] S. M. Kuo and D. R. Morgan, *Active Noise Control Systems*, New York: John Wiley, 1st ed., 1996, pp. 53-146, 187-212.

[10] W. S. Gan , S. Mitra, and S. M. Kuo, "Adaptive feedback active noise control headset: Implementation, evaluation and its extensions," *IEEE Trans. Consum. Electron.*, vol. 51, no.3, pp. 975-982, 2005.

[11] S. M. Kuo, S. Mitra, and W. S. Gan, "Active noise control system for headphone applications," *IEEE Trans. Control Syst. Technol.*, vol. 14, no. 2, pp. 331-335, 2006.

[12] B. Rafaely, "Active noise reducing headset - an overview," in *Proc. Internoise Conf.,* 2001, The Hague, Holland, pp. 589-598.

[13] B. Rafaely and M. Jones, "Combined feedback-feed-forward active noise-reducing headset - The effect of the acoustics on broad-band performance," *J. Acoust. Soc. Amer*., vol. 112, no. 3, pp. 981-989, 2002.

[14] N. Narahari, "Noise cancellation in headphones for audiometry," M.Tech. dissertation, Dept. Elect. Eng., IIT Bombay, Mumbai, 2005.

[15] A. V. Rhijn, "Integrated circuits for high performance electret microphones," *National Semiconductor*, 2011, [Online] Available: https://pantherfile.uwm.edu/type/www/116/Project04/Other_DIYS/HowECMsWork%26newDesiigns.pdf.

[16] National Semiconductor, "Low Power Quad Operational Amplifiers," 2011, [Online] Available: www.national.com/ds/LM/LM124.pdf.

[17] National Semiconductor, "Dual Audio Power Amplifier," 2011, [Online] Available: www.national.com/ds/LM/LM1877.pdf.

[18] Microchip Technology Inc., "dsPIC33FJ32GP302/304, dsPIC33FJ64GPX02/X04, and dsPIC33FJ128GPX02/X04 Data Sheet: High-Performance 16-bit Digital Signal Controllers," 2009, [Online] Available: ww1.microchip.com/downloads/en/DeviceDoc/70292D.pdf.

[19] Texas Instruments Inc., "TMS320C5515 Fixed-Point Digital Signal Processor," 2011, [Online] Available: http://focus.ti.com/lit/ds/symlink/tms320c5515.pdf.

[20] Spectrum Digital Inc., "TMS320C5515 eZdsp USB Stick: Technical Reference," 2010, [Online] Available: http://support.spectrumdigital.com/boards/usbstk5515/reva/files/usbstk5515_TechRef_RevA.pdf.

[21] Texas Instruments Inc., "TLV320AIC3204 Ultra Low Power Stereo Audio Codec," 2008, [Online] Available: http://focus.ti.com/lit/ds/symlink/tlv320aic3204.pdf.

[22] J. G. Proakis and D. G. Manolakis, *Digital Signal Processing*. NJ: Prentice-Hall, 3rd ed., 1996, pp. 630-637.

[23] Texas Instruments Inc., "TMS320C5505 DSP System User's Guide," 2011, [Online] Available: http://focus.ti.com/lit/ug/sprugh5/sprugh5.pdf

ACKNOWLEDGEMENT

I would like to thank my guide Prof. P. C. Pandey for for his precious feedback and supports. I want to give many thanks to Mr. Nandakumar Pai for his valuable help, suggestions and support for programming of the DSP chips and boards. I would also like to express my sincere thanks to my labmates in SPI Lab and Instrumentation Lab for their help and support during the project work. I thank my batchmates for their moral support.

Vinod Kumar Lohar

Author’s Resume

Vinod Kumar Lohar: He received the B. E. degree in electronics and communication engineering from Mugniram Bangur Memorial Engineering College, Jodhpur (Rajasthan) in 2007. He worked as a Lecturer at Shri Balaji College of Engineering & Technology, Jaipur during August 2007 to June 2008. He received PG Diploma in Natural Resources Engineering from the Indian Institute of Technology Bombay in 2009. Presently, he is pursuing the M.Tech. degree in electrical engineering at the Indian Institute of Technology Bombay. His research interests include embedded system design, digital signal processing, and image processing.